A CLINICAL AND MOLECULAR GENETIC INVESTIGATION OF X-LINKED CONGENITAL STATIONARY NIGHT BLINDNESS

LOUISE ELIZABETH ALLEN
M.B.,B.S.(Lond.) F.R.C.Ophth.

Thesis submitted for the degree of Doctor of Medicine at the University of London

2005

ProQuest LLC
789 East Eisenhower Parkway
P.O. Box 1346
Ann Arbor, MI 48106-1346

Abstract

Aims

This study examines the clinical and molecular genetic features of X-linked Congenital Stationary Night Blindness (XLCSNB). The aims are to accurately document the phenotype of affected subjects by investigating functional visual deficit, to evaluate possible disease mechanisms and to confirm or refute the veracity of the "complete" and "incomplete" descriptions of phenotype in common clinical usage. In addition, by identifying causative gene mutations in the pedigrees studied, the study investigates the possibility of a genotype-phenotype correlation.

Methods

Members of fifteen families previously diagnosed as having XLCSNB underwent standardised clinical, psychophysical and electrophysiological phenotypic testing. Comprehensive mutation screening of the genes *NYX* and *CACNA1F* was performed for each pedigree.

Results

Seven different loss-of-function mutations in the *NYX* gene were identified in 11 families and three mutations in the *CACNA1F* gene were identified in another three pedigrees. No mutations were detected in members of the remaining pedigree and this family was excluded from further study. Electrophysiological and psychophysical evidence of a functioning but impaired rod system was present in subjects from each genotype group, although scotopic responses tended to be more severely affected in subjects with *NYX* gene mutations. Scotopic oscillatory potentials were absent in all subjects with *NYX* gene mutations whilst subnormal OFF responses were specific to subjects with *CACNA1F* gene mutations.

Conclusions

NYX gene mutations were a more frequent cause of XLCSNB than *CACNA1F* gene mutations in the 15 British families studied. Since evidence of a functioning rod system was identified in the majority of subjects tested, the clinical phenotypes "complete" and "incomplete" do not correlate with genotype. Instead, electrophysiological indicators of inner retinal function, specifically the characteristics of scotopic oscillatory potentials, 30Hz flicker and the OFF response may prove more discriminatory.

CONTENTS

Table of Contents

Table of Illustrations

Acknowledgements

I was very fortunate to secure funding for this project from The Guide Dogs for the Blind Association. Their support enabled me to take two years sabbatical from my clinical training and funded the equipment and reagents used during the study. I thank for them for their support and forbearance over the protracted writing up period.

Many thanks also go to the numerous families who took part in the study. For many it involved several long trips to complete clinical testing. Many of the young children showed extreme fortitude when it came to give blood for DNA analysis and their electrophysiological testing. Many of the families were referred via consultant ophthalmic and genetic colleagues and I thank them for giving me access to their patients.

I thank Professor John Mollon, Professor of Experimental Psychology at Cambridge University, and Professor Fred Fitzke, Professor of Visual Optics and Psychophysics at the Institute of Ophthalmology, for their help with the psychophysical testing of the subjects and the use of their equipment.

The inspiration for this project and for my chosen specialty of paediatric ophthalmology came from Professor Tony Moore, Consultant Ophthalmologist at Moorfields Eye Hospital and Great Ormond Street Hospital, who has been a great inspiration to me throughout my training. I am very grateful to Professor John Yates, Consultant in Clinical Genetics at Addenbrooke's who first had the idea that CSNB would be an interesting condition to study and who has supervised me locally. I also thank Professor Alan Bird, Professor of Clinical Ophthalmology at Moorfields Eye Hospital, for agreeing to act as my University of London supervisor.

Special thanks go to Professor Dorothy Trump, Professor of Clinical Genetics at the University of Manchester, who led me by the hand through the complex world of millimoles, PCR and sequencing, commiserated with me when my experiments went wrong and advised me during both the molecular genetic work and subsequent writing. In the same vein, I started the research in almost complete ignorance of electrophysiology and I thank Dr Keith Bradshaw at Addenbrooke's Hospital, for his patience in explaining the theory behind the procedures and for all the time that he has put into the project.

Last but not least I must thank my long suffering husband, Nick, who has been unrelenting in his enthusiasm and support for me to finish this thesis, and my three lovely little boys Alexander, George and Charlie, without whom this project might have been finished several years sooner!

Chapter 1 Introduction

1.1 Aetiology of nyctalopia (night blindness)

Nyctalopia, or night blindness, is a common symptom, which may result from dysfunction of rod photoreceptors or their inner retinal connections. Nyctalopia may progress in severity or remain stationary throughout life. Progressive night blindness in association with visual field loss and abnormal ophthalmoscopic retinal appearance may result from inherited disorders of the outer retina such as retinitis pigmentosa and choroideraemia, or choroidal dystrophies such as gyrate atrophy. Acquired progressive night blindness due to vitamin A deficiency is a common result of malnutrition in developing countries and may also be seen as a complication of malabsorption secondary to gastro-intestinal disease in the UK. Acquired night blindness may also rarely occur as a manifestation of distant cancer, particularly cutaneous malignant melanoma.

1.2 Congenital stationary night blindness -historical review

The retinal dystrophy of congenital stationary night blindness (CSNB) was first reported by Cunier (Cunier 1838). He described a condition characterized by congenital non-progressive nyctalopia in members of a seven generation dominant pedigree (the Nougaret family) in Southern France. Affected individuals in this pedigree had good visual acuity and colour vision with a normal fundoscopic appearance. More recently this pedigree, now comprising eleven generations, has been investigated by Nettleship and DeJean and, soon after Cunier's description of autosomal dominant CSNB (ADCSNB), X-linked and autosomal recessive pedigrees were also identified (Nettleship 1907, Donders 1855; Varelmann 1925).

In 1907, Oguchi described an unusual form of CSNB characterized by an abnormal discolouration of the retina, giving a metallic-looking sheen to the fundus. This form of CSNB was subsequently named Oguchi disease (Oguchi 1907).

Lauber reported another form of congenital nyctalopia in 1910. This condition was named fundus albipunctatus for the characteristic multitude of small yellow-white spots

visible in the peri-macular and peripheral retina on fundoscopy (Lauber 1910; Franceschetti and Chrome-Brecioux 1951).

Flecked retina of Kandori was reported as a distinct entity in 1958, since the initial report an additional three affected individuals have been identified (Kandori 1959). Flecked retina of Kandori may be distinguished from the other forms of CSNB by the presence of variably sized, irregular yellow flecks which are larger than those seen in fundus albipunctatus and which occur in the equatorial region but spare the peri-macular retina.

1.3 Classification of congenital stationary night blindness

Following these reports CSNB was classified on the basis of its clinical features and inheritance.

I	**CSNB with *abnormal* fundi**
	Oguchi disease (autosomal recessive)
	Fundus albipunctatus (autosomal recessive)
	Flecked retina of Kandori (autosomal recessive)
II	**CSNB with *normal* fundi**
	Autosomal dominant (Nougaret variety)
	Autosomal recessive
	X-linked recessive

1.4 CSNB with abnormal fundus appearance

1.4.1 Oguchi disease

1.4.1..1 Clinical features

Individuals with Oguchi disease are commonly of Asian ancestry and complain of night blindness but have normal visual acuity, visual fields and colour vision. The characteristic feature of this condition is the retinal appearance on fundoscopy. In light adapted conditions a golden-brown tapetal reflex is visible, on dark adaptation this reflex fades and the fundus appearance becomes normal (Mizuo 1913). This fundoscopic phenomenon (the Mizuo-Nakamura phenomenon) has also been documented in some individuals with X-linked retinoschisis and X-linked cone dystrophy (Mizuo 1913; Noble, Margolis et al. 1989; de Jong, Zrenner et al. 1991). To date two genes have been found to be responsible for Oguchi disease, both are involved in the recovery phase of the phototransduction mechanism: the gene *SAG* encodes the protein arrestin and *RHOK* encodes rhodopsin kinase (Table 1) (Fuchs et al. 1995; Yamamoto et al. 1997).

1.4.1..2 Electrophysiological and psychophysical testing

The rod pathway responses are unrecordable in Oguchi disease. Although early electrophysiological studies indicated that the b-wave amplitude alone was subnormal in the electroretinogram (ERG), more recent studies of subjects with *SAG* gene mutations have demonstrated subnormal a- and b-wave amplitudes indicating that rod phototransduction is abnormal in this condition (Carr and Ripps 1967;Nakazawa et al. 1997). Cone pathway response amplitudes are within the normal range. Dark adaptation is characteristically slow and a final rod threshold may only be achieved after several hours, and even then may be slightly elevated (Nakazawa, Wada et al. 1997).

1.4.2 Fundus albipunctatus

1.4.2..1 Clinical features

Individuals with fundus albipunctatus (FA) are night blind but have good visual acuity, visual fields and colour vision (Margolis, Siegel et al. 1987). This form of congenital stationary night blindness is characterised by the presence of small yellow-white flecks in the retina peripheral to the macula. These flecks appear to lie in the deep retina and

become more numerous and punctate with age (Marmor 1990). Studies of rhodopsin kinetics have confirmed that the condition is associated with a delay in rhodopsin regeneration (Ripps 1982). FA results from loss-of-function mutations in the gene *RDH5*, which encodes the protein 11-*cis* retinol dehydrogenase. This results in markedly reduced conversion of 11-*cis* retinol to 11-*cis* retinal in the retinal pigment epithelium, thereby slowing rhodopsin regeneration (Yamamoto and Simon 1999).

1.4.2..2 Electrophysiological and psychophysical testing

In most cases, rod and cone dark adaptation are markedly prolonged and there is a delay in the acquisition of scotopic ERG thresholds but near normal photopic responses (Marmor 1977; Margolis, Siegel et al. 1987). Variations have been reported in which the dark adaptation curves and ERG are normal or dark adaptation shows a cone segment only (Franceschetti and Chrome-Brecioux 1951). These variations may either represent various degrees of severity of a single disorder or several separate disorders with a similar fundus appearance.

1.4.3 Flecked retina of Kandori

1.4.3..1 Clinical features

This is a rare condition which has only been described in Japanese individuals. It causes mild nyctalopia but the visual acuity, colour vision and visual field examination are normal. The distinguishing feature of this condition is the presence of large (up to 1.5 disc diameters) sharply defined, dark yellow, deep and irregular flecks, which are distributed in the equatorial region of the fundus, sparing the macula.

1.4.3..2 Electrophysiological and psychophysical testing

The cone mediated ERG is normal but prolonged dark adaptation is required before the rod mediated responses are recordable. Dark adaptometry shows initial delay in the recovery of rod sensitivity but attainment of normal thresholds within 40 minutes (Kandori, Tamai et al. 1972).

1.5 CSNB with normal fundus appearance

This is the most common form of CSNB but is probably under diagnosed due to the paucity of symptoms and ocular findings. This form of CSNB is genetically heterogeneous; although X-linked recessive transmission is the most common inheritance pattern, autosomal dominant and autosomal recessive transmission may also occur. Recent molecular genetic investigation of ADCSNB and X-linked recessive CSNB (XLCSNB) has led to the identification of causative gene mutations and improved understanding of the molecular pathophysiological basis of these forms of nyctalopia (see Chapter 4). CSNB is clinically heterogeneous: in general, autosomal dominant inheritance is associated with mild nyctalopia and good visual acuity while the recessive forms of CSNB tend to cause more severe night blindness and are often associated with reduced visual acuity, nystagmus, strabismus and myopia (see Chapter 3).

A clinical classification based on the psychophysical and electrophysiological differences between individuals and families with recessively inherited CSNB is widely used. This sub-classification is based on the ability to detect a scotopic or rod mediated response on electrophysiological or psychophysical testing. Subjects in whom no detectable rod mediated response is evident are classified as having "complete" CSNB, those with a subnormal but recordable rod mediated response are classified as having the "incomplete" form (Miyake, Yagasaki et al. 1986). It has been thought that these two phenotypic forms reflect genetic heterogeneity, although this theory has not been universally accepted due to reports of the presence of both forms within one pedigree (see Chapter 3). The recent identification of the two genes, *NYX* and *CACNA1F*, responsible for XLCSNB enables the investigation of such a genotype-phenotype correlation.

1.6 Molecular genetics of the inherited retinal dystrophies

More than 60 genes responsible for human retinal dystrophies have been identified and this knowledge paves the way for the development of novel therapeutic strategies which may help individuals with these disorders. Classification of retinal dystrophies has previously been based upon clinical phenotype and inheritance patterns. The increasing

knowledge of the molecular pathophysiology of retinal dystrophies shows this purely clinical classification to be simplistic since for example, faults in many different genes result in the symptoms and signs of retinitis pigmentosa. Table 1 summarises our current knowledge of the genes involved in the causation of retinal dystrophies.

1.7 The subject of this thesis

The subject of this thesis is X-linked congenital stationary night blindness with normal fundus appearance; this disorder will hereafter be referred to as XLCSNB in this thesis.

Table 1: Summary of genes responsible for human retinal dystrophies (Adapted from Bessant et al. 2001)

Gene	Locus	Protein/protein function	Inheritance	Associated dystrophies
Phototransduction cascade (Table 2c)				
RHO	3q21-q24	Rhodopsin	AD	RP, ADCSNB
GNAT1	3p22	α1subunit of transducin	AD	ADCSNB
PDEα	5q31.2-qtr	α subunit of PDE	AR	RP
PDEβ	4p16.3	βsubunit of PDE	AR	RP
CNGCα	4p14-q13		AR	RP
Recovery phase(Chapter 2.)				
SAG	2q37.1	Arrestin	AR	Oguchi
RHOK	13q34	Rhodopsin kinase	AR	Oguchi
GUCA1A	6p21.1	Guanylate cyclase Activating protein	AD	Cone dystrophy
GUC2D	17p13.1	Retina specific guanylate cyclase	AD AR	Cone-rod dystrophy Leber congenital amaurosis
Structural proteins				
RDS	6p21.1	Peripherin	AD Digenic	RP, macular dystrophy RP
ROM1	11q13	Rod outer segment protein -1	Digenic	RP
Retinol metabolism				
RLBP1	15q26	Cellular retinaldehyde binding protein	AR	RP
RDH5	12q13-q14	11-*cis* retinol dehydrogenase	AR	Fundus albipunctatus
RPE65	1p31	all-*trans*retinyl ester isomerohydrolase	AR	Leber amaurosis
ABCR	1p21-p13	ATP binding cassette protein	AR	Stargardt disease Cone-rod dystrophy
Transcription factors				
CRX	19q13.3	Cone rod homeobox	AD AR	Cone-rod dystrophy Leber amaurosis
NRL	14q11.1-12.1	Increased rhodopsin transcription	AD	RP
NR2E3	15q32	Ligand dependent transcription factor	AR	Enhanced s-cone syndrome

Table 1 cont.: Summary of genes responsible for human retinal dystrophies (Adapted from Bessant et al. 2001)

Gene	Locus	Protein/protein function	Inheritance	Associated dystrophies
Proteins of uncertain function				
CRB1	1q31-32.1	Crumbs	AR	RP
USH2A	1q41	Usherin	AR	Usher (Type 2a)
EFEMP1	2p16-p21	EGF containing fibrin like extracellular membrane protein	AD	Doyne ret dystrophy
PROML1	4p	Prominin	AR	RP
TULP1	6p21.3	Tubby like protein 1	AR	RP
RP1	8p11-q21		AD	RP
USH1C	11p15.1	Harmonin	AR	Usher (Type 1c)
VMD2	11q13	Bestrophin (RPE)	AD	Best
AIPL1	17p13.1	Arrylhydrocarbon interacting receptor protein	AR	Leber amaurosis
MKKS	20p12	Chaperonin	AR	Bardet-Beidl McKusick-Kaufman
XLRS1	Xp22	Retinoschisin	XL	Retinoschisis
RPGR(RP3)	Xp21	GTPase regulator	XL	RP
RP2	Xp11.3-11.2		XL	RP
NYX	Xp11.23	Nyctalopin	XL	XLCSNB
Miscellaneous				
PHYH	10p15.3-12.2	Phytanoyl CoA hydroxylase	AR	Refsum disease
OAT	10q26	Ornithine aminotransferase	AR	Gyrate atrophy
MYO7A	11q13.5	Myosin VIIa	AR	Usher (type 1b)
TIMP3	22q13-qtr	Tissue inhibitor of metalloproteinase 3	AD	Sorsby fundus dystrophy
NDP	Xp11.3	neuroectodermal protein	XL	Norrie, FEVR
CACNA1F	Xp11.23	alpha subunit of calcium channel	XL	XLCSNB
REP1	Xp21	Rab escort protein	XL	Choroideraemia

Chapter 2 Applied retinal anatomy and physiology

2.1 Functional anatomy of the retina

2.1.1 The cells and layers of the peripheral retina

The retina is a transparent membrane that varies in thickness from 0.1mm to over 0.5mm. It lies in close anatomical and functional apposition to the retinal pigment epithelium (RPE). The RPE is a single layer of cuboidal cells which play a central role in the maintenance of the transduction cascade through chromophore regeneration and participates in the renewal of photoreceptor protein and membrane components(Bok 1985). Six types of neurons may be identified in the retina: the photoreceptor cells, horizontal cells, bipolar cells, amacrine cells, interplexiform cells and ganglion cells. In the peripheral retina, these cells are organised into eight distinct layers (Figure 2a).

Figure 2a. The layers of the retina: (A) As seen in histological section, (B) Diagram of the arrangement of nerve cells. (Snell and Lemp 1989)

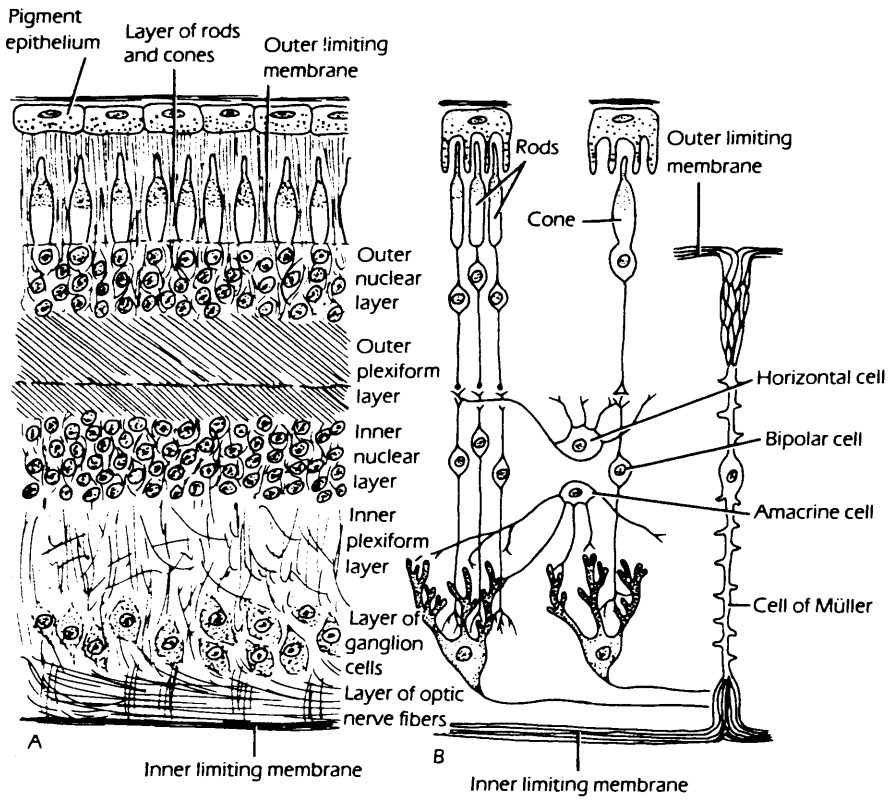

The retina has two types of **photoreceptor cells**, rods and cones (Figure 2b and c), characterized by different sensitivity to light: cones mediate vision in bright lighting conditions and give rise to colour vision, rods mediate vision in dim illumination. Rods and cones are highly specialized cells whose sensory portion, consisting of inner and outer segments, is situated between the retinal pigment epithelium and the external limiting membrane. The **outer limiting membrane** is a row of zonulae adherentes connecting the inner segment of the photoreceptors to the Muller cells and the Muller cells to each other. The Muller cell is of glial origin and spans nearly the full thickness of the retina. It has important roles in the structural development of the retina, the maintenance of potassium homeostasis and the degradation and regulation of synaptic transmitters in the retina. The photoreceptor outer segment is the site of phototransduction. It contains the stacked membranous discs derived from the photoreceptor cells' plasma membrane which contain the photopigments. The rod outer segment consists of a stack of flattened disc membranes (up to 2000 per rod) on which the light–capturing pigment molecules are embedded at high concentration. The entire disc stack is completely covered by a single layer of plasma membrane. Cone outer segments are usually shorter than rods, have a different shape and are not separated from the overlying covering of plasma membrane. Cone opsin is embedded in large, flat membrane surfaces that are not isolated discs but invaginations of the overlying plasma membrane. The **outer nuclear layer (ONL)** is occupied by the cell bodies of the photoreceptors.

The **outer plexiform layer (OPL)** contains the synapses between the photoreceptors and the bipolar and horizontal cells. Bipolar cells act as the major radially conducting element of the retina, transmitting signals either directly or indirectly from photoreceptors to ganglion cells. Bipolar cell axons course inwards into the inner plexiform layer to synapse with the dendrites of amacrine and ganglion cells. Horizontal cells have long processes which run laterally in the OPL and make contact with either rod or cone photoreceptors. Horizontal cells are the interneurons of the outer retina, creating an inhibitory feedback onto the photoreceptors and a feed-forward inhibition of bipolar cells (Masland 2001).

The **inner nuclear layer (INL)** contains the cell bodies of the bipolar cells, horizontal cells, amacrine cells, interplexiform cells and Muller cells. The **inner plexiform layer (IPL)** contains the synapses of the amacrine cells with the dendrites of bipolar cells, interplexiform cells and ganglion cells. Amacrine cells are the interneurons of the inner retina and make lateral contact by synapsing with each other. They provide feedback connections with bipolar cells and feed-forward connections with ganglion cells. Interplexiform cells have processes which project to both plexiform layers. This cell appears to carry information from the inner to outer retina.
Ganglion cells in the **ganglion cell layer** are retinal neurons, their axons form the optic nerve and terminate in the lateral geniculate nucleus and superior colliculus. The dendrites of the ganglion cells receive synaptic inputs from bipolar and amacrine cells. The **nerve fibre layer** contains the ganglion cell axons and some astrocytes. Muller cell foot processes form the **inner limiting membrane**.

2.2 Topography of the retina

Microscopy reveals regional differences in retinal organization. In the human retina, cones are the only type of photoreceptor in the central region of the fovea but outside this area rods begin to appear and sharply increase in number to reach a density of 100.000 rods/mm^2 at 1.2-1.7mm from the foveal center (Figure 2d) (Curcio, Sloan et al. 1990). The foveal region, on the optical axis of the globe, is 1.5mm in diameter. The centre of the fovea, the foveola, is 0.1mm in diameter and is free from cells except for the outer segments of cone photoreceptors. The parafoveal area is a region thickened by the heaped layers of ganglion cells and cells of the inner nuclear layer displaced from the fovea. The macula surrounds the fovea, is approximately 6mm in diameter, and is characterized by a ganglion cell layer which is more than one cell thick.

2.3 Retinal neurophysiology

Whilst most neural cells act on all-or-none (or digital) basis, retinal neurons act through graded slow potentials, which are continuously shaped by the stimulus intensity, colour and geometry. The result is an analog computation which is only converted to a digital message at the last stage of synaptic interaction. This analog

method of synaptic interaction and the depolarization of photoreceptors in darkness allows continuous communication to second order neurons, ensuring that most retinal neurons are continuously modulated by synaptic activity throughout the functional range of light and dark.

2.3.1 Rod phototransduction

All photoreceptors respond to light with hyperpolarization, the degree of which is dependent on the intensity and geometry of the light stimulus. The transduction process in rods has greater amplification than that in cones, making rods more sensitive to light.

Following exposure to light, an enzyme cascade occurs in the rod outer segments (Figure 2c). Absorption of light by rhodopsin leads to isomerization of its 11-*cis* retinal component to the all *trans* form, resulting in a conformational change. This permits the binding and activation of transducin. In the cytoplasm the active alpha sub-unit of transducin activates the enzyme cGMP phosphodiesterase (PDE), which then hydrolyses cGMP (Yamazaki, Hayashi et al. 1990). The resulting drop in intracellular cGMP concentration closes cGMP gated cation channels on the plasma membrane of the rod outer segment, leading to hyperpolarization of the rod cell plasma membrane (Yau and Nakatani 1985).

Several mechanisms are thought to turn the photoresponse off: rhodopsin kinase catalyses the phosphorylation of activated rhodopsin; arrestin, which preferentially binds to light-activated rhodopsin, may block further interaction with transducin; phosducin may bind to transducin preventing participation in multiple cycles of PDE activation (Shinohara, Donoso et al. 1988; Lee, Fowler et al. 1990). Additionally, a calcium-dependant feedback loop involving guanylate cyclase activating proteins (GCAP-1 and GCAP-2) may increase the activity of retina specific guanylate cyclase (RetGC-1 and RetGC-2), thereby restoring the cGMP concentration (Koch 1991). The transduction cascade may also be regulated by various calcium binding proteins: at low calcium concentrations, such as the environment found in light exposed rods, Recoverin may activate retina-specific guanylate cyclase, which would offset the light triggered drop in cGMP. At high calcium concentrations, such as those found in the dark, S-modulin may amplify the on-response by inhibiting rhodopsin phosphorylation and enhancing activation of PDE (Dizhoor, Ray et al. 1991).

Figure 2b: Structure of a rod and cone (from (Snell and Lemp 1989))

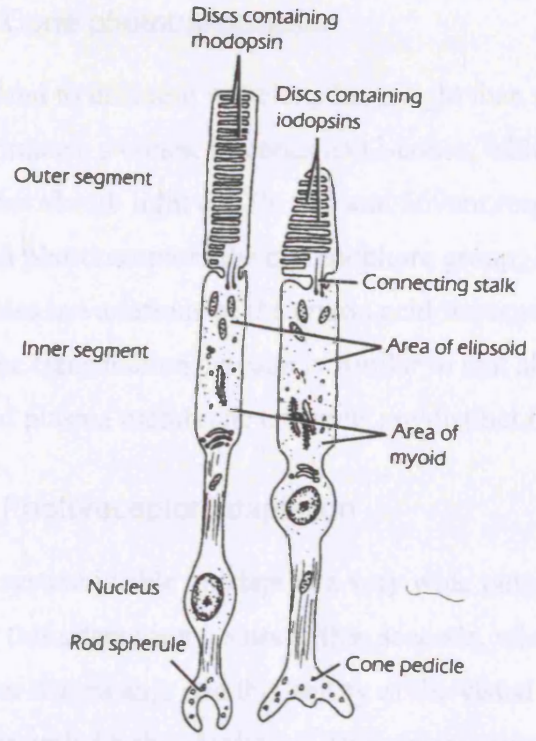

Figure 2c: Transduction cascade

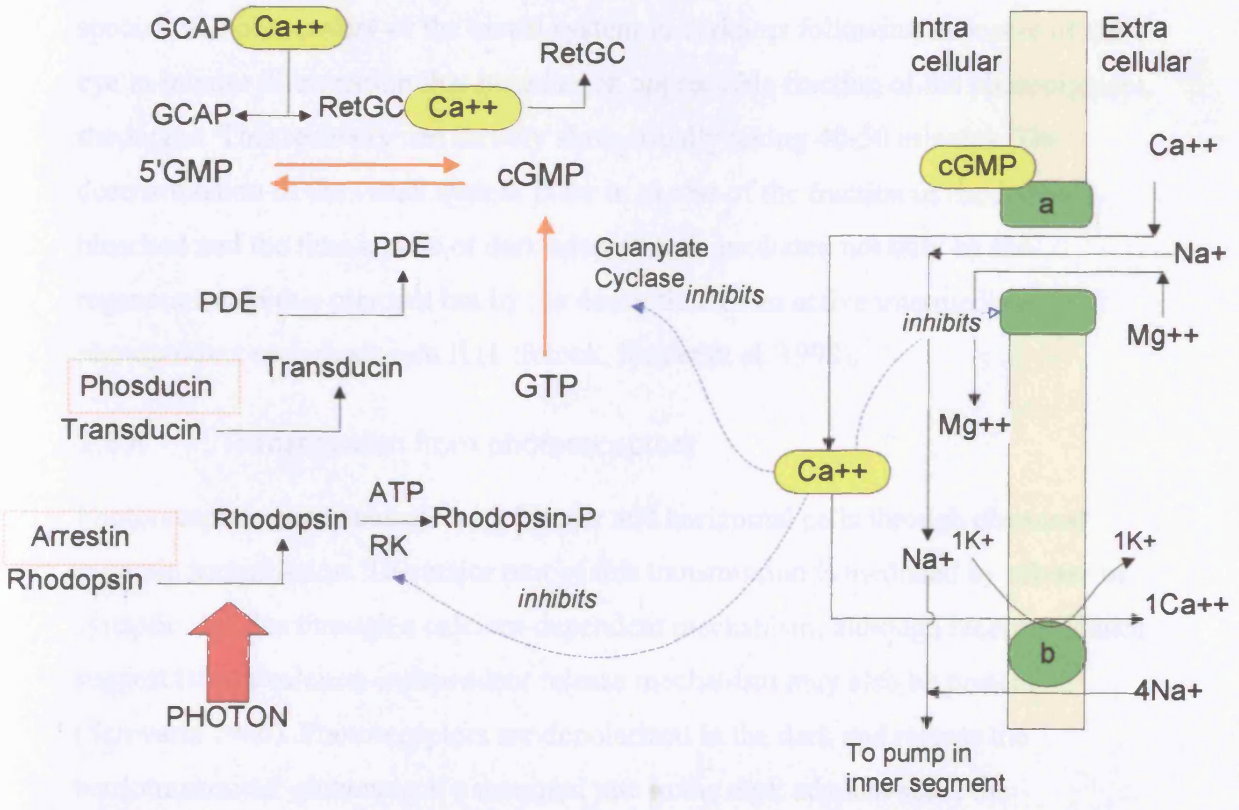

2.3.2 Cone phototransduction

Cones respond to different wavelengths of light than rods. There are three types of cones in primates: s-cones, m-cones and l-cones, which contain blue, green and red pigments that absorb light at 430, 530 and 569nm respectively (Brown and Wald 1964). In all photoreceptors the chromophore group, 11-*cis* retinal, is identical. The difference lies in variations of the amino acid sequence in the protein structure. Although the transduction cascade is similar to that already described for rods, the proteins and plasma membrane channels are distinct but not fully characterized.

2.3.3 Photoreceptor adaptation

The visual system is able to adapt to a very wide range of light intensity. Under many conditions, this adaptation occurs within seconds, whether the background intensity is increasing or decreasing, and this ability of the visual system to rapidly alter its sensitivity is called light adaptation. This process involves the reduction of cone sensitivity caused by depletion of cone photopigment at intense ambient light levels, and modulation of the transduction enzymes by intracellular calcium, the level of which is reduced by constant light exposure. The term dark adaptation refers to the special case of recovery of the visual system in darkness following exposure of the eye to intense illumination that bleaches an appreciable fraction of the photopigment, rhodopsin. This recovery can be very slow, usually taking 40-50 minutes. The desensitization of the visual system is far in excess of the fraction of rhodopsin bleached and the time course of dark adaptation is mediated not only by the regeneration of this pigment but by the decay time of an active intermediate photoproduct metarhodopsin II (Leibrock, Reuter et al. 1998).

2.3.4 Transmission from photoreceptors

Photoreceptors communicate with bipolar and horizontal cells through chemical synaptic transmission. The major part of this transmission is mediated by release of synaptic vesicles through a calcium-dependent mechanism, although recent evidence suggests that a calcium-independent release mechanism may also be present (Schwartz 1986). Photoreceptors are depolarized in the dark and release the neurotransmitter glutamate at a maximal rate in the dark adapted state, the

hyperpolarizing action of light causes a reduction in the rate of neurotransmitter release (Ayoub and D.R.Copenhagen 1991.

2.3.5 Retinal circuitry of the rod and cone pathways

The primary rod and cone pathways are separate. Cones synapse onto several different types of cone bipolar cell. Some of these are depolarizing bipolar cells, forming the cone ON pathway with a sign-inverting synapse. In addition cones synapse with hyperpolarizing (OFF) bipolar cells via a sign-preserving synapse in the cone OFF pathway.

Rods synapse with a single type of bipolar cell named the rod ON bipolar cell (Wassle and Boycott 1991). This, in turn, contacts the AII amacrine cell at a sign-preserving glutamate synapse (Kolb and Famligetti 1974). Signals from the AII amacrine cell then infiltrate the main cone circuitry by exciting ON cone bipolar cells and inhibiting OFF cone bipolar cells (Wassle, Grunert et al. 1995). Thereafter, ON bipolar cells excite ON ganglion cells and OFF bipolar cells excite OFF ganglion cells – this is known as the slow rod pathway. A second rod pathway (the rod-cone coupling pathway, or fast rod pathway) infiltrates the ON and OFF cone bipolar circuitry at the earliest stage, through gap junction contacts allowing synaptic transmission (Kolb and Famligetti 1974).

In the central retina about 10 rods converge onto a single rod bipolar cell, whereas in the peripheral retina about 30 rods converge on a rod bipolar cell - this increases the signal to noise ratio. In comparison one cone, acting via a bipolar cell, may lead to the stimulation of one ganglion cell, preserving high acuity (Daw, Jensen et al. 1990).

Rod-cone interactions occur via the horizontal cells of the inner retina. Horizontal cells have both rod and cone input and feed back in to the cone photoreceptors causing an inhibitory effect on cones in a dark adapted state. The rods, in effect, impose a low-pass filter on the cones (Arden and Hogg 1985).

2.4 Visual function of the rod and cone systems

2.4.1 The effect of retinal position on visual function

Visual acuity rapidly diminishes as a stimulus is moved away from the fovea due to the fall in density of the cone photoreceptors and decrease in relative number of ganglion cells available to carry information away from the retina. The density of rod and cone photoreceptors varies across the retina and this is reflected in changes in visual function elicited with testing. The knowledge of photoreceptor distribution is important since it allows the cone or rod system to be tested in isolation, solely cones will respond to a small stimulus presented to the foveal area. Conversely, tests for both cone and rod sensitivity are optimally performed if the stimulus image stimulates the retina between 10 and 18 degrees from the fovea - an area containing great numbers of both receptor types (Figure 2d) (Siegel and Carr 1979).

2.4.2 The effect of light intensity on visual function

The rod photoreceptors mediate vision at low illumination levels and are responsible for the human retina's exquisite sensitivity to light. Rod photoreceptors operate over a 10^8 range of illumination from near darkness to daylight levels. Cone photoreceptors mediate vision at daylight levels and are responsible for good visual acuity and colour vision. The cones function over a 10^{11} range of illumination. Rod and cone sensitivity to illumination therefore overlap (Figure 2e) (Hood and Finkelstein 1986). The term "rod system" or "cone system" may be used to describe what is really a complex sequence of neural processing after absorption of light rod and cone photoreceptors. The term "scotopic" illumination level is used to describe light levels where only the rod system is able to function, "photopic" level is used when only the cone system is able to function and "mesopic" level is used for the range of illumination which stimulates both the rod and cone system. The luminance of a stimulus can be varied to isolate rod responses from cone responses: dim stimuli presented to a dark adapted eye will cause a purely rod response, whereas very bright stimuli presented to a light adapted eye will elicit a purely cone response.

2.4.3 Spectral sensitivity

The probability of absorption of light energy by the visual photopigments in the outer segments of the photoreceptors is dependent on the wavelength of the incident light. When sensitivity to light is measured in the dark adapted peripheral retina, a broad spectrum with greatest sensitivity at 507nm (blue-green) is observed. The spectral sensitivity curve represents the relative luminosities of the different wavelengths, so if a spectrum was produced in which each wavelength contained the same energy, the blue-green wavelength would appear brightest to the dark adapted eye. In photopic conditions, colour vision is mediated by three types of cone photoreceptors of different but overlapping spectral sensitivities. These are identified by their relative spectral position and are called the long, middle and short wavelength-sensitive cones. The combined activity of the long and middle wavelength-sensitive cones gives a broad spectrum of photopic spectral sensitivity peaking at 555nm (green-yellow). Scotopic (rod) and photopic (cone) spectral sensitivity curves based on the V'_λ and V_λ curves as defined by the CIE (Commission Internationale de l'Eclairage) are shown in Figure 2f. Rod photoreceptors are so insensitive to the extreme red end of the spectrum that it is possible to increase the luminance levels at this wavelength to allow photopic function without serious loss of dark adaptation. This principle is used to advantage in situations where optimum visual acuity is required while maintaining the sensitivity of the dark adapted state, for example, photographic developing.

Figure 2d: Density distribution of rods and cones in the horizontal meridian of the retina. The grey area represents the blind spot projection on the nasal side. The yellow area shows the area in which rod density is highest and cone density is low but constant – an ideal location for stimulation in the assessment of both rod and peripheral cone function. From (Osterberg 1935).

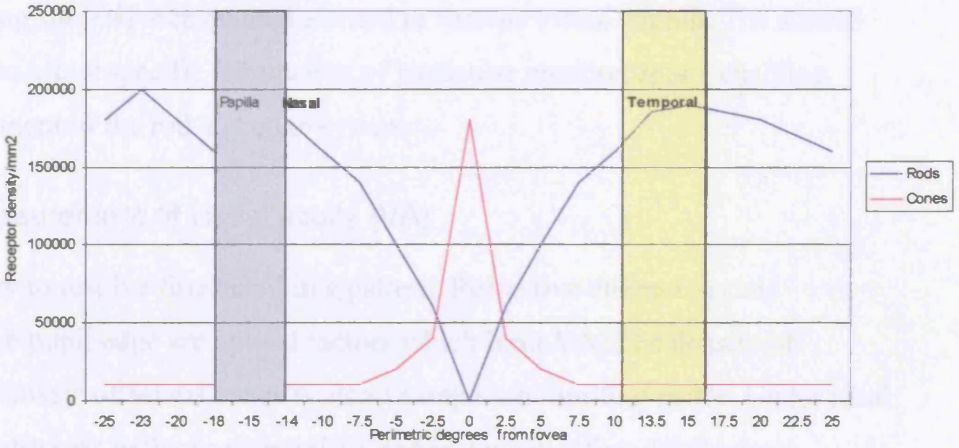

Figure 2e: The functional range of the visual system. The levels of luminance on the top row extends from the minimum detectable to levels at which damage to the retina is possible. The bottom row illustrates the operating range in terms of visual function. Modified from (Bott, Kaufman et al 1986)

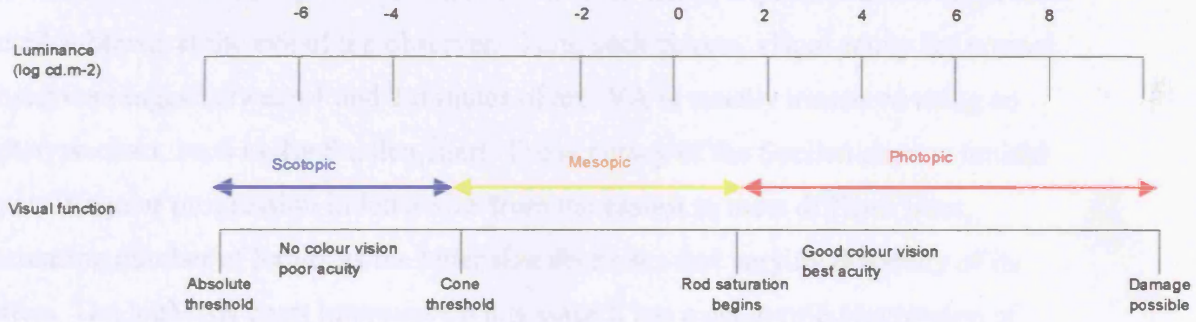

Figure 2f: Rod and cone system spectral sensitivity curves.
The scotopic (rod) curve and photopic (cone) curve relative sensitivities are shown. The rod system is shown to be less sensitive than cones at the longest wavelengths of the visible spectrum.

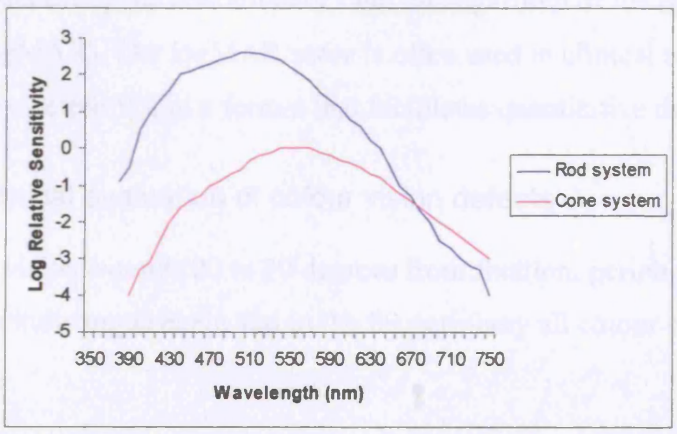

2.5 Introduction to clinical psychophysical testing

Clinical psychophysical measurements are non-invasive assessments of visual function utilizing subjective responses elicited to various visual stimuli. The stimuli may be varied to allow specific stimulation of particular photoreceptors enabling separate assessment of the rod and cone system.

2.5.1 Measurement of visual acuity (VA)

VA is the ability to resolve fine detail in a pattern. Refractive aberrations and diffraction at the pupil edge are optical factors which limit VA. The density of packing in the mosaic of foveal cones is also an important limiting factor. Under ideal conditions, an observer with excellent vision can just resolve fine detail whose angular subtense approaches that of a single cone (Maturana, Lettvin et al. 1960). VA is usually tested clinically by reducing the size of a high-contrast test pattern until the smallest detail in the pattern can just be resolved and is expressed as the angle that detail subtends at the eye of the observer. Using such targets, visual acuity for normal observers ranges between 1 and 2 minutes of arc. VA is usually measured using an optotype chart, such as the Snellen chart. The accuracy of the Snellen chart is limited by its irregular progression in letter size from the easiest to most difficult lines, increasing number of letters as the letter size decreases and varying difficulty of its letters. The logMAR chart improves on this since it has a geometric progression of letter height from line to line, decreasing by 0.1 log units per line and the letters used are of equal difficulty (Ferris, Kassoff et al. 1982). VA may be notated by several different means: the Snellen fraction, the decimal acuity (division of the numerator of the Snellen fraction by the denominator) and the logarithm of the minimal angle of resolution (logMAR). The logMAR score is often used in clinical research since it provides reproducible VA in a format that facilitates quantitative data analysis.

2.5.2 Clinical evaluation of colour vision defects

Trichromatic vision extends 20 to 30 degrees from fixation, peripheral to this red and green become indistinguishable and in the far periphery all colour sense is lost. The

very centre of the fovea (1/8th degree) is blue blind due to the absence of short wavelength sensitive cones.

Defects in colour vision may be identified using a number of different clinical tests. *Pseudoisochromatic plates* are commonly used for screening colour vision and successfully detect 90-95% of congenital abnormalities (Pokorny and Smith 1994). The Ishihara series contains 16 testing plates and one control plate, the incorrect reading of two or more plates can identify protanopic and deuteranopic defects but not tritanopic defects (Figure 2g). The Hardy-Rand-Rittler (HRR) test plates contain symbols in colours close to the neutral points of protanopic, deuteranopic and tritanopic individuals. Colour symbols of low saturation are used as screening plates, and three higher saturations are used for the diagnostic plates. The HRR plates identify and differentiate between protanopia, deuteranopia and tritanopia. The Cambridge Colour Test is a computerised test, previously described by Regan (Regan, Reffin et al. 1994). This test uses luminance noise and masking contours to ensure that that the subject's responses depend solely on chromatic signals. The stimuli, generated by a computer graphics system, consist of spatially discrete patches of varying size and luminance displayed on a black background. The field of the stimulus is formed by a majority of single chromaticity patches and the C shaped target is formed by a subset of patches of contrasting chromaticity to the field (Figure 2h). The orientation and chromaticity of the target is systematically varied in successive presentations. The average luminance of the target is always the same as that of the field. The array is viewed binocularly from a distance of 2.4m in dark surroundings and the subjects presses a button on a console corresponding to the orientation of the target C. Chromatic sensitivity may then be measured along different axes of colour space, protan, deutan and tritan confusion lines calculated and compared to control values.

Chromaticity discrimination tests usually rely on the subject's ability to arrange colours. The Farnsworth D15 and Farnsworth-Munsell 100 Hue test utilize coloured paper strips which differ in hue but have approximately the same saturation and brightness for normal subjects. The City University and the Mollon-Reffin minimalist test (Figure 2g(ii)) use the same hue series. In the latter test, the subject is required to pick out a coloured chip randomly placed in a field of grey chips of varying brightness on the basis of hue only. Score patterns allow the identification,

differentiation and grading of protanopic, deuteranopic and tritanopic defects (Mollon, Astell et al. 1991).

2.5.3 Perimetry

The normal field of vision extends more than 90 degrees temporally, 60 degrees nasally and 70 degrees superiorly and inferiorly. Sensitivity is greatest at the fovea and decreases towards the periphery. An isopter is a line connecting the points in the peripheral visual field where a target of a specific size and intensity would be identified. The shape of an isopter may become characteristically distorted when a disorder affects the visual pathways. Generalized reduction in sensitivity may result from ocular media opacity, constricted pupils or inadequate refraction.

Perimetry is a measurement of the mean minimum detectable light stimulus in selected points in the visual field. Perimeters measure the minimum contrast between background illumination and stimulus, the threshold being the minimum measurable difference in luminance that the patient can detect. Visual fields may be measured by kinetic perimetry (e.g. the Goldmann perimeter) or static automated perimetry (e.g. the Humphrey perimeter). Whilst kinetic perimetry is useful for detecting relatively large field defects rapidly, it is less useful for detecting small scotomas and is less reproducible than static perimetry.

Automated perimetry may be performed with a variety of background and stimulus light intensities and wavelengths in order to assess the threshold sensitivity of specific photoreceptors. Standard automated photopic perimetry (using a white light stimulus) may be mediated by foveal cones and peripheral rods. Rod or cone mediated function may be isolated and measured using short and long wavelength stimuli in scotopic conditions. In dark adapted normal eyes a blue stimulus will be sensed by the rod system and a red stimulus by the cone system (Fitzke 1995). However, the relative sensitivity of the rod and cone system may be altered in retinal disorders, making interpretation of scotopic perimetry more difficult: cone photoreceptors may mediate threshold to a blue stimulus in dark adapted conditions in diseases such as retinitis pigmentosa where there is extensive loss of rod function.

Figure 2g(i): Ishihara and City University colour vision tests

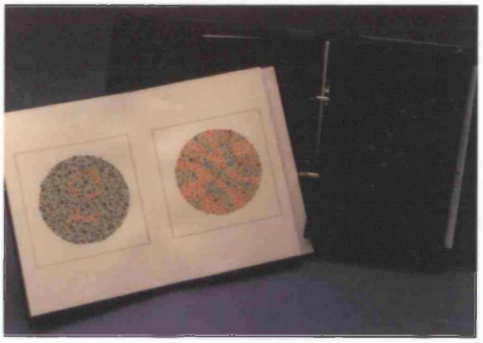

Figure 2g(ii): Hardy-Rand-Rittler and Mollon-Reffin minimalist tests

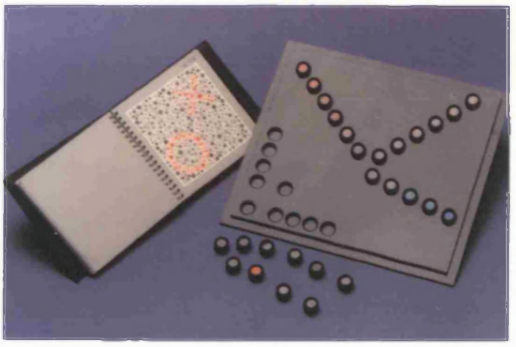

Figure 2h: Stimuli used in the Cambridge Colour Test. The top, middle and lower panels show protan, deutan and tritan test stimuli respectively. The left-hand stimulus of each pair is saturated, the right-hand stimulus represents a more difficult discrimination. (from Regan *et al.* 1993)

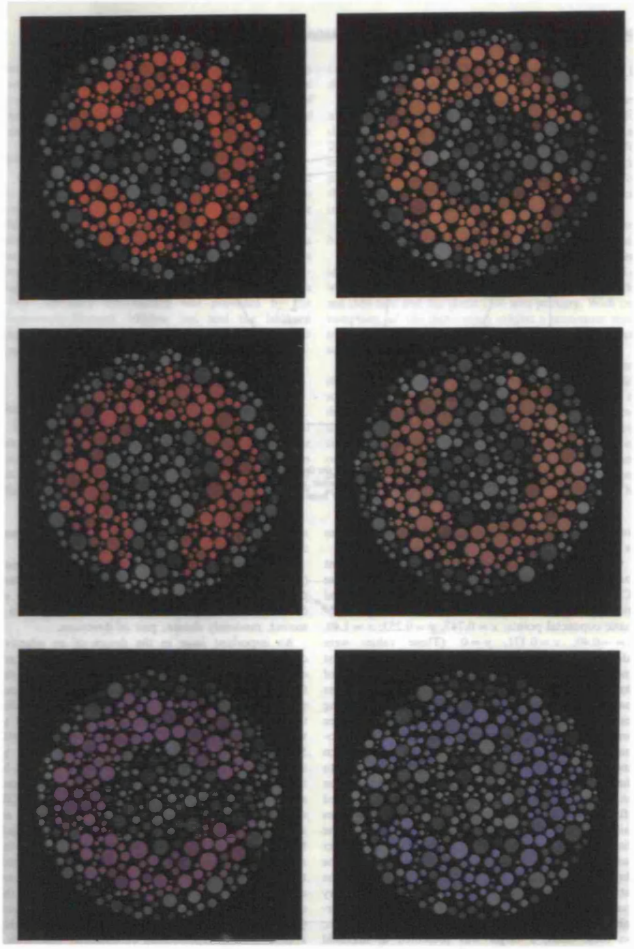

2.5.4 Dark adaptometry

The normal dark adaptation curve following an initial bleaching light is biphasic, reflecting the dark adaptation of the cones and the rods. In the first phase, typically lasting 5-10 minutes, the threshold is determined by the cones as they recover from the pre-adapting bleach. The time course of the process parallels the regeneration of the cone photopigment. Later, the rods recover sufficiently for their thresholds to be lower than those of the cones and they mediate threshold, giving rise to the rod phase. A weak pre-adapting light results in a faster recovery of sensitivity and monophasic curve reflecting the superior sensitivity of the rods. A purely cone response (a monophasic curve with rapid recovery to pre-bleach thresholds) will be seen when dark adaptation is tested at the fovea, therefore dark adaptometry is usually performed between 18 and 20 degrees in the retinal periphery, where rod density is highest. The size, intensity, duration and colour of the stimulus are all important. Cones have almost equal sensitivity to red light as rods so the use of a red stimulus results in a dark adaptation curve with a prominent cone phase and little or no rod phase. Since rods are more sensitive to shorter wavelengths than cones, they mediate threshold earlier in the dark adaptation process when a blue stimulus is used, the resultant curve has a prominent rod phase with an early rod-cone break.

Retinal disease may elevate the absolute threshold of sensitivity and alter the kinetics of the dark adaptation curve. Where there is extensive loss of rod function, cones may mediate threshold even under scotopic conditions so that the dark adaptation curve is monophasic with an elevated final threshold. Conditions in which the regeneration of rhodopsin is abnormally slow, for example fundus albipunctatus, have a prolonged rod phase but normal final thresholds after prolonged dark adaptation.

2.6 Introduction to the electroretinogram (ERG)

2.6.1 Components of the ERG

The electroretinogram (ERG) is a record of the combined electrical response generated by neural and non-neuronal cells within the retina as a response to a light stimulus. The ERG provides an objective measurement of total response of the retina and therefore may not detect localized retinal disease (Figure2i). The **a-wave** is the

initial cornea-negative deflection of the ERG and is known to reflect the hyperpolarization response of the photoreceptors to light. The subsequent **b-wave** is a cornea-positive deflection, which represents a summation of responses but mainly reflects the extracellular current caused by ON bipolar cell depolarization (Newman and Odette 1984). The **c-wave** is a slow cornea-positive deflection comprising a summation of three different potentials, it is generally not used clinically since its long latency makes it subject to artifacts from eye movement. The **d-wave** (OFF response) is a cornea-positive deflection occurring following the abrupt cessation of retinal illumination. It is produced by the OFF (hyperpolarizing) retinal pathway and, since only the cone system utilizes this pathway, is only present in photopic ERG conditions (Daw, Jensen et al. 1990). **Oscillatory potentials** are a series of high frequency, low amplitude wavelets superimposed on the ascending limb of the ERG b-wave after stimulation by an intense light flash. Although the cellular origin of these potentials is uncertain, they are thought to be produced by the cone driven cells of the inner retina, which are supplied by the retinal circulation, such as the amacrine or interplexiform cells (Heynen, Wachtmeister et al. 1985). The **photopic negative wave** (PhNR) has recently been described and forms a negative potential after the b-wave of the photopic ERG (Colotto, Falsini et al. 2000; Viswanathan, Frishman et al. 2001). This response is thought to derive from the inner retina, either directly from the retinal ganglion cells or through mediation by glial cells. The PhNR can be measured in photopic conditions using the standard bright flash or the longer flash stimulus required for measurement of the ON-OFF response.

2.6.2 The normal human ERG

By varying the background lighting conditions and intensity of light stimulus, the ERG can be used to identify specific retinal responses. The response of a dark adapted retina to a dim white or blue flash (scotopic conditions) will yield a purely rod mediated response. The a-wave in these conditions gives information about rod photoreceptor function while the characteristics of the scotopic threshold response (STR), b-wave and oscillatory potentials give information about the rod pathway in the inner retina. Light adaptation and stimulation with a bright or fast flickering stimulus (photopic conditions) will isolate a cone mediated response. As the stimulus intensity and background illumination increase to favor a cone mediated response, the ERG waveform increases in amplitude and decreases in latency. The cone pathway

through the inner retina can be tested by the characteristics of the b-wave, oscillatory potentials, 30Hz flicker response, ON-OFF response and photopic negative response in light adapted conditions.

2.6.3 Factors affecting the ERG

Various factors such as stimulus duration and form of light stimulation affect the amplitude and latency of the ERG. For this reason a standard for clinical electroretinography has been drawn up by International Society for the Clinical Electrophysiology of Vision (ISCEV) (Marmor and Zrenner 1998). An ocular media opacity, such as a cataract, reduces the retinal illumination, thereby reducing the ERG amplitude and prolonging the implicit time. The high axial length associated with myopia of more than –6.0 dioptre spheres (DS) is associated with reduction in ERG amplitude.

Figure 2i: The normal electroretinogram

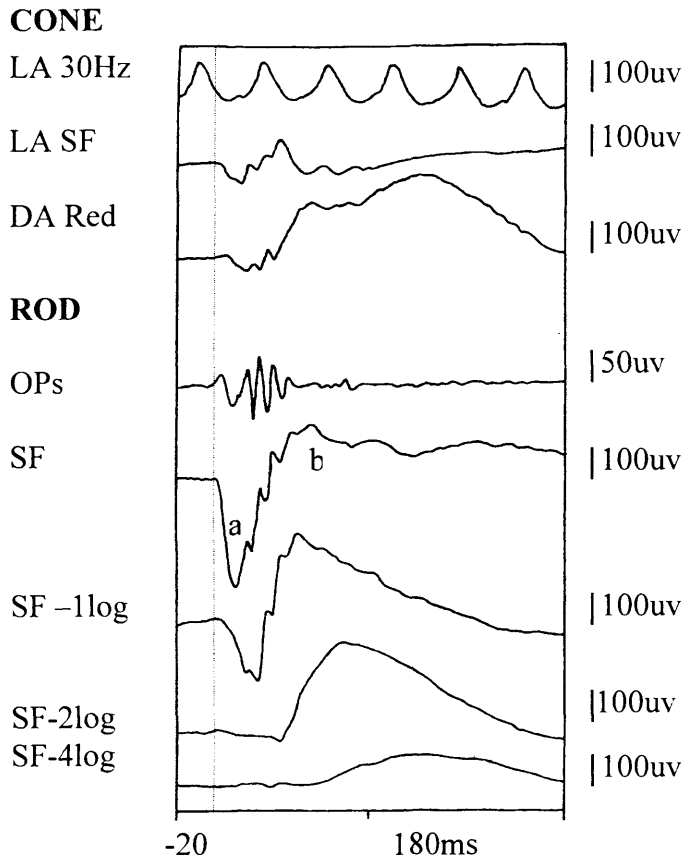

Key

Cone: Cone mediated responses
Rod: Rod mediated responses
LA: Light adapted. DA: Dark adapted
SF: Standard Flash stimulus
OPs: Oscillatory Potentials

Chapter 3 Review of the previous clinical investigation of CSNB

3.1 Clinical and psychophysical manifestations of CSNB

Many of the studies mentioned in this chapter are based on a genetically heterogeneous population of XLCSNB and ARCSNB subjects. This limits the comparisons and conclusions that can be drawn from them.

3.1.1 Symptoms

The cardinal symptom of CSNB is a non-progressive night blindness but a variable reduction in daytime vision may also occur. Since an affected individual has no knowledge of normal night time vision, they may not be symptomatic with their night blindness, particularly if they live in a brightly lit city (Price, Judisch et al. 1988). Children are especially unlikely to complain of night blindness, although their parents may notice that they cling on to them in poorly lit situations. Children are most commonly diagnosed when an ERG is performed to find the cause of their reduced visual acuity and nystagmus. There may be no apparent family history since older members may never have had ERG testing. Before ERG testing was routinely available, these individuals may have been misdiagnosed as having congenital motor nystagmus or ocular albinism.

3.1.2 Visual acuity

Daytime visual acuity is usually subnormal in subjects with XLCSNB, the severity of this visual loss often showing inter and intra-familial variability (Pearce, Reedyk et al. 1990). Previous studies of XLCSNB have reported the visual acuity to range from 6/6 and counting fingers vision (Merin, Rowe et al. 1970; Hill, Arbel et al. 1974). More recent studies have indicated that there is not a significant difference between recorded decimal visual acuities in the "complete" form (0.42 and 0.38) and "incomplete" form (0.41 and 0.30) of AR and XLCSNB (Miyake, Yagasaki et al. 1986; Ruether, Apfelstedt-Sylla et al. 1993).

3.1.3 Refractive state

Although the refractive error in XLCSNB is usually high myopia, it may range from mild hypermetropia (+4.0DS) to high myopia (up to –20.0DS) (Carroll and Haig 1952; Haim 1986; Khouri, Mets et al. 1988; Pearce, Reedyk et al. 1990; Tremblay, Laroche et al. 1995). Miyake reported a significant difference between the refractive error in the "complete" form (-7.0+/-8.1DS) and "incomplete" form (-0.8+/-10.8DS) of AR and XLCSNB but a study by Ruether found no significant difference (Miyake, Yagasaki et al. 1986; Ruether, Apfelstedt-Sylla et al. 1993). Miyake later concurred that hypermetropia, emmetropia and, myopia may coexist within the same pedigree (Miyake 1989). Anisometropia and an astigmatic refractive error may be present but are usually mild (Merin, Rowe et al. 1970; Khouri, Mets et al. 1988; Pearce, Reedyk et al. 1990).

3.1.4 Extra-ocular movements

Strabismus is a frequent finding in individuals with XLCSNB, occurring in 17-100% but there appears to be no predominance between exotropia and esotropia (Hill, Arbel et al. 1974; Miyake, Yagasaki et al. 1986; Ruether, Apfelstedt-Sylla et al. 1993). Exotropias are reportedly more common in "incomplete" AR and XLCSNB and esotropias more so in the "complete" form (Ruether, Apfelstedt-Sylla et al. 1993). Nystagmus commonly accompanies XLCSNB but is not a consistent feature (Haim 1986; Miyake, Yagasaki et al. 1986; Ruether, Apfelstedt-Sylla et al. 1993). In most reports the nystagmus is horizontal in direction and either fine or coarse but fine rotatory nystagmus has also been described (Merin, Rowe et al. 1970; Krill and Martin 1971).

3.1.5 Colour vision

Many studies have reported subjects with XLCSNB as having normal colour vision but mild tritan and protan colour vision defects have been reported in both "complete" and "incomplete" forms of AR and XLCSNB (Hittner, Borda et al. 1981; Wolf and Weber 1984; Miyake, Yagasaki et al. 1986).

3.1.6 Spectral sensitivity

Studies of spectral sensitivity show a reduction in threshold sensitivity to short and long wavelength stimuli. The shape of the spectral sensitivity curve fits the shape of the CIE

scotopic sensitivity curve for wavelengths shorter than 600nm and the CIE photopic sensitivity curve at longer wavelengths, indicating that long wavelengths are mediated by a desensitised cone system and shorter wavelengths are mediated by a desensitised rod system (Sharp et al. 1990).

3.1.7 Visual field examination

Photopic perimetry is usually normal. Specific visual field abnormalities relating to tilting of the optic disc or level of ametropia may be present (Hittner, Borda et al. 1981; Ruether, Apfelstedt-Sylla et al. 1993). A reduction of sensitivity with eccentricity from the fovea has also been identified, a feature associated with high myopia (Terasaki, Miyake et al. 1999). Blue-on-yellow perimetry has identified normal foveal blue cone sensitivity but a significant reduction in sensitivity to the stimulus in the peripheral retina in subjects with the "complete" form of AR and XLCSNB (Terasaki, Miyake et al. 1999).

3.1.8 Ocular examination

Fundoscopy is generally normal in XLCSNB. However, myopic fundus changes may be present and many affected subjects have tilted, pale or dysplastic optic nerve heads. Miyake noted a gold metallic reflex in the mid-peripheral retina in 16 out of 20 subjects with "incomplete" AR and XLCSNB studied (Miyake, Yagasaki et al. 1986). Carr described cases with a granularity at the macula, which blunted the normal foveal reflex (Carr, Ripps et al. 1966). Retinal arteriolar narrowing and peripheral pigment clumping are not seen in this condition. Paradoxical pupillary reflex (pupillary constriction in the dark) has been described in a number of young children with CSNB of unspecified inheritance (Barricks, Flynn et al. 1977; Khouri, Mets et al. 1988). This phenomenon has not been reported in older subjects.

3.1.9 Systemic abnormalities

Systemic abnormalities associated with the recessive forms of CSNB have not been reported.

3.1.10 Dark adaptometry

Psychophysical studies have identified two distinct types of dark adaptation curves in subjects with AR and XLCSNB (Auerbach, Godel et al. 1969; Miyake, Yagasaki et al. 1986). Subjects with the "incomplete" form of recessive CSNB have been shown to have a bipartite curve with elevated final threshold, illustrating the presence of residual rod and cone function. Miyake found subjects with the "complete" form of AR and XLCSNB to have a monophasic curve with an elevated residual cone threshold indicating that rod function is absent and cone sensitivity is reduced (Miyake, Yagasaki et al. 1986; Miyake, Yagasaki et al. 1987). Another group has shown bipartite curves in both AR and XLCSNB but a delayed rod-cone break in the latter (Sharp, Arden et al. 1990).

3.2 Photochemistry in CSNB

Rhodopsin density and its regeneration kinetics have been consistently normal in XLCSNB (Carr 1974; Sharp, Arden et al. 1990). Vitreous fluorophotometry has confirmed that the blood-retinal barrier is intact in AR and XLCSNB (Miyake, Gto et al. 1983).

3.3 The electrophysiology of CSNB

3.3.1 Introduction

The ERG plays an important diagnostic role in CSNB. As might be predicted, the amplitude of the scotopic response is reduced in all forms, however the photopic response may also be abnormal. The two main ERG patterns first described in CSNB were the Schubert-Bornschein (Schubert and Bornschein 1952) and the Rigg's (Riggs 1954) types. More recently, differences have been detected in the Schubert-Bornschein form of CSNB, resulting in its sub-classification into "complete" and "incomplete" types (Table 3a) (Miyake, Yagasaki et al. 1986).

3.3.2 The Rigg's type ERG

The Rigg's type ERG is found in ADCSNB and is characterized by a subnormal scotopic b-wave amplitude but, since the b-wave remains larger in amplitude than the a-

wave, the b-wave to a-wave ratio is greater than one (Figure 3a). The scotopic ERG response also has the temporal characteristics and waveform of the photopic response. The a-wave amplitude has been reported as normal (Riggs 1954;Auerbach et al. 1969) but a more recently, using a brighter flash stimulus, a-wave responses in the dark adapted retina have been reported as subnormal (Sharp, Arden et al. 1990). The Rigg's pattern ERG is most commonly associated ADCSNB (as demonstrated by the Nougaret family) (Carroll and Haig 1952; Francois, Verriest et al. 1956; Sharp, Arden et al. 1990) but has been reported in recessive pedigrees (Auerbach, Godel et al. 1969).
The subnormal and shorter latency waveform seen in the ERG under scotopic conditions is thought to arise as a response from a desensitized retina (Sharp, Arden et al. 1990). The relative bipolar cell: photoreceptor sensitivity may be measured using the b-wave to a-wave ratio. This is normal in Rigg's type CSNB indicating that transmission at the photoreceptor cell / bipolar cell synapse is unaffected (Carr and Siegel 1964). Reduction in the photoreceptor dark current generates the a-wave and this change affects the activity of the post-synaptic neurons, the bipolar cells, resulting in the b-wave. Since both a- and b-waves appear subnormal in this form of CSNB it has been predicted that the fault might lie in the transduction cascade (Sharp, Arden et al. 1990). This theory has since been confirmed by the identification of mutations in genes encoding rod photoreceptor transduction cascade enzymes in affected autosomal dominant pedigrees: α-subunit of cGMP phosphodiesterase (Gal, Orth et al. 1994), α-subunit of transducin (Dryja, Hahn et al. 1996) and rhodopsin (See Chapter 4) (Dryja, Berson et al. 1993; Sieving, Richards et al. 1995; al- Jandal, Farrar et al. 1999).

3.3.3 The Schubert-Bornschein type ERG

The Schubert-Bornschein ERG is characterised by a "negative wave" response occurring to bright light stimulation of the dark adapted retina. Characteristically the a-wave in this form of CSNB is normal both in latency and amplitude but the b-wave is subnormal, resulting in a b-wave to a-wave ratio less than one (Figure 3a)(Schubert and Bornschein 1952). This pattern of ERG has been identified in all hereditary forms of CSNB (Auerbach, Godel et al. 1969; Miyake, Yagasaki et al. 1986; Noble, Carr et al. 1990; Miyake and Kanai 1992). The normal a-wave amplitude reported by many authors in both scotopic and photopic conditions has led to the conclusion that photoreceptor function is normal in CSNB, however, very recent studies have indicated

that there may also be subtle rod photoreceptor dysfunction (Hansen et al. 2001;Langrova et al. 1999). The subnormal b-wave amplitude, leading to a reduced b-wave to a-wave ratio, has indicated that a fault in neurotransmission between the photoreceptor and second order neurons may be the cause (Carr and Siegel 1964). This theory is supported by recent genetic analysis of families with XLCSNB: gene mutations resulting in abnormal glutamate neurotransmitter release from photoreceptor presynaptic terminals have been identified in affected subjects (See Chapter 4) (Bech-Hansen, Naylor et al. 1998; Strom, Nyakatura et al. 1998).

In 1986, Miyake demonstrated that other ERG characteristics could be used to further sub-classify subjects with the Schubert-Bornschein ERG (Table 3a). On the basis of electrophysiological and psychophysical examination two distinct sub-types could be identified(Miyake, Yagasaki et al. 1986). "Complete" AR and XLCSNB was characterized by the absence of a rod mediated response but normal photopic responses. "Incomplete" CSNB was distinguished from the complete form by the presence of a detectable but subnormal scotopic response and, additionally, by a subnormal photopic response. This group also found that the b-wave to a-wave ratio was significantly lower in the "complete" pattern of recessive CSNB than in the "incomplete" form. Miyake demonstrated that subjects from each pedigree could consistently be assigned into either the complete or incomplete sub-groups, with no pedigree showing both types, and postulated that the sub-groups represented different clinical entities. This sub-classification has become accepted despite the description of other pedigrees whose ERG characteristics do not allow their allocation into either "complete" or "incomplete" categories (Khouri, Mets et al. 1988; Pearce, Reedyk et al. 1990; Aldred, Dry et al. 1992).

Table 3a: Classification of CSNB by ERG

Schubert-Bornschein ERG		**Riggs ERG**
Scotopic a-wave: normal		Scotopic a-wave: normal or subnormal
Scotopic b-wave: subnormal or absent		Scotopic b-wave: subnormal
b/a-wave ratio < 1		b/a-wave ratio > 1
Oscillatory potentials: absent / subnormal		
Complete pattern	**Incomplete pattern**	
Scotopic b-wave: absent	Scotopic b-wave: subnormal	
Photopic b-wave: normal	Photopic b-wave: subnormal	
30Hz flicker: normal	30Hz flicker: subnormal	

Figure 3a: Comparison of normal, Schubert-Bornschein and Rigg's and ERG waveforms

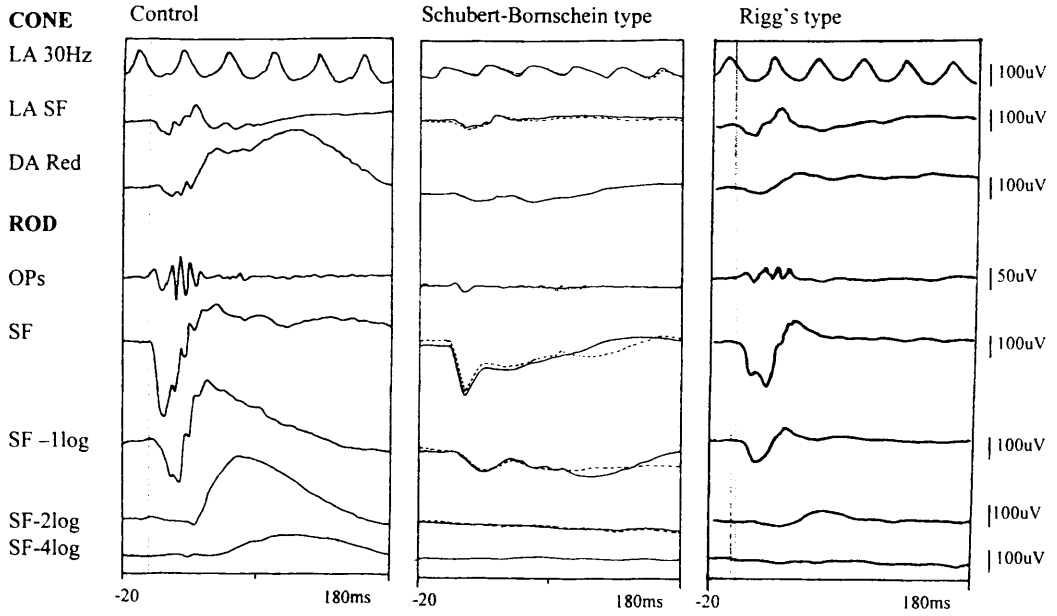

Key
Cone: Cone mediated responses
Rod: Rod mediated responses
LA: Light adapted, DA: Dark adapted
SF: Standard Flash stimulus
Ops: Oscillatory Potentials

3.3.4 The scotopic threshold response

The scotopic threshold response (STR) is a cornea-negative response measured near the psychophysical absolute threshold of vision in the dark adapted eye. At higher intensities this response is masked by the b-wave. Retinal depth recording in the cat eye has shown that the STR originates in the proximal retina at the junction of the inner plexiform and ganglion cell layers. It is thought to reflect the Muller cell response to extracellular potassium ions released by these neurons (Sieving, Frishman et al. 1986). Miyake tested the STR of six subjects with ARCSNB or XLCSNB, two were determined to have the "complete" form and the other four the "incomplete" form on ERG testing. The STR was absent in the subjects with "complete" CSNB. An STR of normal amplitude but delayed latency could be identified in subjects with the "incomplete" form but present, albeit at an elevated stimulus intensity threshold than controls. The authors suggest that, because the STR reflects proximal function in the rod visual pathway, there is a disturbance in the transmission of the rod signal to the rod bipolar cells in "complete" CSNB and that a different mechanism is responsible for the "incomplete" form (Sieving and Nino 1988; Miyake, Horiguchi et al. 1994).

3.3.5 Oscillatory potentials (OPs)

OPs may be detected in the ERG waveform as a response of the dark or light adapted eye to a bright, Standard Flash stimulus. OPs recorded in the dark adapted eye have been reported as subnormal or absent in the "complete" CSNB group but of normal amplitude in the "incomplete" form, conversely, OPs in the light adapted eye have been reported as absent in the "incomplete" form with only one peak identifiable in the "complete" form.(Lachapelle, Little et al. 1983; Miyake, Yagasaki et al. 1986; Tremblay, Laroche et al. 1995) This suggests that in the "incomplete" form the cone system does not respond optimally under the normal operating range (photopic conditions) but rather has its best responses under mesopic or scotopic conditions possibly indicating the disruption of normal rod/cone interaction.(Lachapelle, Little et al. 1983; Tremblay, Laroche et al. 1995)

3.3.6 30Hz flicker response

The amplitude of the 30Hz flicker response has been identified as being subnormal and double peaked in the "incomplete" form of recessive CSNB but of normal amplitude in

the "complete" form.(Miyake et al. 1986 Miyake described an exaggerated increase in response amplitude during light adaptation but this has not been confirmed by other studies.(Miyake, Horiguchi et al. 1987; Tremblay, Laroche et al. 1995) Although the 30Hz flicker response has been demonstrated as being of normal amplitude in "complete" AR and XLCSNB, an unusual "squared off" waveform appearance has been described.(Heckenlively, Martin et al. 1983; Siegel, Greenstein et al. 1987)

3.3.7 The ON-OFF response

The ON and OFF responses are tested in photopic conditions, the positive ON response generated by the ON (depolarizing) bipolar cells and the positive OFF response generated by a combination of the cone photoreceptors and the OFF (hyperpolarizing) bipolar cells. The two responses therefore give complimentary information about the cone pathway through the inner retina. The ON response is, by definition, subnormal in all Schubert-Bornschein type CSNB. The OFF response (or d-wave) has been found to be normal in the "complete" but subnormal and delayed in the "incomplete" form (Miyake et al. 1987c; Quigley et al. 1996; Houchin et al. 1991; Langrova et al. 2002).

3.3.8 The photopic negative response (PhNR)

The PhNR is a negative wave response which follows the b-wave under photopic conditions. The amplitude of the response may either be measured as part of the photopic SF test condition or to a long light stimulus such as that used in the recording of the ON-OFF response. This wave originates from the inner retina, probably as a consequence of the spiking activity of retinal ganglion cells. This response may be a sensitive measure of retinal dysfunction in patients with diseases that affect the inner retina. Reduction in the amplitude of the response has been identified in subjects with glaucoma.(Colotto, Falsini et al. 2000; Viswanathan, Frishman et al. 2001) This response has not previously been evaluated in CSNB.

3.4 Visual evoked potential recording

The visual evoked potential (VEP) is a recording of the electrical response of the brain to a visual stimulus. Many responses are averaged in order to filter out other EEG activity. Individuals with abnormal nerve fibre decussation at the optic chiasm may be

the occipital response, which reverses in distribution when the other eye is tested, may indicate excessive decussation of fibres at the optic chiasm, a characteristic feature of oculo-cutaneous and ocular albinism (see VEP protocol in Chapter 6).

Trembley identified a crossed asymmetry VEP pattern in 9 out of 10 AR and XLCSNB subjects tested who had ERG patterns suggestive of the "incomplete" type (Tremblay et al. 1996). Although is has been suggested that Åland Island eye disease (AIED see 3.6.1) is indistinguishable from "incomplete" CSNB, studies have failed to demonstrate crossed asymmetry of the VEP in AIED families tested (Glass et al. 1993; van Dorp et al. 1985).

3.5 The ERG in female carriers of XLCSNB

Miyake studied the ERGs of 12 obligate female carriers of XLCSNB and determined that whilst the latency and amplitude of their a and b-waves were within normal limits, the amplitude of their oscillatory potentials was subnormal (Miyake and Kawase 1984). This finding was later confirmed by Young who found that this feature could be optimally identified by measurement of the third OP peak amplitude in the response of the dark adapted retina to a blue flash stimulus (Young et al. 1989).

3.6 Other disorders causing a "negative" ERG waveform

The "negative" ERG waveform is not specific to CSNB but may be seen in a variety of retinal disorders, most of which can be excluded by adequate evaluation (Table 3b). Two conditions, however, Åland Island Eye Disease and Oregon Eye Disease do bear a close resemblance to CSNB and are surrounded by controversy.

3.6.1 Åland Island Eye Disease (AIED)

This was first described by Forsius and Eriksson in 1964 and named after the homeland of the original reported family (Forsius and Eriksson 1964). AIED is a non-progressive disorder characterized by reduced visual acuity and dark adaptation, colour vision abnormalities, high axial myopia, astigmatism, nystagmus, foveal hypoplasia, and fundal hypopigmentation (Glass et al. 1993; Rosenberg et al. 1990; Waardenberg et al. 1969). Although initially thought to be a variant of ocular albinism (OA2), the absence

al. 1990; Glass, Good et al. 1993). Although initially thought to be a variant of ocular albinism (OA2), the absence of iris translucency in half the subjects and the limitation of fundus hypopigmentation to the posterior pole in the condition were atypical (Witkop, Quevedo et al. 1983). Additionally, subsequent electrophysiological examination and skin biopsy failed to show the visual pathway misrouting and skin macromelanosomes characteristic of albinism (van Dorp et al. 1985;Witkop et al. 1983). Dark adaptometry has documented abnormal scotopic thresholds and an abnormal rod-cone transition. ERG studies have demonstrated subnormal scotopic and photopic b-wave amplitudes, subnormal 30Hz flicker responses and subnormal scotopic oscillatory potentials (Glass, Good et al. 1993).

The similarity between the clinical and ERG findings in AIED and "incomplete" XLCSNB is striking and has led to the suggestion that these conditions may be a single disease entity, or that AIED may represent a subset of the condition (Weleber, Pillers et al. 1989; Glass, Good et al. 1993). This theory has been supported by linkage studies, which have mapped AIED to proximal Xp11, the same region as the CSNB2 locus (Figure 4a) (Alitalo, Kruse et al. 1991; Schwartz and Rosenberg 1991; Hawksworth, Headland et al. 1995). Andrassi screened 3 families with AIED related phenotype and 1 family with classic AIED for mutations in *CACNA1F*, his group identified loss-of-function mutations in the three AIED related phenotype families but no mutation in the family with classic AIED(Andrassi, Alitalo et al. 1999).

3.6.2 Oregon eye disease

This disorder is clinically similar to AIED/ "incomplete" CSNB but is part of the syndrome of complex glycerol kinase deficiency (Duchenne-type or Becker's muscular dystrophy, glycerol kinase deficiency and congenital adrenal hypoplasia). Pillers reported the clinical features of this disorder in five affected children, they included reduced visual acuity, night blindness, ametropia and variable iris and fundus hypopigmentation. The ERG showed marked reduction in scotopic b-wave amplitudes, subnormal photopic b-wave amplitudes and subnormal oscillatory potentials. Complex glycerol kinase deficiency in these cases was caused by a deletion in Xp21. Due to the marked similarity between the ocular features of this disorder and AIED/ "incomplete" CSNB, the authors suggested that another locus for AIED/ "incomplete" CSNB may

occur in Xp21 (Weleber, Pillers et al. 1989; Pillers, Seltzer et al. 1993). They named the eye condition associated with complex glycerol kinase deficiency Oregon eye disease. Studies of the ERG in boys with Duchenne muscular dystrophy (DMD) have identified a "negative" waveform in a proportion of subjects (Cibis, Fitzgerald et al. 1993; De Becker, Riddell et al. 1994). DMD is caused by deletions in the dystrophin gene located on Xp21 and dystrophin has been identified in the photoreceptor-bipolar synaptic complex, although its function remains unknown (Pillers, Bulman et al. 1993; Schmitz, Holbach et al. 1993). The negative waveform ERG associated with DMD is, unlike Oregon disease, not associated with any visual disturbance or fundal abnormality (Jensen, Warburg et al. 1995).

Table 3b: Conditions associated with a "negative wave" ERG

Condition	**Scotopic ERG response**		**Photopic ERG response**	
	a-wave	**b-wave**	**a-wave**	**bwave**
Congenital stationary disorders:				
Complete CSNB	normal	↓↓↓	normal	+/-↓
Incomplete CSNB	normal	↓↓↓	normal	↓↓
Åland Island Eye Disease	+/-↓	↓↓↓	+/-↓	↓↓
Oregon eye disease	normal	↓↓↓	normal	↓↓
Oguchi disease	+/-↓	+/-↓↓	normal	+/-↓↓
Retinal dystrophies:				
Early retinitis pigmentosa	+/-↓	↓↓	+/-↓	+/-↓
Infantile Refsum disease	↓↓	↓↓↓	↓↓	↓↓↓
Goldmann-Favre vireoretinopathy	↓↓	↓↓↓	+/-↓	↓↓
X-linked retinoschisis	+/-↓	↓↓	+/-↓	↓↓
Cone dystrophy	+/-↓	+/-↓	+/-↓	+/-↓↓
Melanoma associated retinopathy	normal	↓↓↓	normal	↓↓
Vascular disorders:				
Ischaemic central retinal vein occlusion	+/-↓	+/-↓↓		
Central retinal artery occlusion	+/-↓	+/-↓↓	+/-↓	+/-↓↓
Retinal toxicity:				
Quinine	+/-↓	↓↓	+/-↓	+/-↓↓
Vincristine	normal	↓↓↓	normal	normal
Optic atrophy	normal	+/-↓↓	normal	+/-↓

Chapter 4 Previous genetic investigation of XLCSNB

4.1 XLCSNB Linkage studies

The earliest genetic studies excluded linkage of XLCSNB to the loci of colour blindness (Xqter) and to the XG locus (Xpter) (White 1940; Volker-Dieben and Went 1975). Subsequent studies demonstrated that the disorder was closely linked with the locus DXS7 (Gal, Schinzel et al. 1989; Bech-Hansen, Field et al. 1990). Musarella confirmed this finding in pedigrees exhibiting either "complete" or "incomplete" clinical forms of XLCSNB (Musarella, Weleber et al. 1989). The mapping of this locus was further refined to between the loci MAOA and DXS426 (Xp11.3 to Xp11.23) (Aldred, Dry et al. 1992; Bech-Hansen, Moore et al. 1992). At this time there was considerable uncertainty whether the disorder was genetically heterogeneous or if the wide variation in phenotype might result from a single disease locus (Khouri, Mets et al. 1988; Pearce, Reedyk et al. 1990).

The genetic heterogeneity of XLCSNB was clearly established when Bergen demonstrated a novel locus at Xp21.1 in one clinically heterogeneous family (Bergen, ten Brink et al. 1995). Boycott suggested that two loci, one for "complete" (CSNB1) and one for "incomplete" (CSNB2) XLCSNB might account for all reported mapping information. Following genetic and clinical analysis of 32 pedigrees the CSNB2 locus was refined to the region between DXS722 and DXS255, in Xp11.23. The CSNB1 locus was refined to the region between DXS556 and DXS8083, in Xp11.4-Xp11.3 (Figure 4a) (Hardcastle, David-Gray et al. 1997; Boycott, Pearce et al. 1998).

4.2 Identification of the CSNB2 gene – *CACNA1F*

Efforts to identify the CSNB2 gene led to the construction of high-density maps of the Xp11.23 region. Sequencing revealed several new genes including *CACNA1F*, a novel L-type calcium channel α_1-subunit gene spanning 28kb (Strom et al. 1998;Bech-Hansen et al. 1998b). This gene appeared a likely candidate gene for XLCSNB since ERG studies had indicated that the condition might result from a defect in synaptic transmission between photoreceptors and bipolar cells (Hood and Greenstein 1990). Retinal studies in frog retina had also illustrated that glutamate release from

photoreceptor presynaptic terminals is mediated by L-type (long lasting) dihydropyridine sensitive calcium channels (Schmitz and Witkovsky 1997). Additionally, several neurological and neuromuscular disorders in humans and night blindness in Drosophila are known to result from mutations in calcium channel α1-subunit genes (Smith 1996; Doyle and Stubbs 1998).

4.2.1 Properties of the gene *CACNA1F*

CACNA1F is 48 exons in length with a coding sequence of 5901 nucleotides and a predicted protein length of 1966 amino acids (219.5kD). Expression of *CACNA1F* is limited to retinal tissue (Strom et al. 1998;Bech-Hansen et al. 1998b) and RNA in situ hybridisation studies have identified its transcription products in the outer nuclear layer (containing the photoreceptor cell bodies), the inner nuclear layer (containing horizontal, bipolar and amacrine cells) and, more weakly, in the ganglion cell layer (Strom, Nyakatura et al. 1998).

4.2.2 Structure and function of the L-type calcium channel

L-type calcium channels consist of 4 subunits (α_1, α_2, β, and γ, the calcium conducting pore and the voltage sensor being located in the α_1-subunit (Catterall 1995). Three autosomal L-type calcium channel α_1-subunit genes have previously been cloned: α_1s from skeletal muscle (Hogan, Powers et al. 1994), α_1c from cardiac muscle and brain (Schultz 1990) and α_1d from neural and endocrine tissues (Williams 1992).
Figure 4b illustrates the structure of the α_1-subunit of an L-type calcium channel. The α_1-subunit is comprised of four repeat segments (I-IV), each containing six transmembrane domains (S1-S6). The similarity between the amino-acid sequence of the human α_1d-subunit gene and that of *CACNA1F* is 70% overall and 84% in the transmembrane segments. Sequence identity between *CACNA1F* and the other L-type channels is present in the charged residues of the S4 regions which act as voltage sensors (Stuhmer 1989) and the dihydropyridine binding sites at IIIS5-S6 and IVS6 (Schuster 1996). The amino acids at the β-subunit binding site after the first segment is also conserved (Pragnell 1994).

4.2.3 Mutation analysis of the gene *CACNA1F*

Having identified *CACNA1F* as a candidate gene for "incomplete" XLCSNB, Strom and Bech-Hansen screened a total of 33 pedigrees with this clinical form of the disorder for mutations. Using a single-stranded conformation polymorphism (SSCP) technique, Strom screened 39 of the 48 exons for mutations and identified nine different mutations in 10 of the 13 pedigrees (five missense mutations, four protein truncating mutations) (Strom, Nyakatura et al. 1998). Bech-Hansen screened 20 families with "incomplete" CSNB for mutations in *CACNA1F* using direct DNA sequencing and identified mutations in all 20. The six different mutations resulted in premature stop codons causing protein truncation (Bech-Hansen, Naylor et al. 1998).

4.2.4 Pathophysiological effect of *CACNA1F* loss-of-function mutations

Loss-of-function mutations in *CACNA1F* result in inactivity of the L-type calcium channel. This form of XLCSNB is not the only example of a retinal channelopathy; rod monochromatism has recently been determined to result from loss-of-function mutations in *CNGA3*, a gene located on chromosome 2q11. This gene encodes the α-subunit of the cone photoreceptor cGMP-gated cation channelling a potassium channel sub-unit in the cone photoreceptor (Kohl, Marx et al. 1998).

On the basis of the ERG pattern of Schubert-Bornschein type CSNB, it has been postulated that the disorder is caused by defective neurotransmission between photoreceptors and bipolar cells. The a-wave of the ERG response is of normal amplitude, indicating that the photoreceptor current is normal but the b-wave is severely reduced in amplitude, reflecting an abnormally reduced level of light induced depolarization in the ON bipolar cells of the inner retina. Theoretically this pattern could result either from a decrease in the amount of neurotransmitter released from the photoreceptors or the effectiveness of the transmitter at the post-receptoral site (Hood and Greenstein 1990).

In darkness, glutamate is tonically released from the photoreceptor presynaptic terminal whilst light-induced photoreceptor hyperpolarization diminishes the release of the neurotransmitter. The reduced stimulation of the ON bipolar cell by released glutamate in light conditions results in its depolarization (Stockton and Slaughter 1989). Loss-of-function mutations affecting the α_1-subunit of the L-type calcium channel impair the influx of calcium ions into the photoreceptor presynaptic terminals thereby diminishing

the tonic release of glutamate and allowing the ON bipolar cells to be relatively depolarized (light adapted) in darkness. The effect of this is to limit the synaptic gain between the first and second order retinal neurons (Bech-Hansen, Naylor et al. 1998; Strom, Nyakatura et al. 1998).

4.3 Identification of the CSNB1 gene - NYX

More recently the CSNB1 locus has been identified on Xp11.4 using positional cloning and a candidate gene approach (Bech-Hansen, Naylor et al. 2000; Pusch, Zeitz et al. 2000). Analysis with gene finding software predicted a novel gene, *NYX* at this locus.

4.3.1 Properties of the gene *NYX*

NYX is a 3 exon gene with a full length sequence of 1443 nucleotides encoding a protein of 481 amino acids named nyctalopin. Transcript size and tissue distribution were not detectable by Northern analysis due to the low level of expression of this gene, however RT-PCR results indicated expression in retina, kidney, brain, muscle, placenta and testis (Bech-Hansen, Naylor et al. 2000; Pusch, Zeitz et al. 2000). As is the case with *CACNA1F*, *NYX* is apparently expressed in the photoreceptor, bipolar, amacrine and ganglion cells (Bech-Hansen, Naylor et al. 2000; Pusch, Zeitz et al. 2000).

4.3.2 Structure and function of nyctalopin

Nyctalopin contains an N-terminal signal peptide and a C-terminal glycosylphosphatidyl (GPI) anchor. The central part of the protein encodes 11 consecutive leucine-rich repeat (LRR)motifs which are flanked by N- and C-terminal cysteine rich LRRs. This structure qualifies nyctalopin as a new extracellular member of the subfamily of the small leucine-rich proteoglycan (SLRP) family (Iozzo 1997). Figure 4c illustrates a three-dimensional model of nyctalopin.

Members of the LRR superfamily are involved in regulation of cell growth, cell adhesion and axon guidance (Kobe and Deisenhofer 1994; Hocking, Shinomura et al. 1998). Nyctalopin has approximately 30-35% identity with other SLRP family members including Karatocan (mutations in which have been shown to cause corneal plana) and chondoadherin (Pellegata, Dieguez-Lucena et al. 2000). Other superfamily members that have GPI-anchors include *Drosophila* chaoptin, an extracellular photoreceptor neuron-specific cell adhesion molecule (Krantz and Zipursky 1990), and *Drosophila*

connectin, which acts as a repulsive guidance molecule during motoneuron growth cone guidance and synapse formation (Nose, Takeiki et al. 1994). Nyctalopin may therefore have important function as a developmental regulator of synaptic formation between rod photoreceptor cells and postsynaptic neurones including bipolar and amacrine cells.

4.3.3 Mutation analysis of *NYX*

Two groups have performed *NYX* mutation analysis by direct DNA sequencing on 46 pedigrees with "complete" CSNB, to date 29 different mutations have been identified. These mutations include point mutations (16 different missense mutations, 2 nonsense mutations), 8 deletions and 3 insertions. These identified mutations all result in loss-of-function of nyctalopin by disrupting vital regions of the protein, for example the deletion of 326 base pairs in exon 3 of one family and a nonsense mutation in another both result in absence of the GPI anchor, thereby making the protein soluble rather than membrane bound.

4.3.4 Pathophysiological effect of *NYX* mutations

The functional role of nyctalopin in the retina remains to be clarified but loss of protein function evidently causes the diverse clinical features of CSNB1. If the protein is required to establish or maintain functional contacts between rod photoreceptor cells and postsynaptic neurons of the inner retina, loss of function might be predicted to result in a disconnection of these synaptic circuits.

4.3.5 The nob Mouse Model

A naturally occurring mouse model of XLCSNB was described in 1998 (Pardue, McCall et al. 1998). The nob (no b-wave) mouse demonstrates similar electroretinographic features as human subjects with XLCSNB. Recently mutations in the mouse nyx gene have been identified in affected mice, making it an extremely useful model for defining the role of nyctalopin in signal transmission between photoreceptors and retinal bipolar cells (Gregg, Mukhopadhyay et al. 2003). Using this mouse model, Ball et al. have demonstrated that the absence of nyctalopin does not result in the disruption in the expression pattern of other proteins known to be required for synaptic transmission, such as the α_1-subunit of the L-type calcium channel and dystrophin (Ball, Pardue et al. 2003).

Figure 4a: Diagrammatic representation of the X chromosome, illustrating the position of the CSNB1 and CSNB2 gene loci.

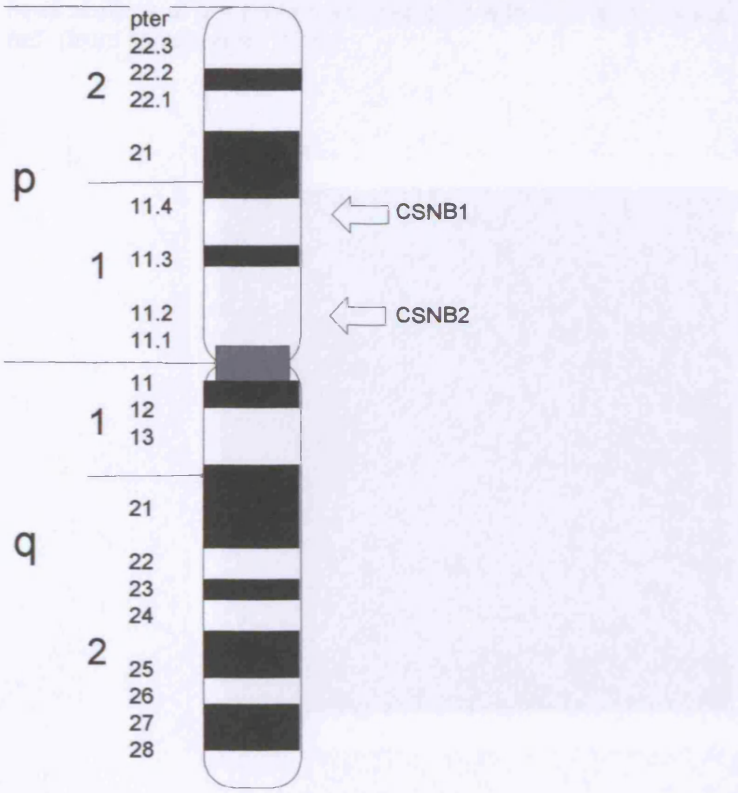

Figure 4b: Structure of the voltage-gated calcium channel alpha$_1$-subunit. The subunit contains 4 repeat domains containing 6 transmembrane domains (S1-S6) (from Strom et al 1998).

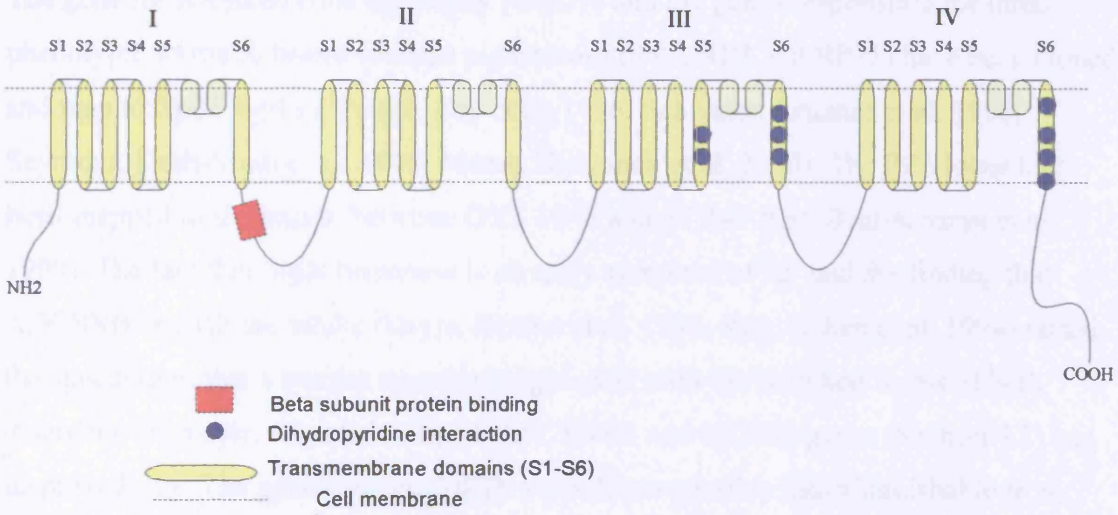

Figure 4c: 3D modelling of nyctalopin.
The structure is represented as a ribbon, beta-sheets in light blue, alpha-helices in yellow and numbering of the leucine-rich repeats is highlighted in blue. Basic amino acid residues lining the inner surface of the protein are depicted with their side chains in blue and acidic amino acids in red. (from Pusch et al. 2000)

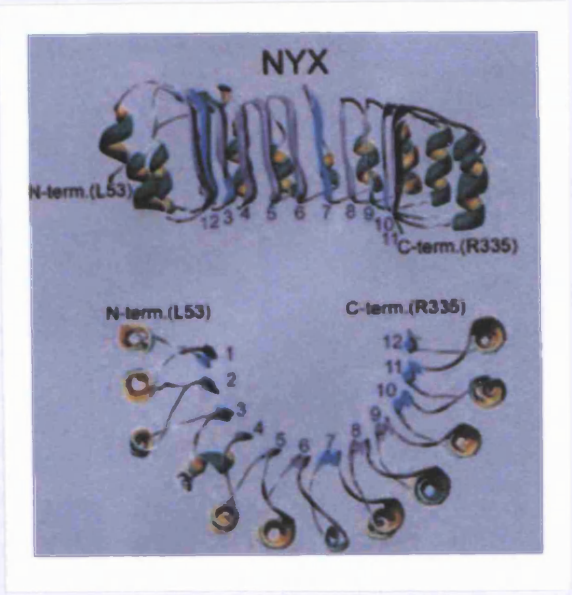

4.4 Other inherited retinal conditions mapping to Xp

Many other retinal disorders also map to this area of the X chromosome (Figure 4d). The gene for X-linked cone dystrophy (COD1) and the genes responsible for three phenotypic forms X-linked retinitis pigmentosa (RP2, RP3 and RP15) have been cloned and map to Xp21.1-p11 (Meindl, Dry et al. 1996; Schwahn, Lenzner et al. 1998; Seymour, Dash-Modi et al. 1998; Mears, Hiriyanna et al. 2000). The RP6 locus has been mapped to the region between DXS 1048 and STR44 (Ott, Bhattacharya et al. 1990). The fact that night blindness is an early symptom of RP and the finding that ADCSNB and RP are allelic (Dryja, Berson et al. 1993; Rao, Cohen et al. 1994) raised the speculation that a similar situation might exist with the X-linked forms of both disorders. However, recent cloning of the CSNB1 and CSNB2 genes (Section 4.3) has disproved this. The gene causing AIED, a condition possibly indistinguishable from "incomplete" XLCSNB, has been localised to the region between DXS7 and DXS255, a region overlapping the CSNB2 gene locus. This indicates that the conditions may be one and the same or allelic (Glass, Good et al. 1993).

Figure 4d: Inherited ocular disease map for proximal Xp

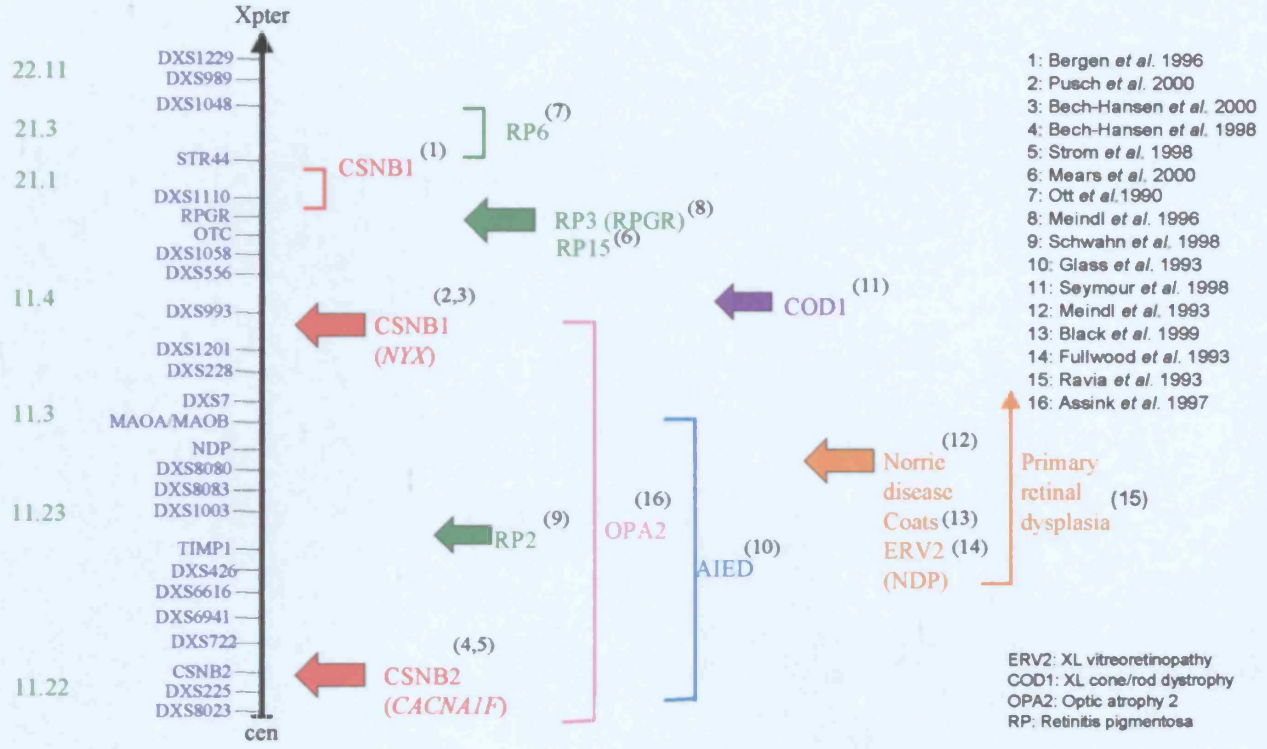

Chapter 5 Summary of review

5.1 Summary of review and problems remaining

From this review of the literature it can be seen that there are many controversies surrounding CSNB.

Many of the problems associated with the clinical classification of CSNB lie with the absence of standardisation of electrophysiological procedures. Most of the studies were performed before the ISCEV standardisation of ERG protocols in 1989. Additionally, ERG results from two different sets of recording equipment are not directly comparable. This lack of standardisation may explain why some authors have suggested that some subjects can not be classified as having either "complete" or "incomplete" CSNB according to Miyake's criteria, and that both forms of the condition may occur in one pedigree. Miyake's study included subjects with XLCSNB and ARCSNB and could not attempt to make a genotype-phenotype correlation. The molecular genetic studies that have been performed have, necessarily, involved subjects who have been examined in many different centres across the world and do not provide adequate information on phenotype.

The improvement in the standardization of psychophysical and electrophysiological testing and the advancement in the understanding of the molecular genetics of XLCSNB by the recent identification of the two genes responsible for the condition provide an exceptional opportunity to investigate the presence of a genotype-phenotype correlation in this condition.

5.2 Aims of this project

The aims of this study are:

1) To accurately document the phenotype of affected subjects in families with XLCSNB.

2) To investigate the functional deficit of the scotopic and photopic system in subjects with XLCSNB, evaluate possible disease mechanisms and to confirm or refute the existence of the "complete" and "incomplete" clinical subtypes.

3) To test families with XLCSNB for a causative gene mutation and investigate the possibility of a genotype-phenotype correlation.

Chapter 6 Investigation of XLCSNB: Methods and protocols

6.1 Ethical Committee approval

Ethical committee approval was given for this study by the Cambridge Regional Ethical Committee in 1998.

6.2 Diagnostic criteria

The criteria for diagnosis of XLCSNB were:

1) The symptom of non-progressive nyctalopia
2) Normal visual field examination
3) Grossly normal fundoscopic examination
4) The presence of a 'negative wave' ERG in affected males.

6.3 Identification of pedigrees and recruitment of patients

Families with CSNB were identified mainly from the Genetic Clinic database at Moorfields Eye Hospital and from the East Anglian Regional Genetic Clinic Database. A letter providing information about the study and inviting the referral of additional pedigrees was sent to Clinical Geneticists and Consultant Ophthalmologists throughout the UK. Subjects with a diagnosis of CSNB were contacted by post with information regarding CSNB, details of the proposed project and a questionnaire regarding their family history of the condition (Appendix A). Twenty three affected subjects from 15 pedigrees who fulfilled the above criteria gave written informed consent to participate in the study.

6.4 Ophthalmic examination

Twenty subjects from 12 of the original 15 pedigrees were able to attend for standardised ophthalmic examination. Individuals from the other 3 pedigrees agreed to give blood for DNA analysis. The twenty affected subjects and immediate family members were examined prospectively. Information was recorded on a standardised

data sheet (Appendix B) subsequently data was entered onto a computerised database for analysis. A general ophthalmic history was recorded with particular attention paid to the history of nyctalopia, deterioration in visual acuity, colour vision deficiencies, previous therapy for amblyopia or strabismus and family history. A full ophthalmic examination including refraction and slit-lamp biomicroscopy was performed. A-scan measurements of the ocular axial length were performed in older children and adults.

6.5 Psychophysical examination

Visual acuity was tested using Snellen and logMAR charts. Colour vision was tested using the HRR plates, Ishihara plates, City University plates, the Mollon-Reffin 'minimalist test' and where possible the Mollon-Reffin digital colour vision test. Photopic perimetry was tested using a Goldmann perimeter. Older children and adults were invited to attend a further appointment for further psychophysical testing (scotopic perimetry and dark adaptometry) at the Institute of Ophthalmology, London.

6.5.1 Scotopic perimetry

A Humphrey Field Analyser (HFA) was modified to allow measurements in scotopic conditions and control by an external computer for spectral sensitivity measurement and dark adaptometry. The apparatus and method for scotopic perimetry and dark adaptometry using this equipment has been described previously (Steinmetz, Haimovici et al. 1993; Downes, Fitzke et al. 1999).
In amblyopic subjects the non-amblyopic eye was tested; where the visual acuity was the same in each eye, the right eye was selected for testing. Testing followed pharmacological mydriasis with 1% cyclopentolate and 40 minutes of dark adaptation. scotopic perimetry was performed prior to dark adaptometry.
Scotopic perimetry was recorded using red (predominant wavelength 650nm) and blue (predominant wavelength 450nm) targets corresponding to Goldmann size V over the 30-2 HFA grid. Threshold intensity for these targets was determined at two pre-assigned retinal locations (-9, +9 and +9,-9 on the HFA 30-2 grid).

6.5.2 Dark adaptometry protocol

The 450nm and 650nm Goldmann size V targets were used for dark adaptometry. An initial pre-bleach threshold value for each target was determined at –9,+9 and +9.-9

on the HFA 30-2 grid. A 2 minute period of light adaptation (equivalent to 7.5 scotopic troland seconds), sufficient to bleach more than 95% of available rhodopsin, was achieved using lights installed within the perimeter bowl. The testing strategy used a method of ascending limits in which the stimulus was presented at 3.5 second intervals, and after each response the stimulus intensity for each location and target stimulus was reduced by 7dB for the first three responses and 3dB for subsequent responses. They were then increased by 1dB until the next response was recorded. Threshold measurements were continued in the dark for at least 45 minutes (or longer depending on the subject's tolerance). Dark adapted thresholds were considered abnormal if there was a 10dB (1 log unit) or greater elevation when compared with age matched controls. The rod-cone break was determined by visual inspection. Return of pre-bleach sensitivity was defined as the time at which the average of the last five measurements came within 5dB (0.5 log units) of the average of the pre-bleach threshold measurements.

6.5.3 Spectral sensitivity protocol

Spectral sensitivity to additional stimuli of wavelength 488nm, 520nm, 590nm and 633nm was also assessed prior to dark adaptometry.

6.6 Electrophysiological examination

All twenty subjects underwent standardised electroretinography. During the course of the research project a new piece of testing apparatus became available which enabled the recording of the ON-OFF response in a number of the subjects.

6.6.1 ERG protocol

Several international professional bodies have published recommendations for recording the ERG. While the ERG protocol used for this project complies with the standards set by the International Society for Clinical Electrophysiology of Vision (ISCEV) (Marmor and Zrenner 1998), we have used gold foil electrodes for our subjects and controls rather than the contact lens electrode used with a speculum which they recommended. Although gold foil electrodes are not as sensitive as contact lens electrodes, they are in more common clinical use across the UK and are much more likely to be tolerated by children without the need for sedation or the risk

of corneal abrasion. Other workers have also justified the use of gold foil electrodes. In children too young to tolerate the gold foil electrode, a gold skin electrode was used (Kriss and Russell-Eggitt 1992).

The ERG was recorded by means of a gold foil electrode located in the inferior fornix of the tested eye. In children who were unable to tolerate the foil electrode, a gold disc electrode was positioned on the lower eyelid. Gold disc electrodes were positioned mid-frontally (Fz) and on the forehead as reference and ground electrodes respectively. The ERG signal was amplified with a gain of 1 x 104 over a bandwidth of 0.8-800Hz and fed into an analog-to-digital converter of the laboratory computer system. The computer sample rate was 1 kHz and the sweep time 200ms (rod responses) or 100ms (cone responses). Four to 64 responses were averaged, depending on signal size.

The stimulus was a 10μs Xenon flash (Grass Instruments PS22) delivered via a diffusing sphere (Ganzfeld) so as to provide full-field even illumination of the eyes. Stimulus intensity was measured with an integrating photometer fitted with a luminance barrel and photopic filter. The maximum stimulus intensity was $7cd.s^{-1}.m^{-2}$, which complies with the recommended level for the Standard Flash 'Maximal response' ISCEV standard. Stimulus intensity was controlled by means of neutral density filters (Kodak Wratten). During the course of the test the subject's eyes were monitored with a low light level camera.

The pupils were dilated with 1% tropicamide and the eyes dark adapted for 20 minutes. The ERG recording electrodes were positioned under dim red illumination and rod responses were then recorded to stimuli of increasing intensity. Cone function was tested using a red flash under dark adapted conditions. The eyes were then exposed continuously to a rod desensitising background of $25cd.m^{-2}$ for 10 minutes. Cone responses were then recorded to the Standard Flash and to a 30Hz flicker. Scotopic oscillatory potential amplitudes were isolated by passing the ERG response elicited in dark adapted conditions using the Standard Flash through a 100-300Hz digital filter, photopic oscillatory potential amplitudes were isolated by the same means under light adapted conditions.

The ERG responses of 26 adult control subjects aged 19-62 years were used to provide normal latency and amplitude data.

6.6.2 Scotopic Threshold Response protocol

The STR intensity series was recorded with a gold foil electrode in the same manner as the ERG protocol above. The pupils were fully dilated with 1% tropicamide and recording initiated after 20 minutes of dark adaptation. The stimulus was presented at 2 second intervals. The STR intensity series was recorded initially with the Standard Flash stimulus attenuated by up to -7.2 log units by a neutral density filters then with increasing stimulus intensity in 0.3 log unit steps until the STR was abolished by the scotopic b-wave. The dark adapted ERG was then recorded.

6.6.3 ON-OFF response protocol

The ON-OFF responses were elicited using a long flash stimulus in a second ganzfeld system. The system incorporated two independent 250 watt tungsten halogen lamps mounted in fan cooled lamphouses. The colour temperature of the light was approximately 3000 deg K. Light was collected from each lamphouse over a wide angle by an aspheric lens mounted adjacent to the exit port of the lamphouse. A second aspheric lens brought the beam to a focus at the centre of a fast electronic shutter. Infra-red and ultra-violet wavelengths were removed by appropriate filters in the light path. Additional neutral density filters in each light path controlled stimulus and background intensity. A 20mm fiber optic bundle collected the light at exit from the shutter. The bundle then split into 4 tails which were positioned at equidistant points around the front of the ganzfeld bowl and directed the beam via diffusers onto the inner surface of the bowl. The tails from the two systems were interleaved around the front of the bowl. One system with the shutter continuously open provided the background adapting light which was set to 48 ph cd.m^{-2}; the other system provided the stimulus which was set to 320 ph cd.m^{-2}. The flash duration was controlled by an electronic shutter with 90% rise and fall times of 5ms. The duration of the light period was 200ms and that of the dark period 150ms. The data acquisition sweep time was 300ms and 50 responses were averaged for each trial. At least two responses were recorded to ensure data quality and reliability and the two or more responses were then averaged off-line for response peak cursoring.

6.6.4 VEP protocol

The VEP protocol followed the recommendations made by Apkarian (Apkarian, Reits et al. 1983). The stimulus was a large (60') appearing (300ms onset) and disappearing (500ms offset) black and white chequerboard pattern of field 20 (horizontal) by 18 (vertical) field generated on a computer display screen. The white square luminance was 80cd.m^{-2} and the contrast was 98%. The screen was viewed at a distance of 100cm and a 10' red square centered within the stimulus field served as the fixation spot. Adequate fixation was assessed by closed circuit television. VEPs were recorded using 5 disc electrodes placed 3cm apart in a horizontal row, 3cm above the inion with the central electrode located at the midline. Reference for all electrodes was the common ground electrode was located on the mid-frontal position (Fz) on the forehead. Signals were amplified with a gain of 10^5 over a bandwidth of 1-100Hz. Each trial was the average of one hundred presentations.
Monocular left and right eye responses were recorded. At least two independent trials were obtained to stimulation of each eye for confirmation that the waveform was reproducible. The two (or more) responses were computer averaged off-line and the hemispheric 'difference' signal computed by subtracting the right hemispheric response from the left hemispheric response when each eye was stimulated in turn. The difference potential resulting from stimulation of each eye was then plotted and the polarity of the difference potential compared qualitatively in the period 80-110ms after pattern onset. The presence of reversal in the difference potential from right to left eye stimulation was considered to be evidence of response asymmetry due to misrouting.

6.7 Molecular genetic analysis

6.7.1 DNA extraction from blood samples

Following informed consent and after clinical examination, 20mls of peripheral venous blood was taken in EDTA tubes from all subjects and was stored at +4°C prior to DNA extraction. Genomic DNA was extracted from peripheral blood samples using the Nucleon II kit (Scotlab Ltd, Strathclyde, Scotland) at the Molecular Genetic Laboratory at Addenbrooke's Hospital. This process involves the segregation of leucocytes from erythrocytes and disruption of the leucocyte nuclear and cytoplasmic

membranes to release genomic DNA. Cellular proteins are then removed by denaturation and extraction using organic solvents and DNA precipitated from aqueous solution by the addition of ethanol.

6.7.2 Mutation screening of the genes *CACNA1F* and *NYX*

The DNA from affected males in 15 pedigrees was screened for mutations in the *CACNA1F* gene by the author at the Cambridge Institute for Medical Research in Cambridge. During the course of the project the *NYX* gene was identified: DNA from the subjects in whom *CACNA1F* gene mutations had not been detected was then screened for mutations in *NYX* by Dr Alison Hardcastle and colleagues in the Department of Molecular Genetics at the Institute of Ophthalmology, London.

Affected male DNA was PCR amplified for the 48 exons of *CACNA1F* using primers and conditions outlined in Table 6a (Strom, Nyakatura et al. 1998). Buffer recipes are described in Appendix C. Affected male DNA was subsequently PCR amplified for the exons of *NYX*, primers and conditions are outlined in Table 6b. The magnesium ion concentrations required are shown and all reactions were annealed at 60°C with 1µl of DMSO in NH_4 Reaction Buffer (Bioline, London, UK).

The PCR products were purified using the Qiagen purification kit (Qiagen Ltd, Crawley, UK) according to the manufacturer's instructions and then directly sequenced using a Big-dye terminator cycle sequencing kit (Perkin-Elmer-Applied Biosystems, Warrington UK) and a fluorescent sequencer (ABI 373) according to the manufacturer's instructions (Appendix C). Segregation analysis of observed sequence changes was performed using the gain or loss of a restriction endonuclease site in all available family member DNA. Previously unreported nucleotide sequence changes were determined to represent significant mutations rather than polymorphisms by screening a population of 100 unrelated Caucasian males for the nucleotide change. Where the same mutation was identified in multiple pedigrees, the possibility of a founder effect was evaluated by amplification of microsatellite markers around the gene as previously described (Hardcastle, Thiselton et al. 1999).

Table 6a: Primers and conditions for polymerase chain reaction (PCR) of *CACNA1F* exons

Exon primer	Annealing Temperature °C	Buffer	Exon primer	Annealing Temperature °C	Buffer
1F: ACAAACGTCCCATTTGCAC **1**R: GCAATGGGTGGGTCAGAG	61	NEB	**15**F:AGCCTATTTGAGCCCAACCT **15**R:ACCCATCCCATGGTCTCC	61	P1
2F: ATACCCTGTCCCTCCCTGAC **2**R: CTCCTGGTACCCTGATGACC	Touchdown 63,61,59	NEB	**16**F:GAGCTCCACAGTGACTTCCC **16**R:ACCCTGCCTATAGACCACCC	66	P1
3F: GAGGTTCCCAAGGGAGTAGG **3**R: GTCTGGCTGGAAGGAGTGAG	65	P1	**17**F:GTGGTCTATAGGCAGGGTGC **17**R:GACTGTGTTAGGGGTGGAGC	60	P1
4F:CTCGGTCCTGACTATGCTCC **4**R: GGTAGGAAGGCGACTAGGGT	60	NEB	**18**F:GTAGTGATCCCCCTTAGCCC **18**R:ACAGGTAGTGGTGGGAGTGG	Touchdown 63,61,59	P1
5F: ATCCCAAGGCCTGACCTC **5**R: ACCCTCCACCTCCGACCT	58	P1	**19**F:CCTCACCATTGATGACTCCC **19**R:TGTCTGCCTGAGCTCTTTCC	60	NEB
6F: CTTATTTCTGCCTCCCCCTC **6**R: AGCATTGGATCTAGGAACCG	Touchdown 63,61,59	P1	**20**F:TTTTGCTTTTCTCTGGTGCC **20**R:GGCTCACCTAGGGCTCTTCT	61	NEB
7F: CAAGCTCCAGTCTTCCTGC **7**R: TGAGTGTCAGGGAGGAAAGG	60	P1	**21**F:TCAGGGCCAGAACTGTATCC **21**R:GTCCCCTCAGCTCCTAGCTC	61	NEB
8F: GGATGCATGCCTTTTCTCTC **8**R: GTTTGCCAGGCACAAAGAAG	61	P1	**22**F:GAAGTCACCTAGGATCCCCC **22**R:CAACTGAGGGTAGGACTGGG	62	P1
9F: TAGCCCTCTATCCTCCTCCC **9**R: GGAGGGCAGACCACATCTAA	61	NEB	**23/24**F:TCCCCAGGTCTGAGTCTAGC **23/24**R:GTCCTGTGGGTTTGGGTG	63	P1
10F:AATTGTCCTTTCTCTCCCTGC **10**R:TCCAATCTTTGGCTTTCACC	62	P1	**25/26**F:GTAGCCATATGCTTGGGTGC **25/26**R:AGTCTTTGGGAGGGGTCCT	Touchdown 65,63,61	P1
11F:AGGTCCTGACCACTATCCCC **11**R:GGACTTGAGTCAGGGTTTGG	61	NEB	**27**F:AACCTGTTTGCACATCCACA **27**R:CTGCCTCATCCCCTGATAAA	58	NEB
12F:TTTACGACACACACCTCCCA **12**R:ATCCAAAGGTCATGAGGGCT	60	P1	**28**F:ACCTGCCCCCACCTCTAC **28**R:ACCATCCATAGGGGGTCAG	60	P1
13F:AGGGCAGGCTTAGGTAGGTG **13**R:AGAAGGAATAGGAGGCTGGG	61	P1	**29**F:ATGCCCTGCCCTGGTATG **29**R:ATAGGGTCAGGAGTCTGGCG	58	P1
14F:GATCATCCCTGCCTCTCTCC **14**R:CTTCCCCCTCCCCTAATACA	61	NEB	**30**F:AATATTTGGTTGGGTGTGGC **30**R:CCCAAGGAATTCATCCACTG	57	P1

Table 6a– continued: Primers and conditions for PCR of *CACNA1F* exons

Exon Primer	Annealing Temperature °C	Buffer	Exon primer	Annealing Temperature °C	Buffer
31F:GACAGGGCACTGCTTTTCTC **31**R:CAGGAGTAGGGAGGATGTGC	61	NEB	**40**F:TCTTCCTATTGGCTCATGCC **40**R:AGCGATCATCTGCCATTCAG	62	NEB
32F:CTCCACCTTGTTCATTTGGGC **32**R:GGACATGGGAAAAGAAGCAG	Touchdown 65,63,61	NEB	**41**F:CCCTGTGTGATCTTGCCTTC **41**R:CCATCCACACTAGGCCCTG	61	NEB
33F:AAATGCAAACTGAGCATCCC **33**R:ATTTGGAAATGGGTATGGCA	60	P1	**43**F:GTGCATGCAACACTCAGTCC **43**R:CTCAACTTCCTGCCTCCTGA	58	P1
34F:GACTGCATCTCCCAGTAGGC **34**R:ATTCTTAACCCATCCCCTGC	59	P1	**44**F:ATCTGGTCTGCCTAACGTGC **44**R:CAGTTCCCACCCCTCCTC	Touchdown 65,63,61	NEB
35F:GTAGGGGTGGCAGGTAGACA **35**R:GTGGCAGGGGAGTGAGTAGA	60	NEB	**45**F:GACTGTTTGTGCCCCATCTC **45**R:TTCCCCAGATCTCTGTCCTG	61	P1
36F:GATGTAGCCCCTGGTGAGAA **36**R:GGTGGTTGTGAGGAAATGGT	59	NEB	**46**F:CTGACATTGCTATTTGCCCC **46**R:CATCTCTCCAGACCCCAGAC	Touchdown 65,63,61	NEB
37F:ACAGTGTTCTGCCCTTCACC **37**R:TAATGAGATGCAGCAGTCGG	61	NEB	**47**F:AGCGGTGAGTCCTAGACCCT **47**R:GACTCCTTTCCGTCCTCCTC	Touchdown 65,63,61	NEB
38F:AGTGGTACCTCCCCAACTCC **38**R:CCACCCTTGCCATGTGATAG	61	P1	**48**F:AACACTGATCCCACCTGTGC **48**R:GAATTCAGAGGGCGTGGAC	61	P1
39F:ACATTCGTTCCTGCATACCC **39**R:ATGAGTTTGCTCCTTGCACC	61	P1			

Table 6b: Primers and conditions for PCR of *NYX* exons

Exon Primer	Annealing Temperature °C	Buffer MgCl2	Exon Primer	Annealing Temperature °C	Buffer
1F:ACCTTTACTTCTCTCAAACCA **1**R:GGCATCACTGACAACCCAGC	61	15mM	**3b**F:ACAACCTGTCCTTCATCACGC **3b**R:CAGGTTGAGCGGCGCAGG	61	10mM
2F:ATGAAAGGCCGAGGGATGTTG **2**R:CCAACATCCCTCGGCCTTTCA	61	10mM	**3c**F:GACTGTGGCGTCCTGGAGC **3c**R:GGTCACCTGGCTGAGGTCC	61	10mM
3aF:GACCTTTGGCTGACGGTTGC **3a**R:GTGCAGGTAGCGCAGGTCG	61	15mM	**3d**F:ATGGAGGGCTCCGGACGTG **3d**R:TTACCACAAACACAACTCAAGCC	61	15mM

Chapter 7 Molecular Genetics Results

Mutation screening for *CACNA1F,* using direct DNA sequencing, was performed on the 15 pedigrees which fulfilled the diagnostic criteria for XLCSNB.

7.1 Mutation screening of CACNA1F

Comprehensive mutation screening of the *CACNA1F* gene revealed 3 different mutations in 3 families, all predicted to cause protein truncation and therefore loss of function (Table 7a, Figure 7a). The novel nonsense mutation detected in exon 7 (family X10) occurs after the fifth transmembrane domain (Figure 4c) therefore deleting part of Segment I and all of Segments II, III, IV, the EF-hand motif and cytoplasmic C-terminus. This sequence change results in loss of a digest site for the restriction enzyme BseR I and was found to segregate with the disease in this family (Figure 7b). The single base deletion in exon 9 detected in family X11 results in a frameshift at amino acid position 341 resulting in loss of domains and motifs downstream from Segment I and predicted loss of function. This mutation has previously been identified in one other family (Bech-Hansen, Boycott et al. 1998). The third loss-of-function mutation (family X12) was identified in exon 24 resulting in protein truncation in Segment III and has also been previously identified in a single family (Strom, Nyakatura et al. 1998).

Two polymorphic variants were detected in the *CACNA1F* gene (1647C>T and 3114T>C), which were not predicted to alter the amino acid sequence. A third polymorphism was found in families X04 and X05, namely a G>A transition at nucleotide position 5595, which resulted in a conservative amino acid substitution from arginine to histidine. The sequence change was confirmed by the presence of a new HpH I restriction enzyme digest site (Figure 7c), this sequence change was identified two of the first 50 normal males to be tested, indicating that this was not a disease causing mutation (Figure 7d). These polymorphisms have not previously been reported. Subsequently, *NYX* gene mutations were identified in both X04 and X05 pedigrees.

Table 7a: *CACNA1F* sequence changes identified in subjects with CSNBX.

Pedigree	Exon	Sequence change*	Codon change	Type
X10	7	637G→T	E213X	Stop (Novel mutation)
X11	9	1023delC	D341delC	Frameshift (stop378)
X01	14	1647C→T	None	Polymorphism
X12	24	2719C→T	R904X	Stop
X02	28	3114T→C	None	Polymorphism
X04 X05	48	5595G→A	R1865H	Polymorphism

* position according to Af067227

7.2 Mutation screening of NYX

Mutation screening of the *NYX* gene was subsequently performed on affected males from the 12 pedigrees in which *CACNA1F* mutations were not identified. A total of 7 different mutations segregating with disease were identified in the *NYX* gene in 11 different families (Table 7b), which were not detected in over 100 control chromosomes.

A splice site mutation, G>C, was detected in family X03 at position +1 in intron 2. The first nucleotide of a donor splice sequence is generally 100% conserved (Horowitz and Krainer 1994), hence the transition identified at this site is very likely to affect RNA splicing.

One missense mutation was identified in 2 families (X01 and X07), which results in an asparagine to serine change at amino acid 216 in the seventh LRR. This mutation was also identified in one family from Canada (Bech-Hansen, Naylor et al. 2000) and appears to involve a conserved residue within the LRR repeats of nyctalopin. In family X08 a nonsense mutation was detected resulting in protein truncation at amino acid 299 with loss of the eleventh LRR, the C-terminal cysteine rich LRR and GPI-anchor. Loss of the GPI-anchor is also the predicted result of a 1 base pair (bp) deletion in family X15 and therefore emphasises the crucial role of the GPI-anchor for nyctalopin function.

Several deletions were detected, including an in-frame 15 bp deletion in families X04 and X06, resulting in the loss of 5 amino acids (glutamate, leucine, arginine, leucine and alanine) from the third LRR and therefore a smaller protein (477 amino acids). This

mutation is predicted to alter the structure of the protein and has also been identified in one other family (Pusch, Zeitz et al. 2000). A 17 bp deletion was found in family X13, which produces a frameshift, predicted to create 91 novel amino acids and a premature stop codon. The third deletion identified in three families (X05, X09 and X14) was a 335 bp deletion causing disruption of the C-terminal cysteine rich LRR and loss of the GPI-anchor (Hardcastle, David-Gray et al. 1997; Pusch, Zeitz et al. 2000), this deletion was shown to segregate with the disorder in the pedigrees concerned. No polymorphisms were detected in the *NYX* gene.

To evaluate the possibility of a founder effect among the families sharing the same mutations (families X05, X09 and X014, families X04 and X06 and families X01 and X07) microsatellite markers were amplified to create a haplotype around the *NYX* gene. Markers DXS574, DXS993, DXS8012 and DXS1201 were amplified in affected males from the families, as previously described (Hardcastle, David-Gray et al. 1997), to reveal a common haplotype in families X05, X09 and X14 suggesting that the 335 bp deletion of *NYX* occurred as a single event in a common ancestor. The other families analysed appeared to be unrelated as no common haplotype was observed in families with the same mutation. Previous *NYX* gene screens also revealed recurring mutations, most notably a 24 bp deletion identified in 7 families (Bech-Hansen, Naylor et al. 2000).

Table 7b: NYX gene sequence changes identified in subjects with CSNB

Pedigree	Exon	Sequence change*	Codon change	Type
X03	2	37+1G→C		Splicing Mutation (Novel)
X13	3a	48-64, 17bp deletion		Frameshift (stop) (Novel)
X04 X06	3a	339-353, 15bp deletion		Amino acid deletion
X01 X07	3b	647A→G	N216S	Amino acid substitution
X08	3c	895C→T	Q299X	Stop (Novel)
X05 X09 X14	3c-d	1122-1457, 335-bp deletion		Protein truncation (Novel)
X15	3d	1309delC	L437delC	Frameshift Stop (Novel)

* position 1 at ATG start site according to AJ278865

7.3 Summary of molecular genetic analysis

Mutation screening of *CACNA1F* and *NYX* genes identified a causative mutation in 14 of the 15 families studied. One novel mutation in the *CACNA1F* gene and five novel mutations in the *NYX* gene have been identified in addition to confirming five previously reported mutations in these genes. In one definitely X-linked pedigree (X02) a mutation was not identified on sequencing. As a result of the mutation screening the XLCSNB subjects were classified by genotype into two groups: subjects with identified *NYX* gene mutations (CSNB1; pedigrees X01, X03-X09) and subjects with *CACNA1F* gene mutations (CSNB2; pedigrees X10-X12).

Figure 7a: *CACNA1F* sequencing results

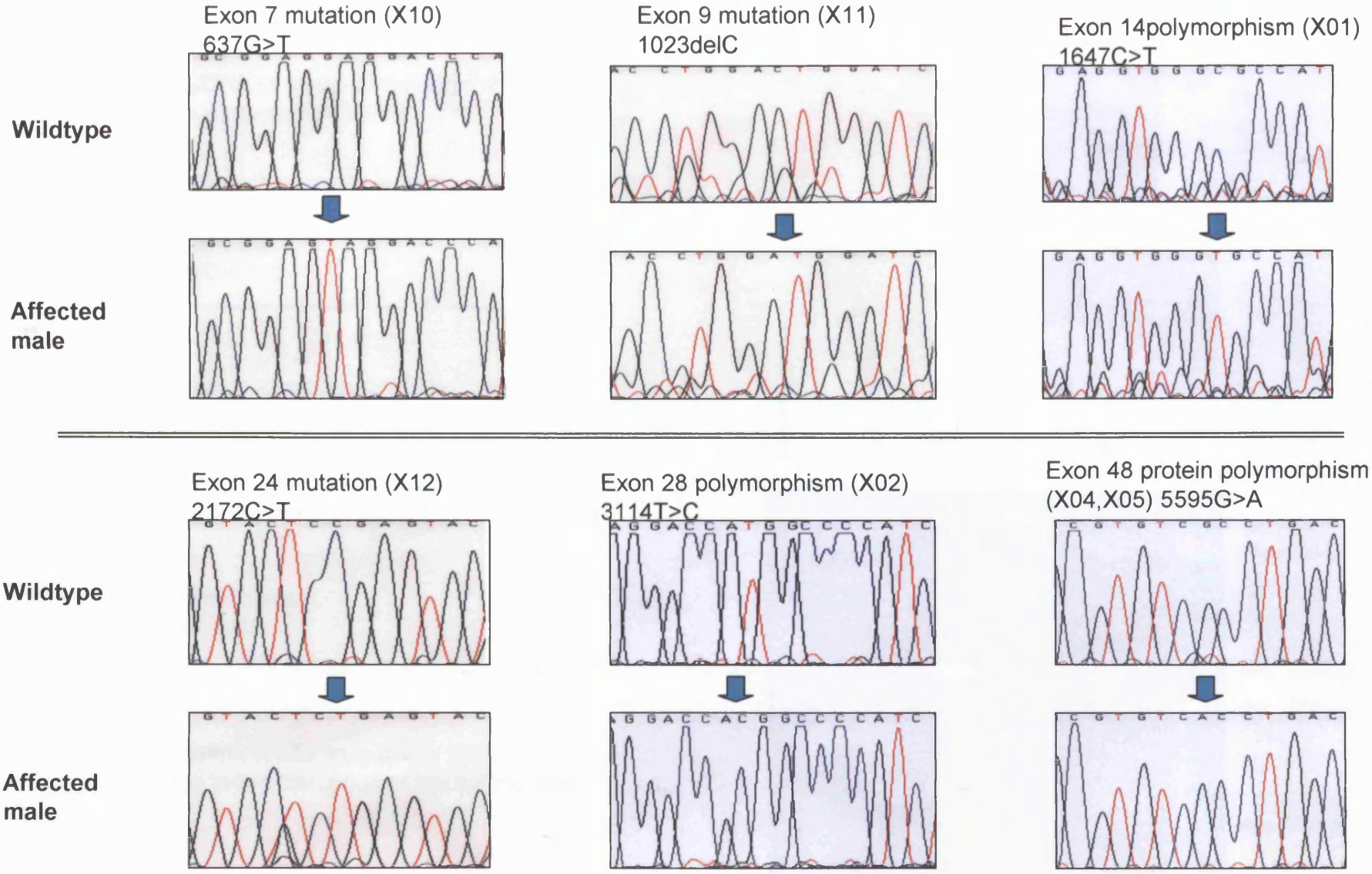

Figure 7b: Enzyme digestion confirmation of novel mutation in exon 7 - pedigree X10

Bse RI cleaves DNA at a site containing the base pair (bp) sequence GAGGAG.

A. Bse RI digestion of wildtype exon 7

Bse RI digestion produces a 170 bp fragment and a 60bp fragment in the normal sequence

B. Bse RI digestion of mutant exon 7

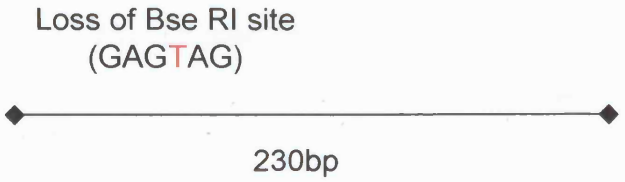

Bse RI digestion produces a single 230bp product due to the disruption of the cutting site

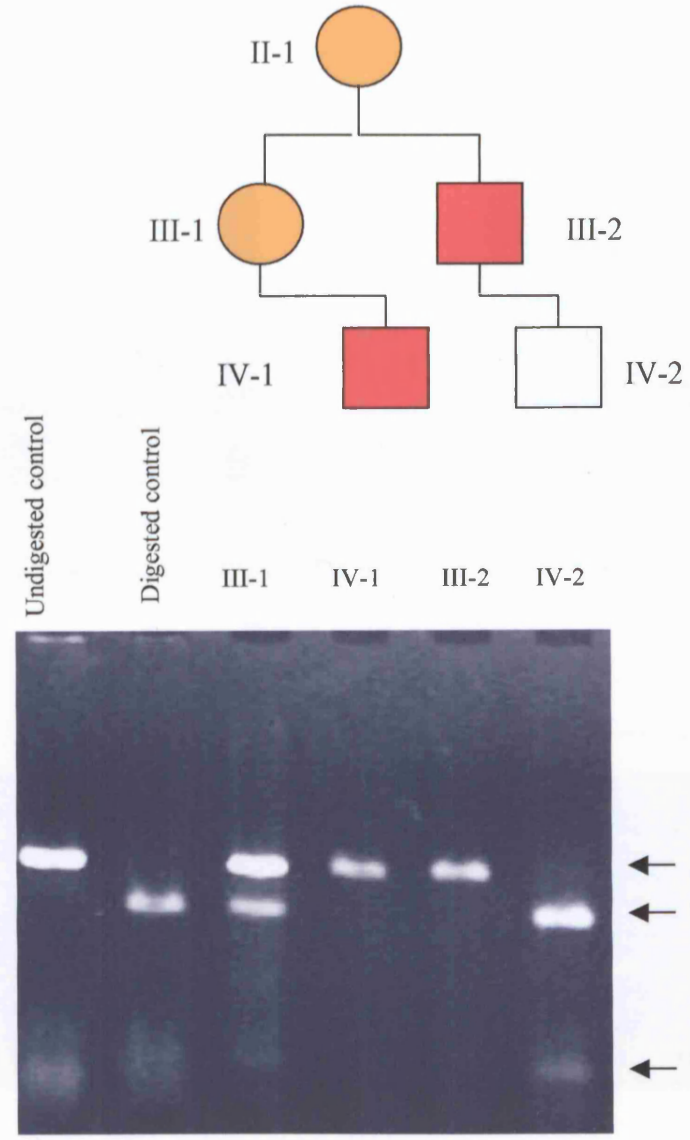

Figure 7c: Enzyme digest confirmation of exon 48 polymorphism – pedigrees X04 and X05

Hph I cleaves DNA at sites with the nucleotide pattern GGTGAnnnnnnn-n'.

A. Hph I digestion of wildtype exon 48

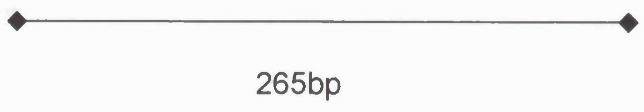

Wildtype exon 48 does not contain this cutting site, a 265bp fragment results from digestion.

B. Hph I digestion of exon 48 polymorphism

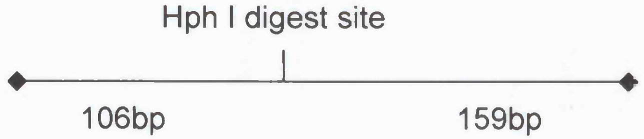

Digest with Hph I results in two fragments.

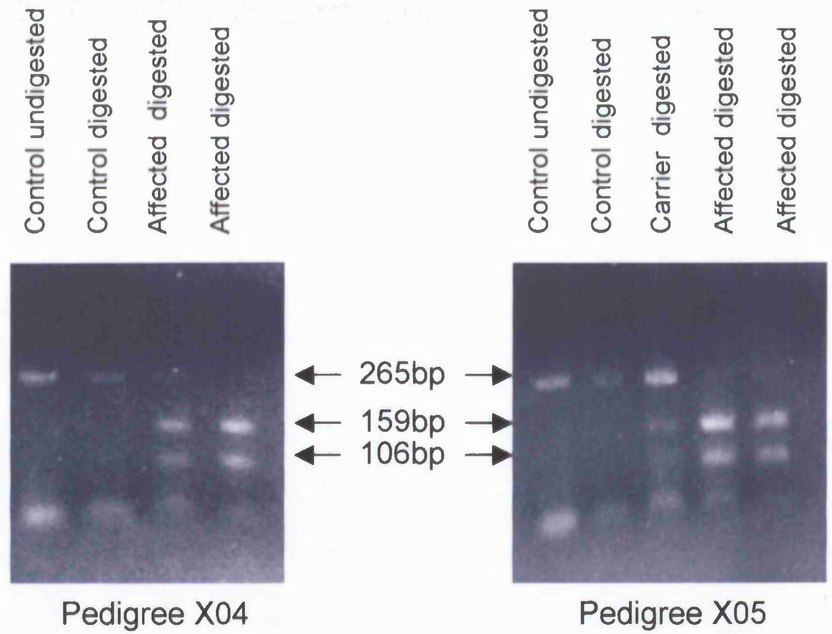

Figure 7d: Screening of controls for exon 48 sequence change

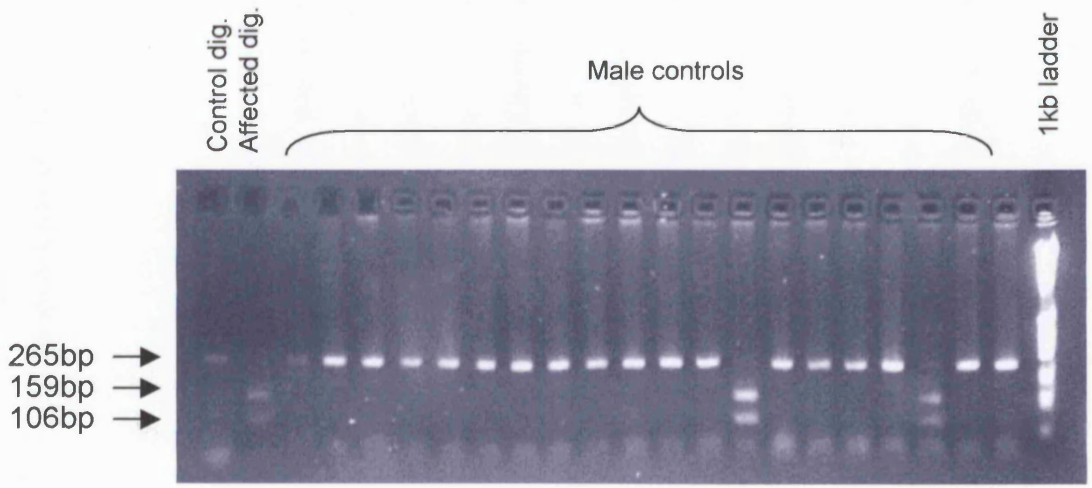

Chapter 8 Clinical examination results

Mutation screening of the genes *CACNA1F* and *NYX* (Chapter 7) enabled the genotypic classification of the XLCSNB subjects in this study into genotype groups CSNB1 (*NYX* gene mutation) and CSNB2 (*CACNA1F* gene mutation). The X-linked family without detected mutations (X02) have been excluded from clinical comparison. Subjects from two pedigrees with *NYX* mutations (X13& X14) were unable to attend either centre for clinical, electrophysiological or psychophysical assessment. The only affected male from pedigree X15 available to take part in the study had a history of bilateral retinal detachments. Since this pathology would be expected to influence his clinical test results, he was excluded from the phenotype study. In total 20 patients from the 11 remaining pedigrees were assessed clinically, 14 in the 8 pedigrees with the CSNB1 genotype and 6 in the 3 pedigrees with the CSNB2 genotype. Pedigrees X01, X03-X09 were in the CSNB1 genotype group and pedigrees X10-X12 were in the CSNB2 group.

8.1 Visual acuity

Symptomatically, although the night blindness had remained stationary with age, the visual acuity had deteriorated in several subjects, both in the CSNB1 genotype group: one subject (pedigree XO3 II-9) had severe visual field loss due to glaucoma, another (pedigree X08 III-1) had developed myopic macular degeneration and had required laser therapy. Corrected visual acuity in each eye and with both eyes open was recorded (Table 8a.). In both the CSNB1 and CSNB2 groups the mean logMAR score was 0.4+/-0.2 units (6/18 equivalent). Figure 8a illustrates a scatterplot and error bar chart of the best binocular corrected visual acuity. Six subjects (32%) had had significant amblyopia (difference in visual acuity of > 0.2 logMAR units between eyes) since childhood. Two subjects had suffered reduced visual acuity as adults: Subject II-9 from pedigree X03 had developed glaucoma for which he had had bilateral trabeculectomies, subject III-1 from pedigree X08 had developed myopic macular degeneration with staphyloma formation and had required macular laser therapy.

8.2 Refractive Error

All 20 subjects were myopic, the mean spherical equivalent ranging from -2DS to –18.5DS. Mean refractive error in the CSNB1 group was –7.25+/-4.5DS and in the CSNB2 group was –8.0+/-1.5DS (Figure 8b&c). The astigmatic element of the refractive error is illustrated in Figure 8c. The mean axial lengths were 26.9+/-1.4mm in the CSNB1 group and 27.9+/-0.4mm in the CSNB2 group, confirming the myopia to be axial rather than refractive.

8.3 Nystagmus and strabismus

Nystagmus was present in 15 of the 20 subjects (75%) and was of similar type (horizontal) in the CSNB1 and CSNB2 groups, the amplitude of nystagmus tended to be larger in subjects with the worse visual acuity. The four patients who did not have detectable nystagmus had a binocular logMAR visual acuity of 0.1-0.2 (6/9).
Strabismus was present in 18 of the 20 subjects (90%). Three subjects had undergone strabismus surgery in childhood (pre-operative deviation is shown in Table 8a). All subjects in the CSNB2 group were esotropic whereas 8 of the 14 subjects (57%) in the CSNB1 group were esotropic and 4 (29%) were exotropic. Two subjects (14%) in this group were orthophoric without strabismus surgery (Figure 8d).

Figure 8a: Scatterplot of best corrected binocular visual acuity (logMAR) between genotypes

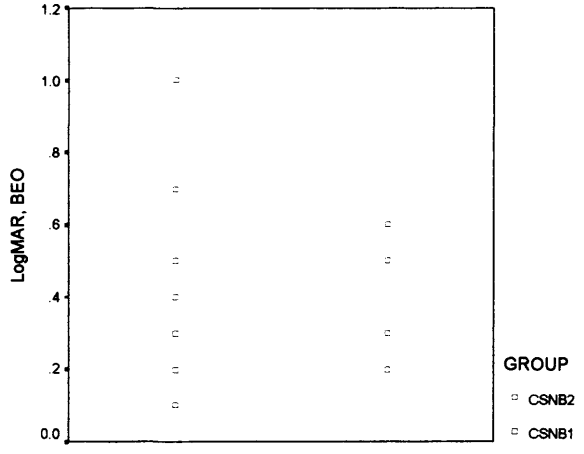

Figure 8b: Scatterplot of mean spherical equivalent between genotypes

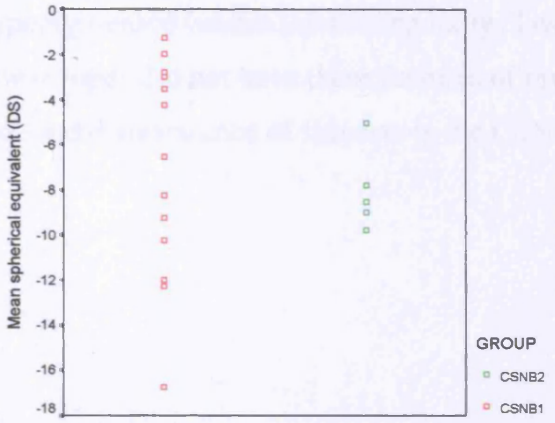

Figure 8c: Refractive error (each axis represents a retinoscopic axis)

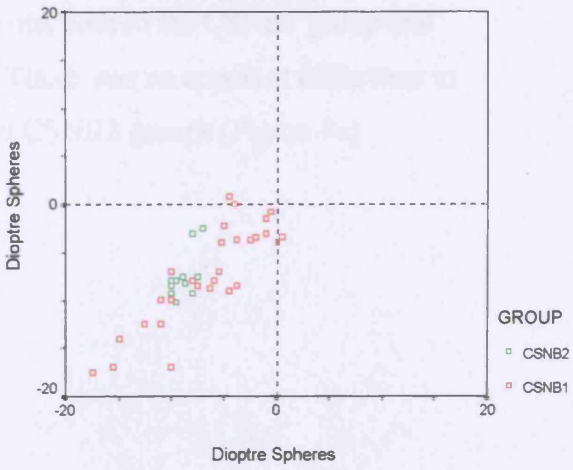

Figure 8d: Comparison of strabismus types between genotype groups

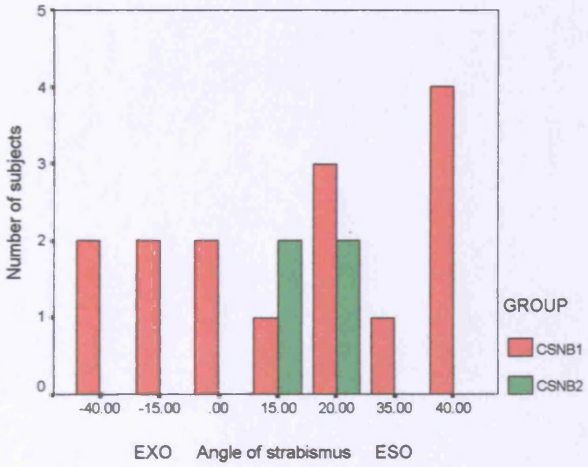

8.4 Slit lamp examination (SLE)

8.4.1 Anterior segment examination

17 of the 20 subjects had normal anterior segment appearance on SLE (Table 8b). One subject had iris translucency (IV-9 from pedigree X03). Subject II-9 from pedigree X03 had features consistent with previous bilateral trabeculectomies. Another had evidence of previous anterior uveitis (III-3 from pedigree X10).

8.4.2 Fundoscopy

18 of the 20 patients (89%) had tilted optic nerve heads and, of these, most had a tigroid, hypopigmented fundus inferotemporally. Two patients, both in the CSNB1 group and low myopes did not have these features of myopia. There was no apparent difference in the fundal appearance of subjects in the CSNB1 and CSNB2 groups (Figure 8e)

Table 8a: Clinical examination of CSNBX subjects

CSNB1 Pedigree	Subject	Age	LogMar OD	OS	OU	Snellen Equiv. OU	Nystagmus	Strabismus	Mean Sph Equiv. (DS)	Mean Axial Length (mm)
X01	IV-2	16	0.2	0.3	0.1	6/9	None	40PD ET	-2.75	25.45
X03	II-9	75	0.5	0.6	0.5	6/18	Fine, horiz	OT	-1.25	
	II-11	67	0.5	1	0.4	6/18	Fine, horiz	OT	-3.5	26.02
	IV-9	36	1	0.3	0.3	6/12	Fine, horiz	20PD ET	-8.25	27.13
	IV-17	17	0.4	1	0.4	6/18	Fine, horiz	20PD ET	-9.25	
X04	IV-2	30	0.8	1	0.5	6/18	Fine, horiz	40PD ET	-10.25	28.43
X05	V-2	54	0.5	0.6	0.4	6/18	Fine, horiz	40PD XT	-4.25	26.12
	VI-6	24	0.4	0.8	0.4	6/18	Fine, horiz	40PD ET	-16.75	28.54
	VI-7	21	1	0.8	0.7	6/36	Coarse, horiz	40PD ET	-12.00	28.10
X06	III-5	62	0.5	0.2	0.2	6/9	None	20PD ET	-2.0	25.13
X07	III-1	48	0.2	0.6	0.2	6/9	Fine, horiz	35PD ET	-6.5	27.85
X08	III-1	40	1	1	1	6/60	Fine, horiz	40PD XT	-12.25	28.21
	IV-2	11	0.2	0.8	0.2	6/9	None	15PD XT	-8.25	
X09	IV-6	63	0.3	0.2	0.2	6/9	None	15PD XT	-3.0	25.32
CSNB2 pedigree										
X10	III-3	51	0.8	0.6	0.6	6/24	Coarse, horiz	20PD ET	-9.0	28.14
	IV-8	26	0.6	0.6	0.5	6/18	Coarse, horiz	15PD ET	-5.0	
X11	III-3	79	0.7	0.6	0.6	6/24	Coarse, horiz	15PD ET	-8.5	
	IV-2	17	0.4	0.3	0.3	6/12	Fine,horiz	15PD ET	-9.75	27.65
	IV-5	8	0.5	0.3	0.3	6/12	Fine, horiz	20PD ET	-7.75	
X12	IV-2	11	0.2	0.2	0.2	6/9	None	15PD ET	-8.5	

PD=prism dioptres

Table 8b Slit lamp examination features of XLCSNB subjects

CSNB1 Pedigree	Subject	Age	Iris translucency	Optic disc tilt	Fundal Hypopigmentation	Other Features
X01	IV-2	16	No	No	No	
X03	II-9	75	No	Yes	Infero-temporal	Glaucomatous disc cupping L>R
	II-11	67	No	Yes	Infero-temporal	
	IV-9	36	Yes	Yes	Infero-temporal	
	IV-17	17	No	Yes	Infero-temporal	
X04	IV-2	30	No	Yes	Infero-temporal	
X05	V-2	54	No	Yes	Macula and IT	
	VI-6	24	No	Yes	Macula and IT	
	VI-7	21	No	Yes	Macula and IT	
X06	III-5	62	No	Yes	Infero-temporal	
X07	III-1	48	No	Yes	Inferotemporal	
X08	III-1	40	No	Yes	Inferotemporal	Bilateral staphylomata, laser scars
	IV-2	11	No	Yes	No	
X09	IV-6	63	No	No	No	Mild atrophic macular change
CSNB2 pedigree						
X10	III-3	51	No	Yes	Infero-temporal	Bilateral cataracts
	IV-8	26	No	Yes	No	
X11	III-3	79	No	Yes	Infero-temporal	
	IV-2	17	No	Yes	Infero-temporal	
	IV-5	8	No	Yes	No	
X12	IV-2	11	No	Yes	Infero-temporal	

IT=infero-temporal

Figure 8e: Fundus appearance

CSNB1 (*NYX* mutation)

X03 IV-9

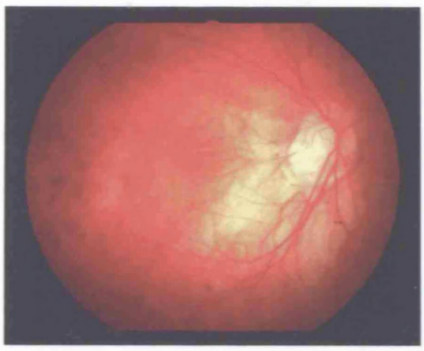

X09 IV-6

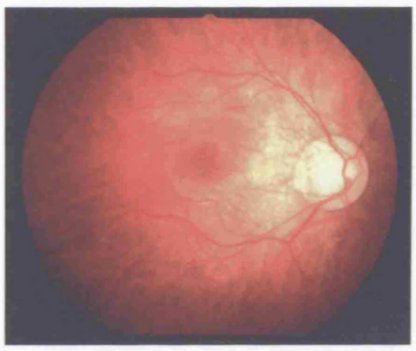

X04 IV-2

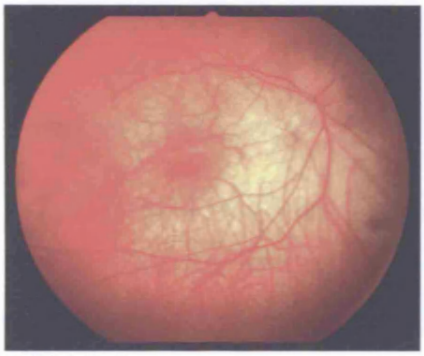

CSNB2 (*CACNA1F* mutation)

X05 VI-6

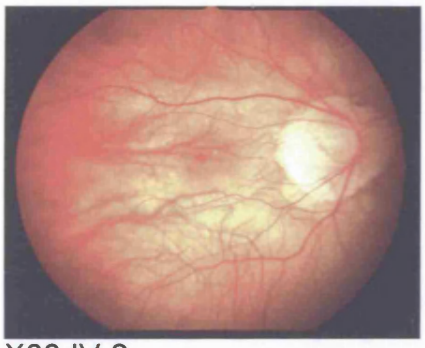

X10 III-3

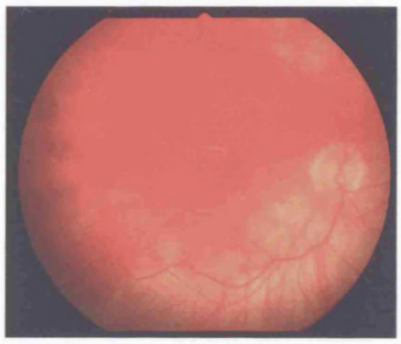

X08 IV-2

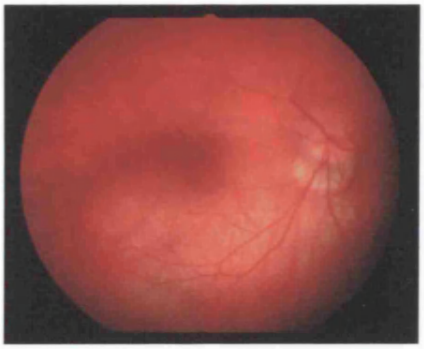

X11 IV-2

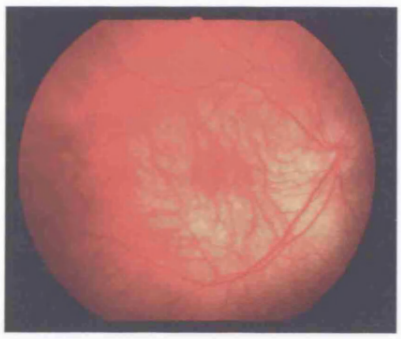

Chapter 9 Psychophysics results

9.1 Colour vision

A summary of the colour vision testing results in shown in Table 9a. No specific colour vision abnormalities detected in the majority of subjects. The subjects with the more severe colour abnormalities had other pathology that might explain this. Subject X03 II-9 had glaucomatous optic disc cupping, Subject X05 V-2 had bilateral macular staphylomata, Subject X08 III-1 had bilateral myopic maculopathy previously treated with focal laser therapy.

9.2 Photopic Perimetry

Photopic perimetry identified normal or near normal foveal sensitivities but a gradual reduction in sensitivity with eccentricity from the fovea in most subjects (Figure 9a). Central sensitivities were reduced in the subject with myopic maculopathy (X08 III-1) and extensive visual field loss was present in the subject with glaucomatous disc cupping (X03 II-9). There was no evidence of visual field constriction or mid-peripheral scotomata.

9.3 Scotopic Perimetry

Scotopic static perimetry was performed on 9 adult subjects, 7 in the CSNB1 group and 2 in the CSNB2 group according to the protocol (Chapter 6.5.1). Examples of the results are shown in Figure 9b. The first graph is a grey scale representation of scotopic sensitivity. Normal values when the short wavelength, blue stimulus is used is 46dB or a clear grey scale (10dB=1 log unit) and for the long wavelength, red stimulus, 34dB or a lightly stippled gray scale. Mean sensitivity measurement was calculated by averaging the values measured at retinal locations -9,+9 and +9,-9 on the HFA grid.. The range of mean threshold elevation in subjects with *NYX* mutations (CSNB1) was 2.5-4.4 (mean 3.5) log units with the blue and 1.6-3.1(mean 2.0) log units with the red stimulus. Subjects with *CACNA1F* mutations (CSNB2) showed a range of mean threshold

elevation of 1.3-2.3 (mean 2.0) log units for the blue and 1.8-1.9 (mean 1.9) log units for the red stimulus. In every subject there was a relative reduction in sensitivity in the superior visual field, i.e. the inferior retina, of up to 1 log unit compared to the inferior field.

Table 9a: Results of colour vision assessment

CSNB1 Pedigree	Subject	Ishihara	City University	HRR test	M-R Minimalist Normal = P1,D1,T1	Cambridge Colour Test Normal= P<100, D<100, T<150
X01	IV-2	Normal	Normal	Normal	Normal	Normal
X03	11-9	Missed most R-G plates	Normal	Missed most R-G plates Normal	P3,D4, T1	N/A
	II-11	Normal	Normal	Normal	Normal	N/A
	IV-9	Normal	Normal	Normal	Normal	Normal
	IV-17	Normal	Normal		Normal	Normal
X04	IV-2	Missed most R-G plates	Normal	Missed most R-G plates	P1,D3,T2	P266,D448,T164
X05	V-2	Missed most R-G plates	3 R-G plates incorrect Normal	Missed all R-G and B-Y plates	P2,D3,T1	P1100, D1100,T1100 Normal
	VI-6	Normal	Normal	Normal	Normal	Normal
	VI-7	Normal		Normal	Normal	
X06	III-5	Normal	Normal	Normal	Normal	Normal
X07	III-1	Normal	Normal	Normal	P1,D1,T3	N/A
X08	III-1	Normal	Normal	Missed most R-G plates Normal	P6,D6,T2	N/A
	IV-2	Normal	Normal		P3,D2,T2	P311,D100,T153
X09	IV-6	Normal	Normal	Normal	Normal	P232,D219,T204
CSNB2 Pedigree						
X10	III-3	Normal	Normal	Missed most B-Y plates Normal	Normal	P163,D154,T322
	IV-8	Normal	Normal		Normal	N/A
X11	III-3	Normal	Normal	Normal	Normal	N/A
	IV-2	Normal	Normal	Normal	Normal	N/A
	IV-5	Normal	Normal	Normal	Normal	N/A
X12	IV-2	Normal	Normal	Normal	Normal	N/A

Figure 9a: Photopic perimetry from representative subjects. Photopic perimetry identified a gradual reduction in sensitivity with eccentricity from the fovea in most subjects from each genotype group.

CSNB1 X04 IV-2

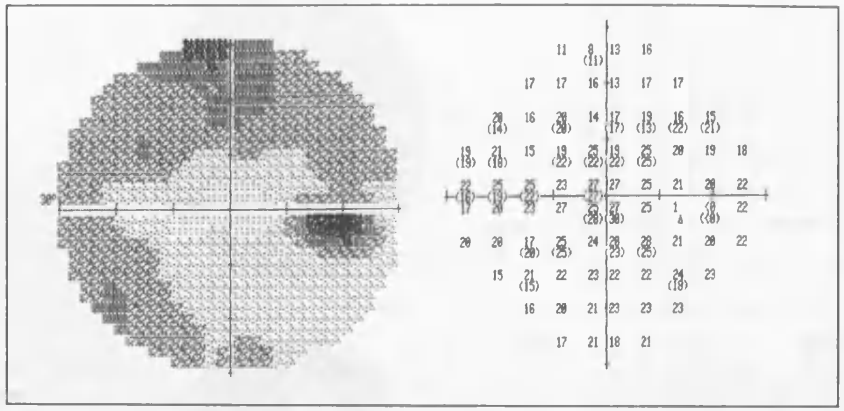

CSNB1 X03 IV-9

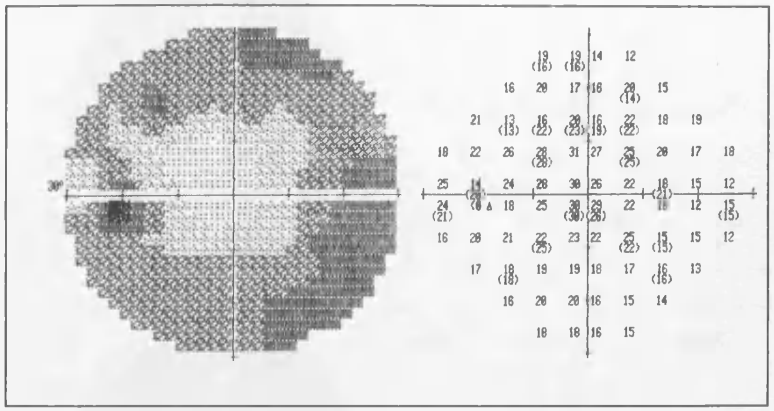

CSNB1 X09 IV-6

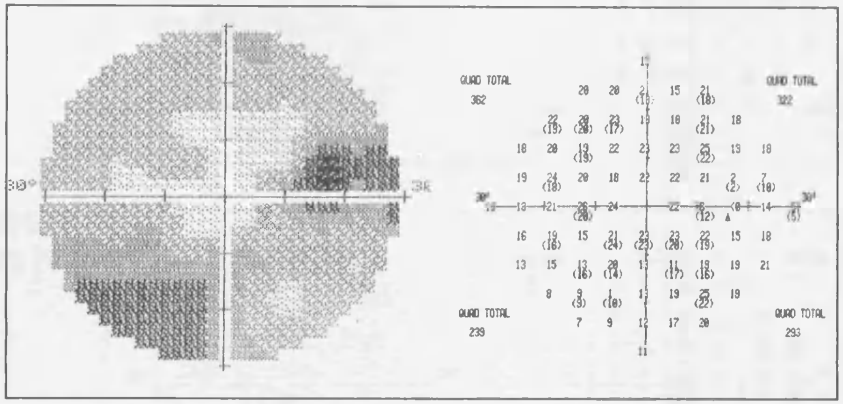

CSNB2 X10 IV-8

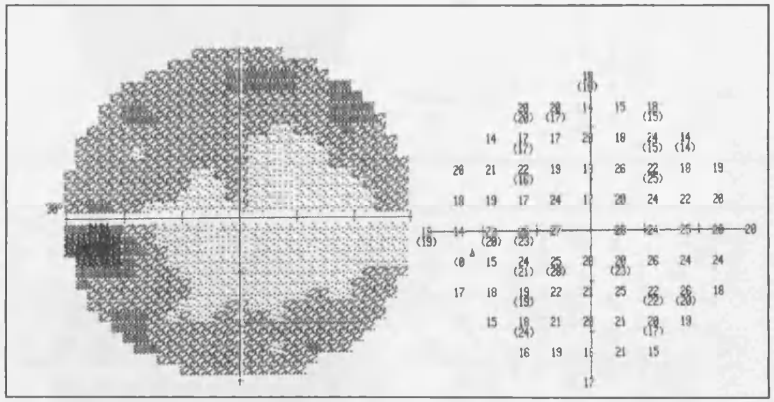

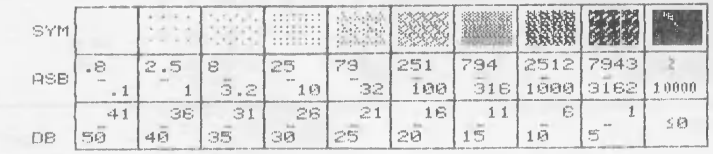

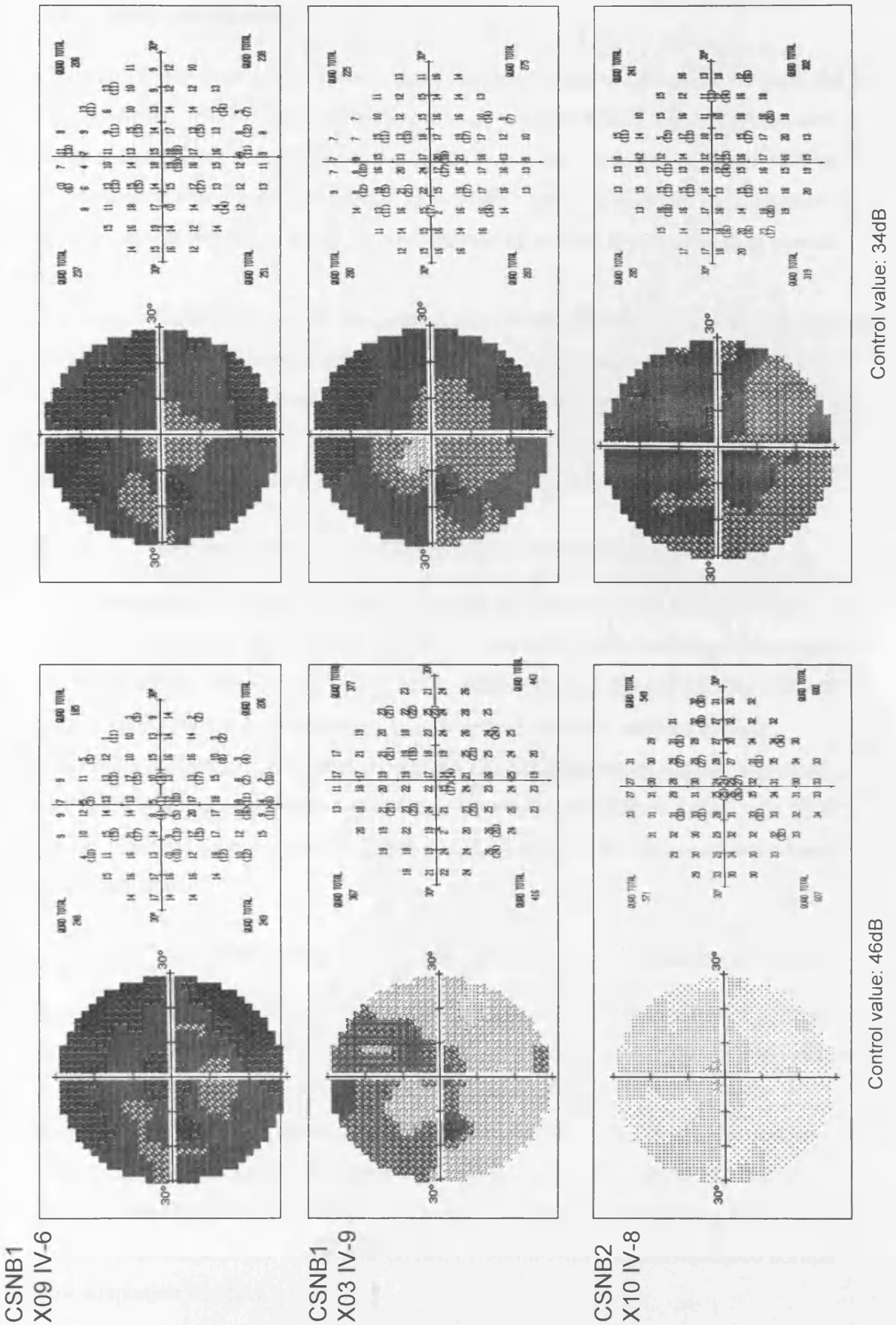

Figure 9b: Scotopic perimetry:

9.4 Dark adaptometry

Dark adaptation was tested in two retinal locations using a red stimulus (650nm) and a blue stimulus (450nm) as stated in the protocol (Chapter 6.5.2). Representative dark adaptation curves for these four stimulus conditions are illustrated in Figure 9c. Due to differences in technique, the absolute values differ from the scotopic static perimetry determinations, therefore all results are reported as relative to corresponding normal values.

The control curve in Figure 9c demonstrates the threshold intensity for the blue and red stimulus at the two retinal locations tested. The threshold increases by approximately 4log units following the bleach and a blue stimulus rod/cone break occurs after approximately 9 minutes of dark adaptation. Pre-bleach threshold measurements are reached after approximately 30-40 minutes of dark adaptation.

9.4.1 Dark adaptometry in subjects with *NYX* mutations (CSNB1)

The mean absolute threshold for the two retinal test locations was elevated by 2.4 - 4.3 log units for the blue stimulus and by 1.9 - 3.2 log units for the red stimulus compared to control values. Four of the seven CSNB1 subjects tested showed definite rod/cone breaks for the blue stimulus, occurring after approximately 9 minutes of dark adaptation, the other curves were unreliable. The dark adaptation curves are plotted together for the blue stimulus tested at retinal location -9,9 (Figure 9d(i)). All CSNB1 subjects reached their pre-bleach thresholds by 30 minutes and demonstrated normal adaptation kinetics.

9.4.2 Dark adaptometry in subjects with *CACNA1F* mutations (CSNB2)

Two subjects with CSNB2 underwent dark adaptometry. The blue stimulus absolute threshold was elevated by 0.6 - 1.5 logunits and the red stimulus absolute threshold by 0.7 - 1.8 log units compared to controls. Although 1 of the 2 CSNB2 subjects demonstrated a rod/cone break (Figure 9d(ii)), subject X10 III-3 showed a monphasic curve with increased sensitivity compared to the control. This subject had bilateral cataracts which presumably prevented a complete bleach prior to testing. Both CSNB2 subjects reached their pre-bleach thresholds by 30 minutes and demonstrated normal dark adaptation kinetics.

Figure 9c: Dark adaptation curves: red and blue stimuli, retinal locations –9,9, 9,-9. Rod/cone breaks were demonstrated in subjects from each genotype groups to the blue stimulus only.

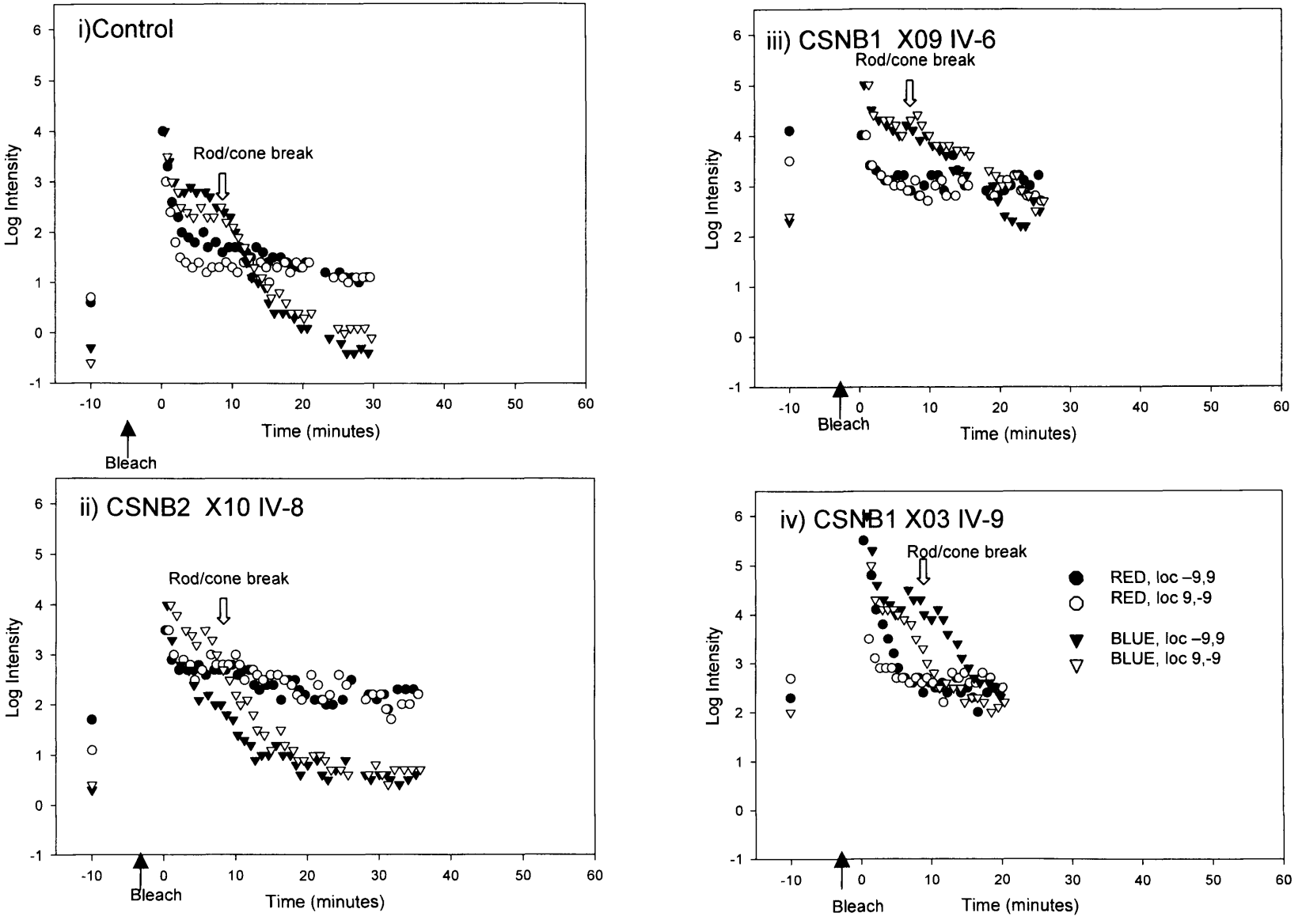

Figure 9d: Dark adaptation curves: Blue stimulus, retinal location –9,9

i) CSNB1 subjects

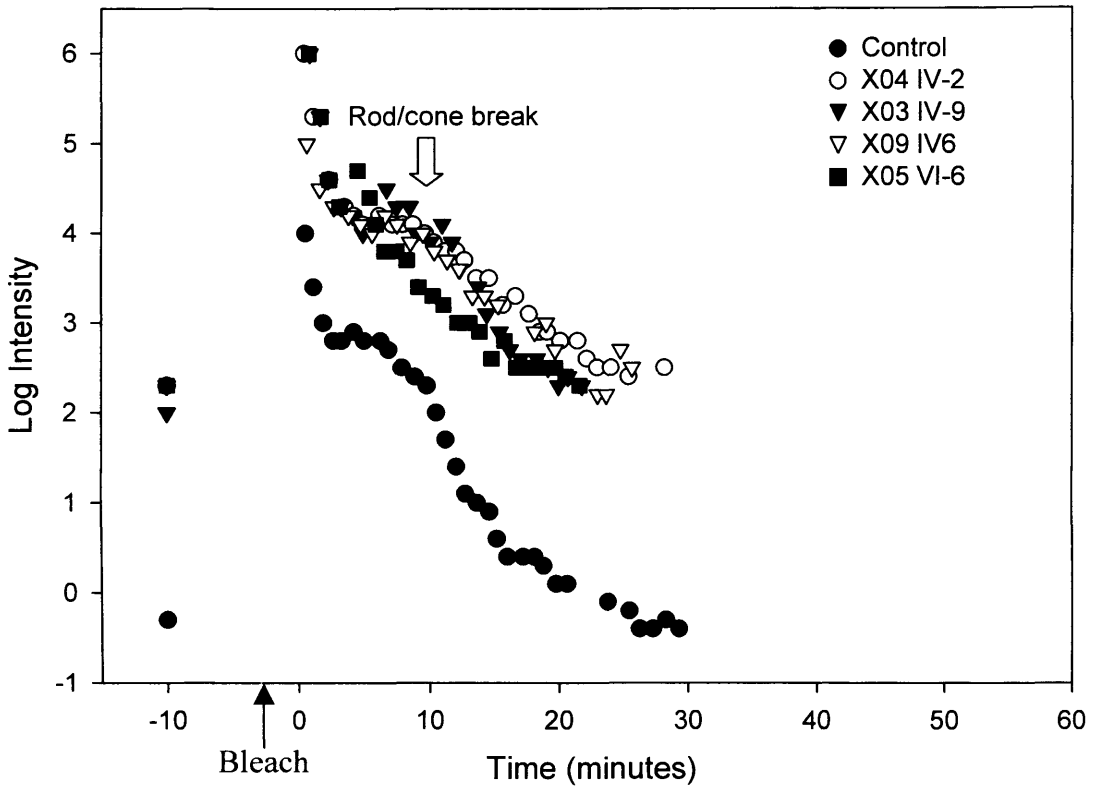

ii) CSNB2 subjects

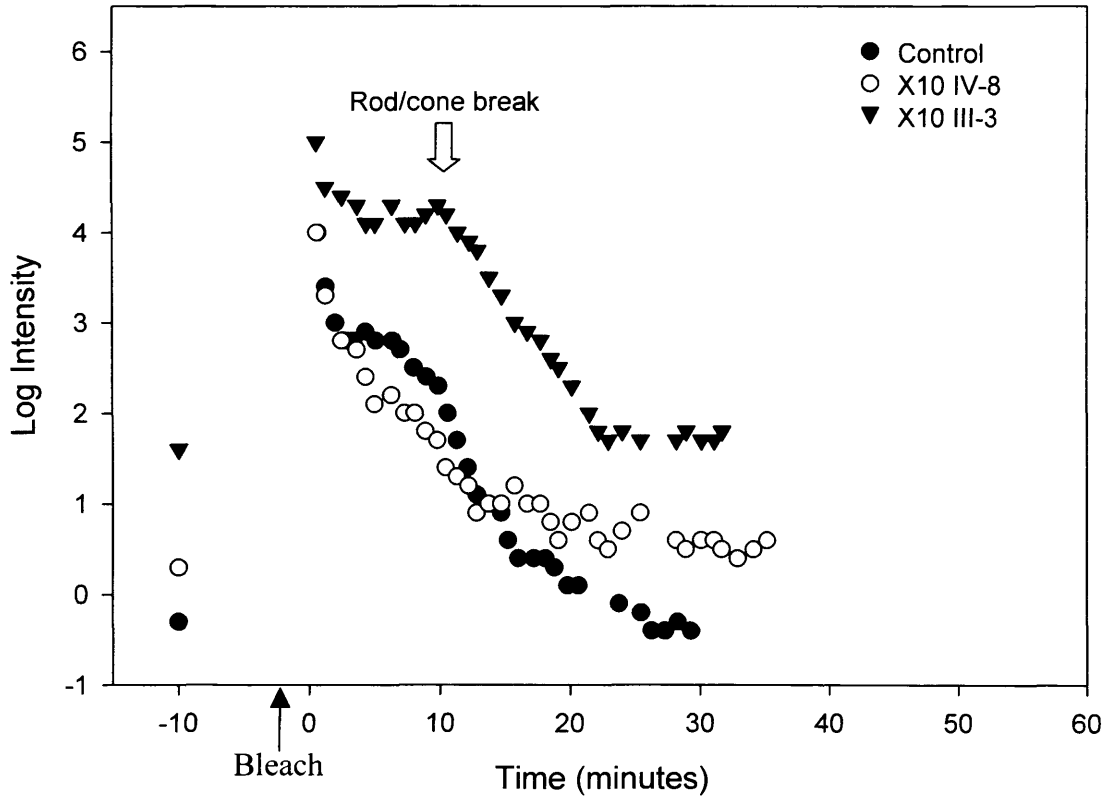

9.5 Spectral sensitivity curves

Four CSNB1 subjects and 2 CSNB2 subjects underwent assessment of spectral sensitivity. Spectral sensitivities to the 5 different wavelengths (450nm, 488nm, 590nm and 633nm) were calculated and plotted for the two retinal locations tested (Figure 9e). The CIE scotopic sensitivity curve shown in Figure 9e has been shifted downwards on the y-axis to enable comparison of curve shape with the XLCSNB subjects tested. The spectral sensitivity curves of all subjects in each genotype group fitted the CIE curve with no apparent shift in peak sensitivity towards longer wavelengths.

Figure 9e: Spectral sensitivity curves for retinal position 9,-9.

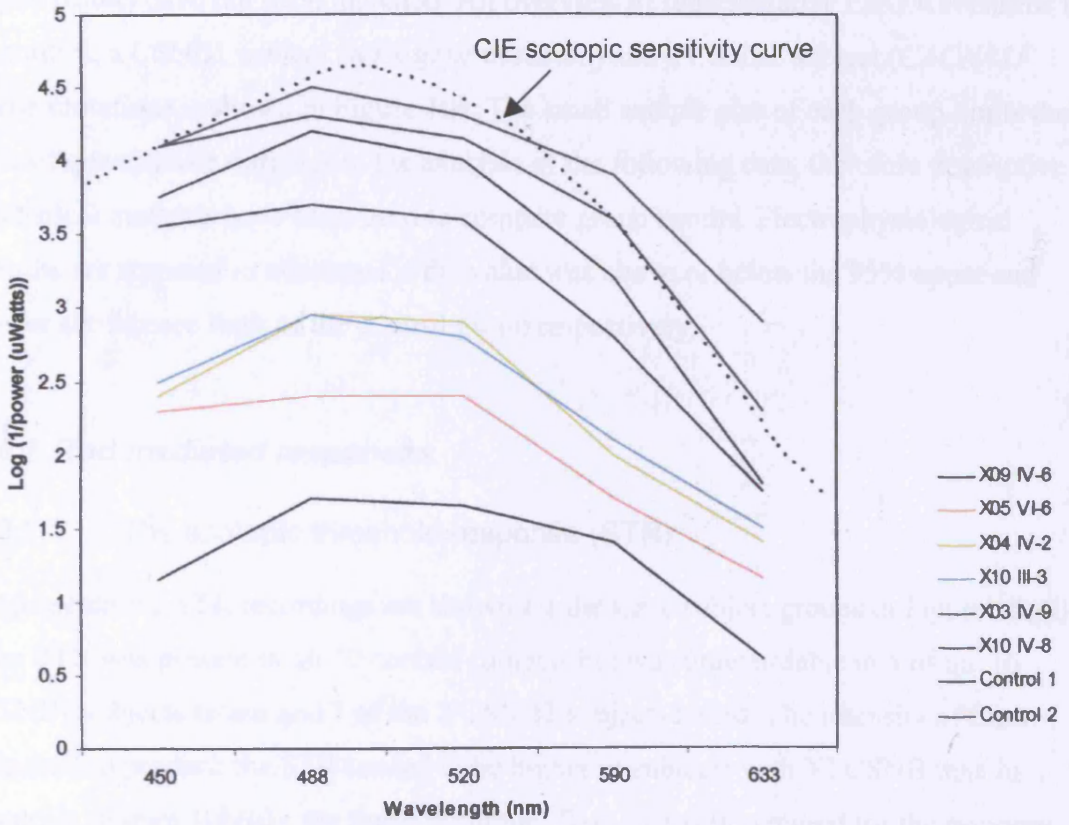

Chapter 10 Electrophysiology

ISCEV standard ERGs were performed in the manner described in Chapter 6. Eleven pedigrees had previously been identified as having an *NYX* gene mutation (Chapter 8). Eleven affected male subjects from 8 of these 11 pedigrees were assessed electrophysiologically using foil electrodes. One pedigree (X15) was excluded due to the subject's history of bilateral retinal detachments. Affected members from 2 pedigrees were unavailable for testing. Four affected males from the 3 pedigrees with identified *CACNA1F* gene mutations were also assessed. Where possible scotopic threshold responses, ON-OFF responses and visual evoked potentials were also performed. Skin disc electrodes were used for one child in each genotype group and these results have not been included. An overview of representative ERG waveforms for a control, a CSNB1 subject (*NYX* gene mutation) and a CSNB2 subject (*CACNA1F* gene mutation) is shown in Figure 10a. The small sample size of each group limits the use of quantitative statistics in the analysis of the following data, therefore descriptive statistical methods have been used to compare group results. Electrophysiological results are reported as abnormal if the value was above or below the 95% upper and lower confidence limit of the control group respectively.

10.1 Rod mediated responses

10.1.1 The scotopic threshold response (STR)

Representative STR recordings are shown for the three subject groups in Figure 10b(i). The STR was present in all 10 control subjects but was unrecordable in 5 of the 10 CSNB1 subjects tested and 1 of the 2 CSNB2 subjects tested. The intensity of flash required to produce the STR tended to be higher in subjects with XLCSNB than in controls (Figure 10b(ii)): the mean minimum flash intensity required for the response was SF-6.9 log units in controls and SF-5.3 log units in XLCSNB subjects. The intensity of the stimulus required to produce the maximum response was comparable in the subject groups. The maximum STR amplitudes tended to be larger in control subjects than XLCSNB subjects (Figure 10b(iv)). The latency of the response was delayed in 4 of the 5 CSNB1 subjects and 1 CSNB2 subject.

Figure 10a: Comparison of ERG waveforms

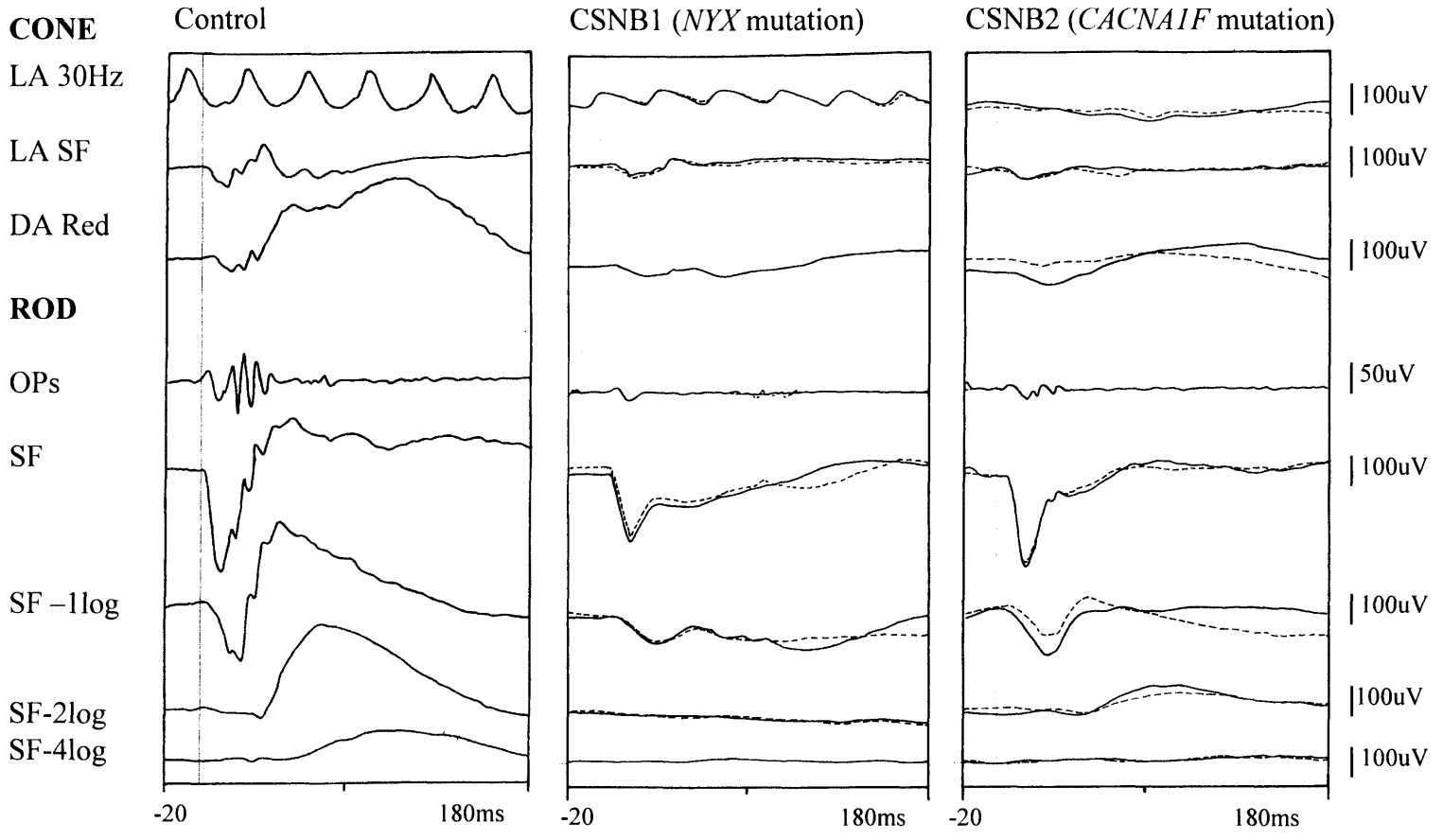

Key

Cone: Cone mediated responses
Rod: Rod mediated responses
LA: Light adapted, DA: Dark adapted
SF: Standard Flash stimulus
Ops: Oscillatory Potentials

Figure 10b: The scotopic threshold response

i) Representative STR waveforms

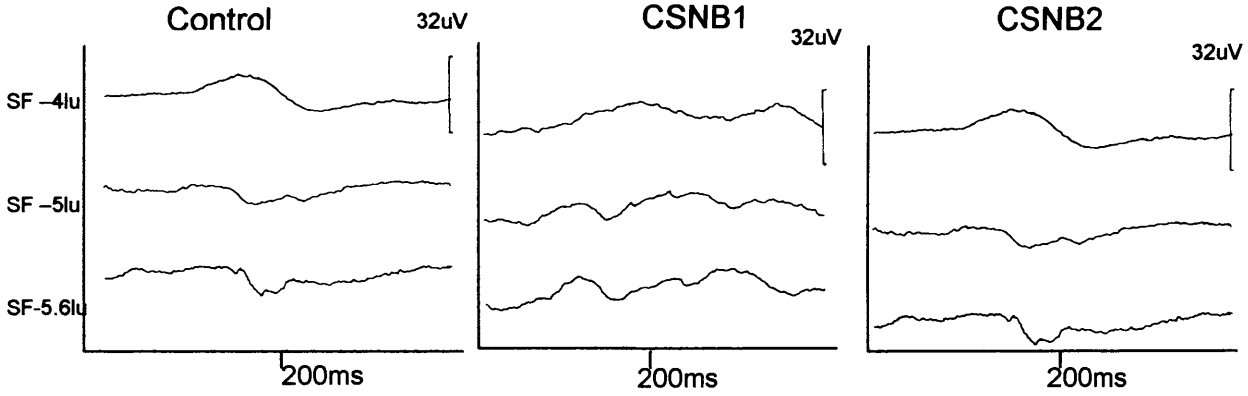

ii) Intensity of stimulus at first recorded scotopic threshold response

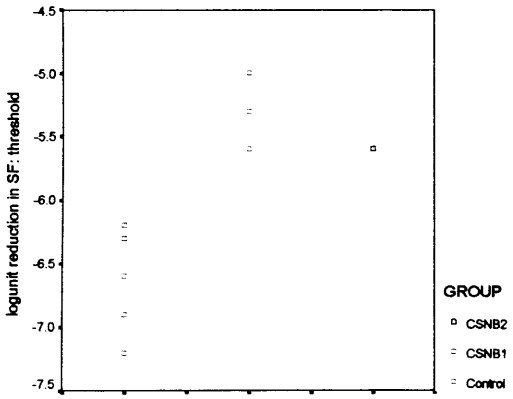

iii) Intensity of stimulus at maximum recorded scotopic threshold response

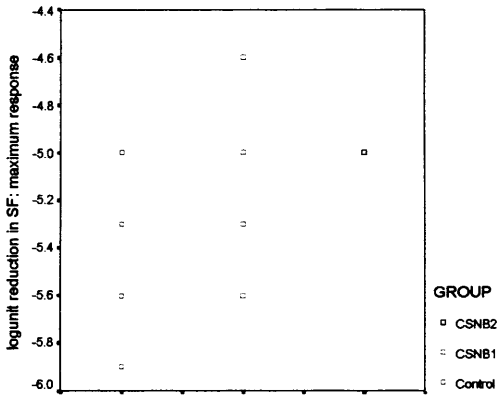

iv) Maximum scotopic threshold response amplitude scatterplot and error bar chart

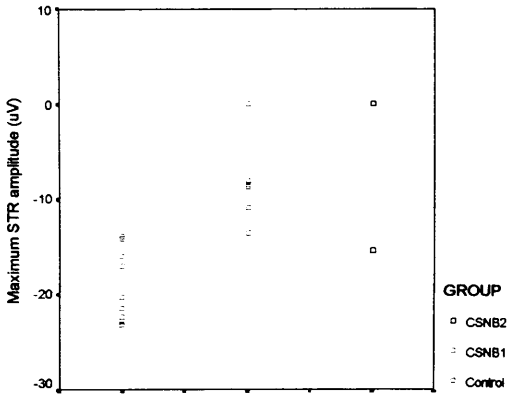

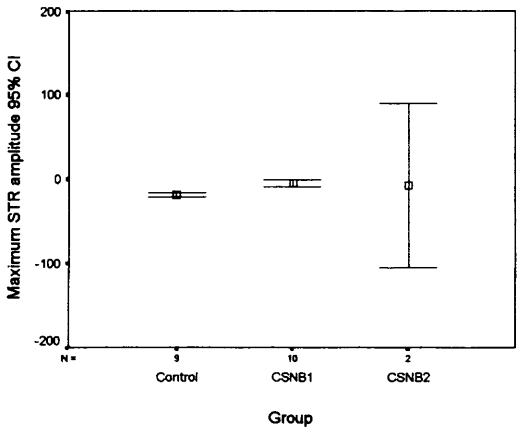

10.1.2 The scotopic ERG

The scotopic ERG was measured to three different intensities of stimulus: Standard Flash (SF)– 4 log units, SF-2.6 log units and SF–1 log unit. The a-wave becomes measurable at SF–1 log unit flash intensity. The characteristics of the b-wave are most accurately assessed in these scotopic conditions where the a-wave is not a complicating feature of the waveform. Representative responses to ISCEV standard scotopic stimulation (SF-2.6 log unit filter) are shown in Figure 10c(i).

Scotopic ERG responses are summarised in Table 10a.The a- and b-wave latency for each stimulus intensity results were normal in both genotype groups. The b-wave amplitude was subnormal in all XLCSNB subjects for each stimulus intensity (Figure 10c(ii)). A response to the ISCEV standard scotopic stimulus (SF –2.6 log units) was detected in 9 of the 11 (82%) CSNB1 subjects and 3 of the 4 (75%) CSNB2 subjects. The mean b-wave amplitude did not appear to differ markedly between genotypes.

Summary

- a- and b-wave latencies were generally normal in both forms of CSNB
- A b-wave response to the standard ISCEV scotopic stimulus (SF -2.6logunits) was present in the majority of XLCSNB subjects from each genotype group.
- The b-wave response was subnormal in all subjects with CSNB.

Table 10a: Table of scotopic ERG properties

Stimulus intensity	Property	Control (n=19)	NYX mutation group (n=11)	CACNA1F mutation group (n=4)
SF-4lu	b-wave amplitude (uV)	78+/-29	3+/-5	11+/-7
	Response recorded in N° (%)	19 (100%)	3 (27%)	3 (75%)
SF-2.6lu	b-wave amplitude (uV)	267+/-66	17+/-13	49+/-39
	Response recorded in N° (%)	19(100%)	9(82%)	3(75%)
SF	a-wave amplitude (uV)	-315+/-60	-307+/-84	-268+/-43
	Response subnormal in N° (%)	0	2 (18%)	0
	b-wave amplitude (uV)	472+/-85	190+/-57	204+/-51
	Response subnormal in N° (%)	0	11 (100%)	4 (100%)
	Maximal OP amplitude (uV)	62+/-25	0	26+/-8
	Response subnormal in N° (%)	0	11 (100%)	0
	b-wave:a-wave ratio	1.5+/-0.2	0.6+/-0.1	0.8+/-0.1

lu=log units
uV=microvolts

Figure 10c: Rod mediated ERG results (dark adapted eye)

i)Representative rod ERGs (SF-2.6lu).

Note differing scales and lower amplitude responses in both XLCSNB groups.

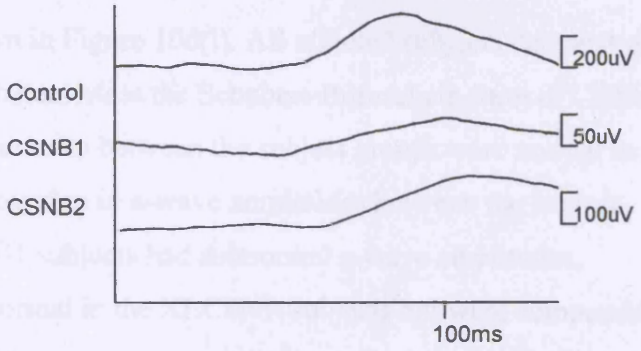

ii) B-wave amplitude scatterplots. Subnormal b-wave amplitudes are illustrated in both genotype groups, the CSNB1 subjects (NYX mutations) having the most attenuated response.

SF-4.0 log unit intensity

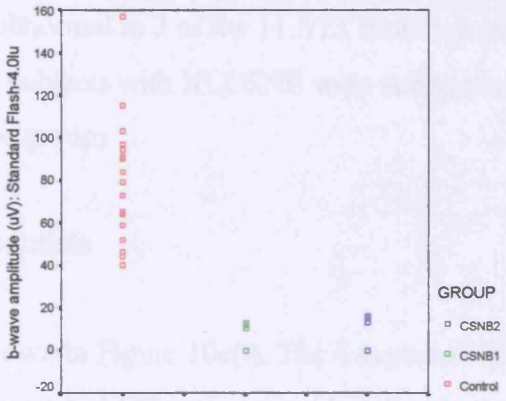

SF-2.6 log unit intensity (Standard scotopic stimulation)

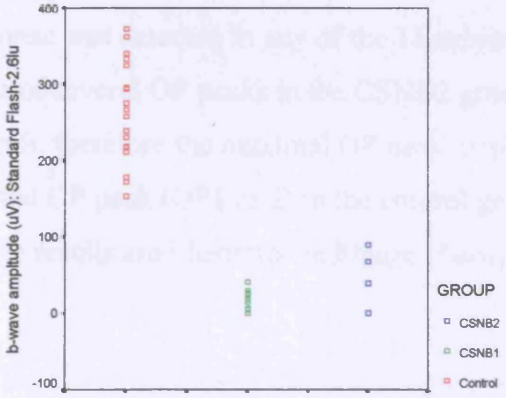

SF-1.0 log unit intensity

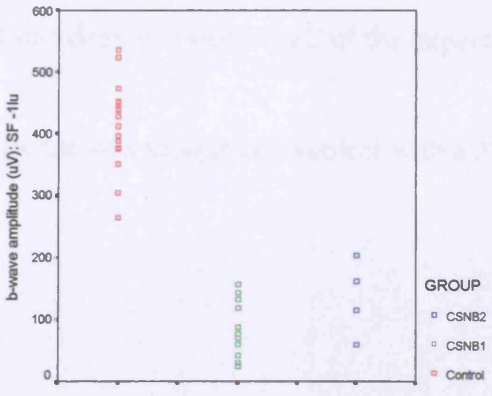

10.1.3 The Dark Adapted Standard Flash ERG

Representative responses are shown in Figure 10d(i). All affected subjects demonstrated the 'negative wave' ERG which characterises the Schubert-Bornschein form of CSNB. The a- and b-wave latency measurements between the subject groups were normal in both genotype groups. There was overlap in a-wave amplitudes between the subject groups, two of the 11 (18%) CSNB1 subjects had subnormal a-wave amplitudes. The b-wave amplitudes were subnormal in the XLCSNB subjects but were comparable between genotypes (Figure 10d(ii)).

Summary

- The a-wave amplitude was subnormal in 2 of the 11 *NYX* mutation subjects
- The b-wave amplitudes in all subjects with XLCSNB were subnormal but comparable between genotype groups

10.1.4 Scotopic oscillatory potentials

Representative OP waveforms are shown in Figure 10e(i). The 4 expected OP peaks were identified in all control subjects, several OP peaks were identified in the subjects with CSNB2 but no measurable response was detected in any of the 11 subjects in the CSNB1 genotype group. The absence of several OP peaks in the CSNB2 group made assignment of the peak number difficult, therefore the maximal OP peak amplitude was measured and compared to the maximal OP peak (OP1 or 2) in the control group and peak latencies were not compared. The results are illustrated in Figure 10e(ii).

Summary

- Scotopic OP responses were abnormal in all CSNBX subjects
- Subjects with *CACNA1F* mutations demonstrated only 2 of the expected 4 OP peaks
- No measurable scotopic OP response was seen in any subject with a *NYX* mutation

Figure 10d: Dark adapted Standard Flash ERG results

i) Representative waveforms.
Note the "negative" waveform in XLCSNB and the smooth contour of the ascending limb of the b-wave in CSNB1 (*NYX* mutation).

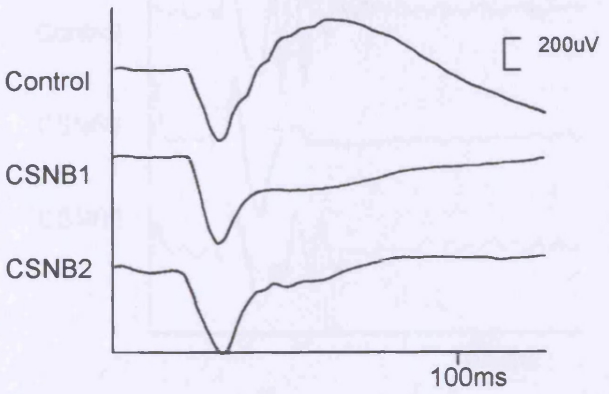

ii) B-wave amplitude scatterplot and error bar chart. Subnormal b-wave amplitude are illustrated in both XLCSNB groups to this stimulus, the mean response being similar in both genotype groups.

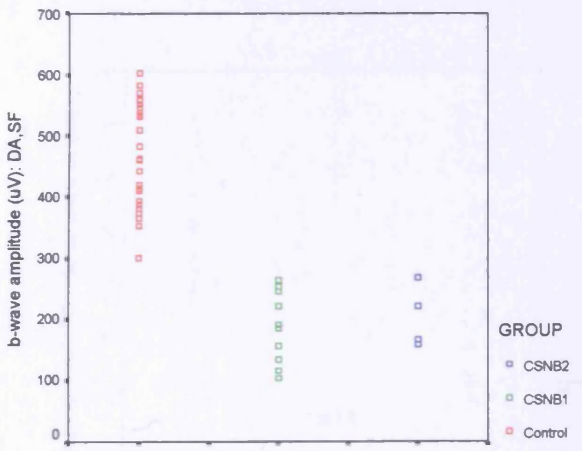

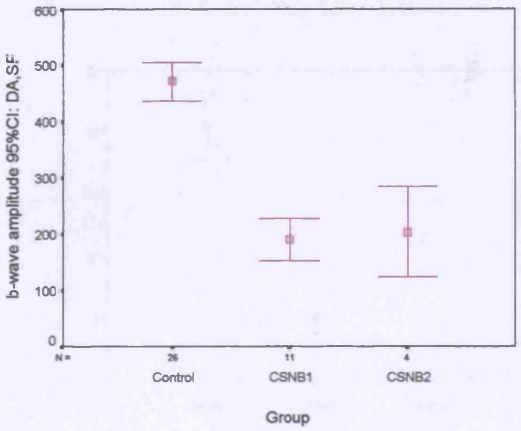

Figure 10e: Oscillatory potentials

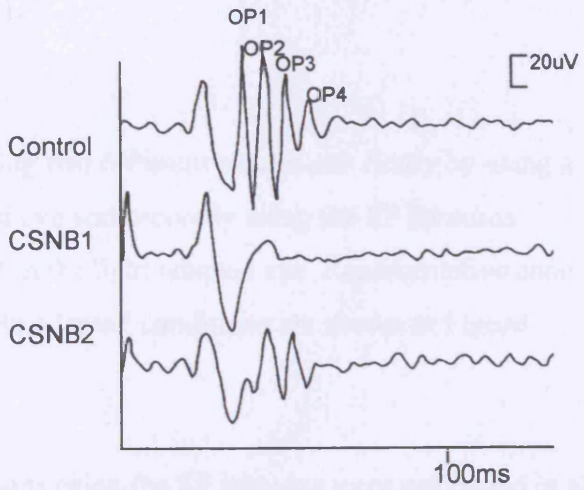

i): Representative scotopic OPs. Note the absence of a recordable OP waveform in CSNB1 (*NYX* mutation) and the abnormal waveform in CSNB2.

ii) Maximum OP amplitude scatterplot and error bar chart. The OP response was unrecordable in all 11 subjects in the CSNB1 group and the maximum OP amplitude subnormal in subjects in the CSNB2 group.

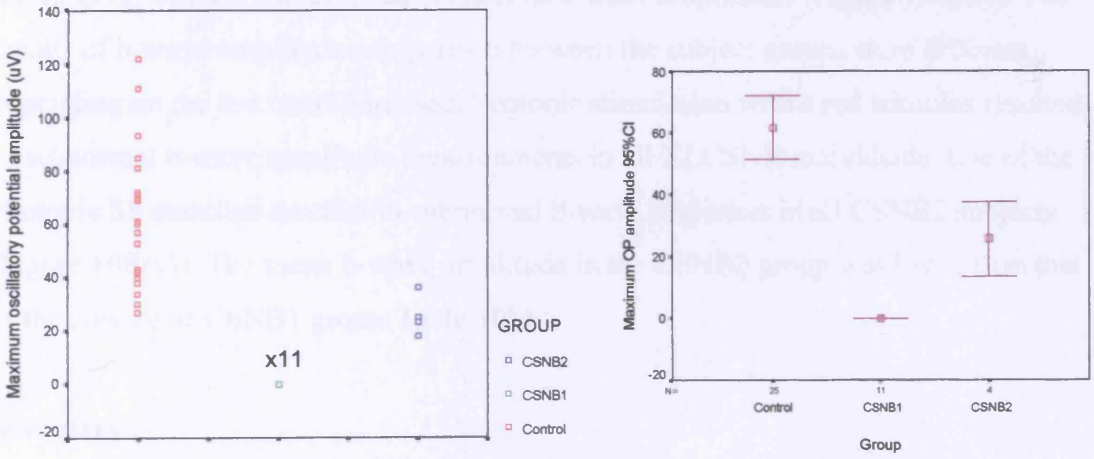

10.2 The cone mediated ERG

Cone mediated responses were tested using two different conditions: firstly by using a red coloured stimulus in the dark adapted eye and secondly using the SF stimulus against a rod saturating light background in the light adapted eye. Representative cone derived responses to a SF stimulus in light adapted conditions are shown in Figure 10f(i).

The a-wave latencies in photopic conditions using the SF stimulus were prolonged in all 11 subjects with CSNB1 (Table 10b, figure 10f(ii)). These findings were confirmed with the red stimulus. B-wave latency was prolonged in 4 of the 11 (36%) CSNB1 subjects and only 1 of the 4 (25%) CSNB2 subjects.

The calculated mean a-wave amplitudes in the subject groups were similar when the red stimulus was used. In photopic conditions, 3 of the 4 (75%) CSNB2 subjects and 1 of the 11 (9%) CSNB1 subjects had subnormal a-wave amplitudes (Figure 10e(iii)). The results of b-wave amplitude comparison between the subject groups were different depending on the test condition used. Scotopic stimulation with a red stimulus resulted in subnormal b-wave amplitude measurements in all XLCSNB individuals. Use of the photopic SF stimulus resulted in subnormal b-wave responses in all CSNB2 subjects (Figure 10f(iv)). The mean b-wave amplitude in the CSNB2 group was lower than that of the control or CSNB1 group(Table 10b).

Summary

- The a-wave latency was prolonged in all subjects with *NYX* mutations
- The b-wave latency was prolonged in subjects from each XLCSNB genotype group.
- The majority of subjects with *CACNA1F* mutations had a subnormal photopic a-wave amplitude
- The photopic b-wave amplitude was subnormal in all subjects with *CACNA1F* mutations

Table 10b: Table of photopic ERG properties

Stimulus	Property	Control (n=19)	*NYX* mutation group (n=11)	*CACNA1F* mutation group (n=4)
SF	Mean a-wave latency (ms)	13+/-6	16+/-1	16+/-1
	Response prolonged in N° (%)	0	11 (100%)	3 (75%)
	Mean a-wave amplitude (uV)	-62+/-15	-66+/-18	-38+/-20
	Response subnormal in N° (%)	0	0	2 (50%)
	Mean b-wave amplitude (uV)	129+/-41	100+/-30	46+/-15
	Response abnormal in N° (%)	0	0	2(50%)
30Hz Flicker	Mean latency (ms)	11+/-2	15+/-5	15+/-3
	Response prolonged in N° (%)	0	8(73%)	1 of 2 recordable (50%)
	Mean amplitude (uV)	96+/-28	84+/-23	25+/-13
	Response subnormal in N° (%)	0	0	2of 2 recordable (100%)
ON-OFF response		Control (n=15)	*NYX* (n=2)	*CACNA1F* (n=2)
	Mean a-wave latency (ms)	22+/-1	28+/-5	31+/-2
	Response prolonged in N° (%)	0	2(100%)	2(100%)
	Mean a-wave amplitude (uV)	-36+/-8	-32+/-0	-17+/-7
	Response subnormal in N° (%)	0	0	1(50%)
	Mean b-wave amplitude (uV)	67+/-14	19+/-9	18+/-2
	Response subnormal in N° (%)	0	2(100%)	2(100%)
	Mean d-wave amplitude (uV)	49+/-16	52+/-24	16+/-1
	Response subnormal in N° (%)	0	0	2(100%)

Figure 10f: Cone mediated ERG results.

i)Representative cone ERGs.
Note differing scales and lower amplitude CSNB2 response.(Standard Flash, light adapted eye)

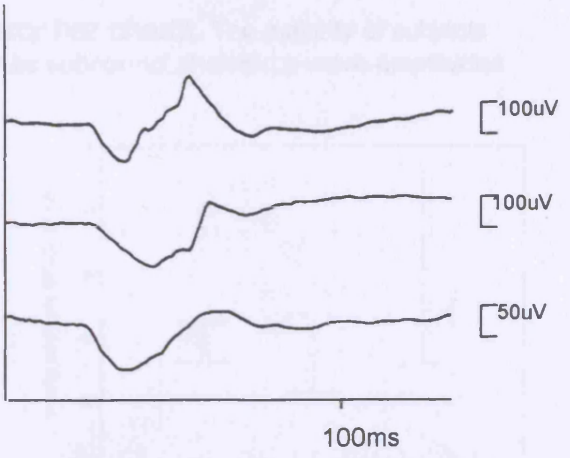

ii) A-wave latency scatterplots and error bar charts. The latency was prolonged in all CSNB1 subjects (*NYX* mutations) and the majority of CSNB2 subjects (*CACNA1F* mutations).

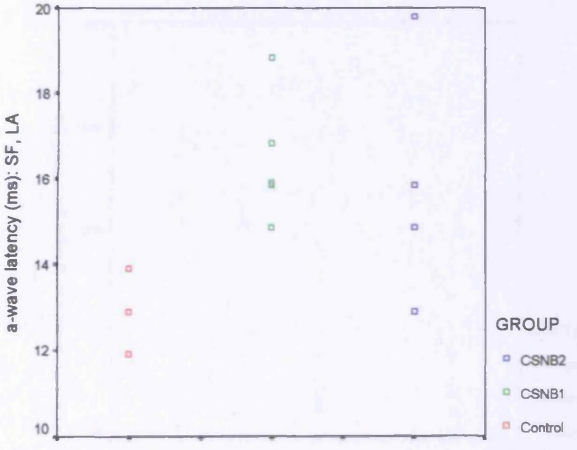

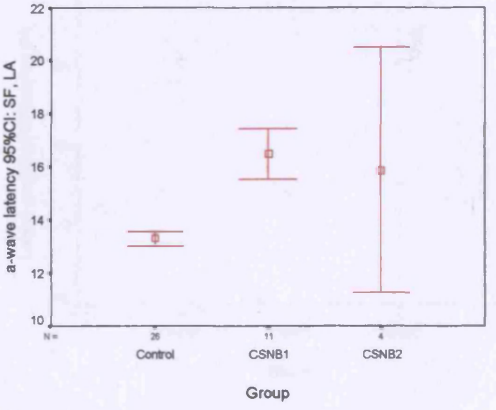

Figure 10f: Cone mediated ERG results – continued

iii) A-wave amplitude scatterplots and error bar charts. The majority of subjects (75%) in CSNB2 group (*CACNA1F* mutations) had subnormal photopic a-wave amplitudes.

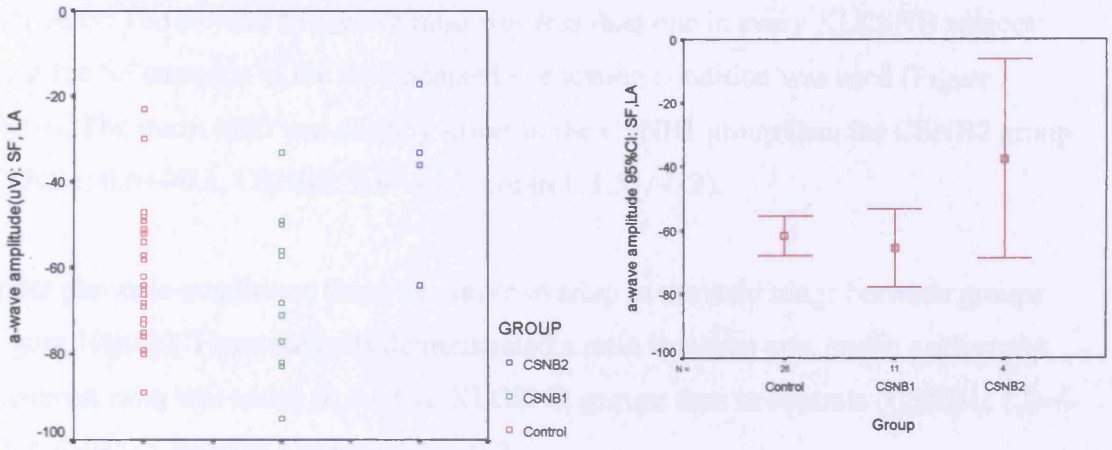

iv) B-wave amplitude scatterplots and error bar charts

Dark adapted red flash stimulus. B-wave amplitudes were subnormal in all subjects with XLCSNB.

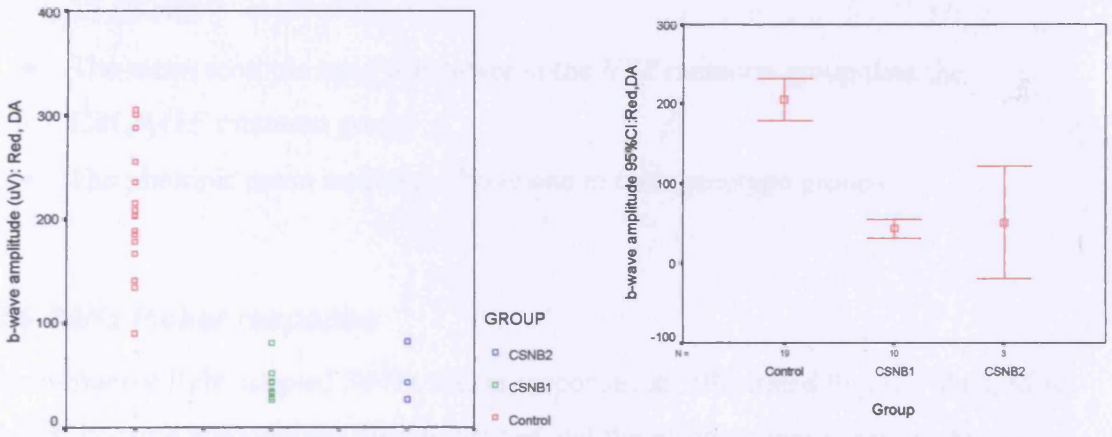

Standard Flash stimulus to dark adapted eye. B-wave responses were subnormal in all CSNB2 group subjects.

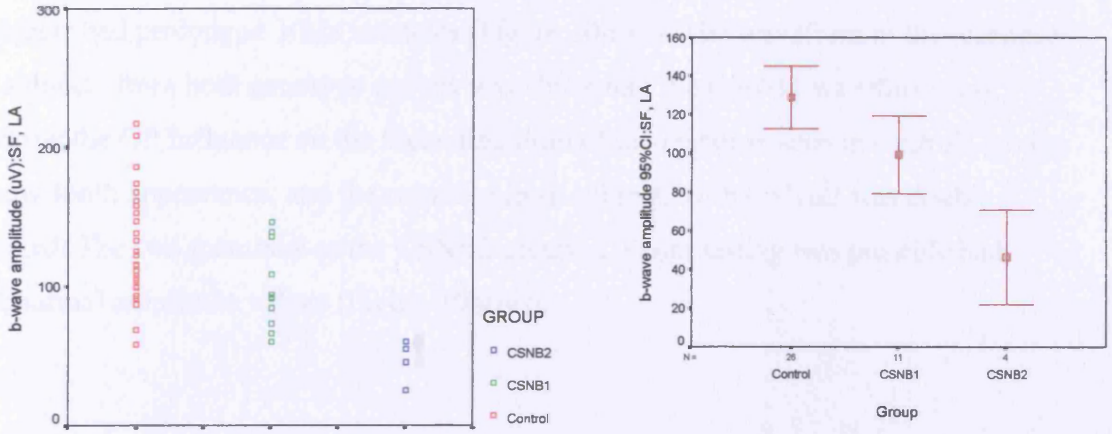

10.3 b-wave to a-wave ratio

The characteristic 'negative' waveform ERG results in a b-wave to a-wave ratio less than unity. The b-wave to a-wave ratio was less than one in every XLCSNB subject when the SF stimulus in the dark adapted eye testing condition was used (Figure 10g(i)). The mean ratio was slightly lower in the CSNB1 group than the CSNB2 group (CSNB1: 0.6+/-0.1, CSNB2: 0.8+/-0.1, control: 1.5+/-0.2).

Under photopic conditions there was more overlap in the ratio range between groups (Figure 10g(ii)). Three subjects demonstrated a ratio less than one, one in each group. The mean ratio was lower in the two XLCSNB groups than in controls (CSNB1: 1.6+/-0.3, CSNB2: 1.3+/-0.4, Control: 2.0+/-0.7).

Summary

- The scotopic b-wave: a-wave ratio was less than one in every subject with XLCSNB
- The mean scotopic ratio was lower in the *NYX* mutation group than the *CACNA1F* mutation group
- The photopic mean ratio was above one in both genotype groups

10.4 30Hz flicker response

Representative light adapted 30 Hz flicker responses are illustrated Figure 10h(i). Most subjects became photophobic during this test and the response was unrecordable above muscle artifact in 2 of the 4 subjects in the CSNB2 group. Although the calculated group means were similar, 8 of the 11 (73%) CSNB1 and 1 of the 2 (50%) CSNB2 subjects had prolonged 30Hz latencies (Figure 10h(ii)). The waveform of the response in subjects from both genotype groups was abnormal: the CSNB1 waveform was lacking the OP influence on the ascending limb of the response seen in controls, giving a saw-tooth appearance, and the response from subjects with CSNB2 was double peaked. The two members of the CSNB2 group in whom testing was possible had subnormal amplitude values (Figure 10h(iii)).

Summary

- The 30Hz waveform was abnormal in the two XLCSNB groups and appeared specific to genotype
- The latency appeared prolonged in the majority of subjects with *NYX* mutations
- The response amplitude was subnormal in both subjects with *CACNA1F* mutations tested
- The mean response amplitude in the *NYX* mutation group was comparable to the control group

Figure 10g: B-wave to a-wave ratios

i) Dark adapted b-wave:a-wave ratio scatterplot and error bar chart.
The b/a-wave ratio was less than one in every XLCSNB subject, and the mean ratio was lower in the CSNB1 (NYX mutation) group.

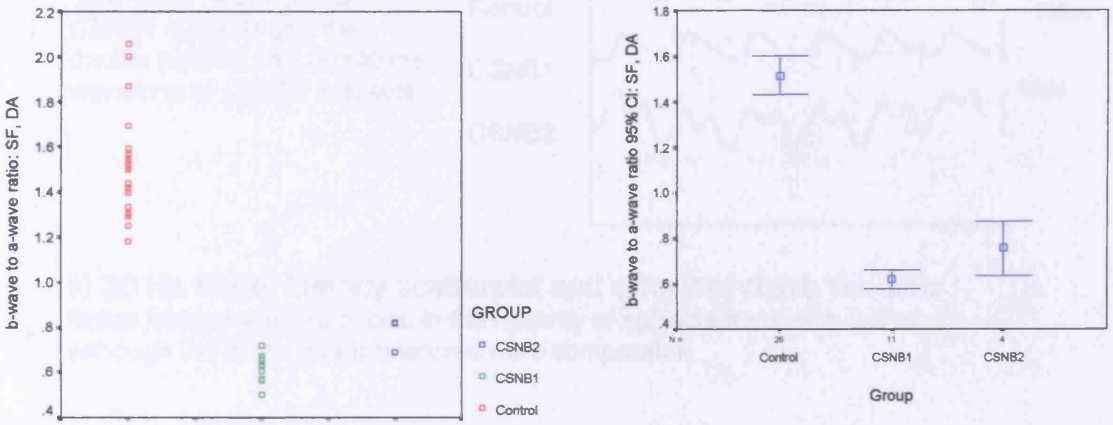

ii) Light adapted b-wave:a-wave ratio scatterplot and error bar chart. The photopic b/a-wave ratio was over one in all subjects with XLCSNB. The mean ratio was lower in the CSNB2 group (*CACNA1F* mutations).

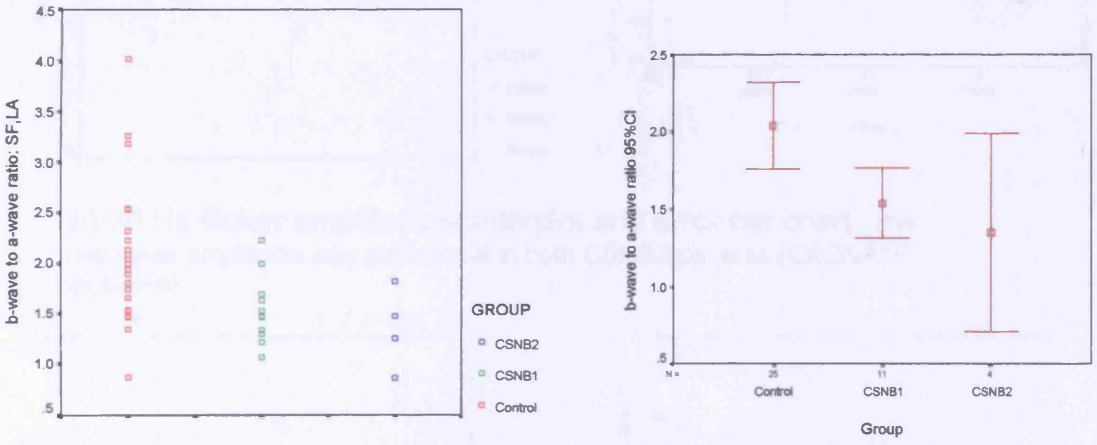

Figure 10h: 30 Hertz flicker results

i) Representative 30 Hz flicker responses. Note the "saw-tooth" waveform of CSNB1 subjects and the double peaked, low amplitude waveform of CSNB2 subjects.

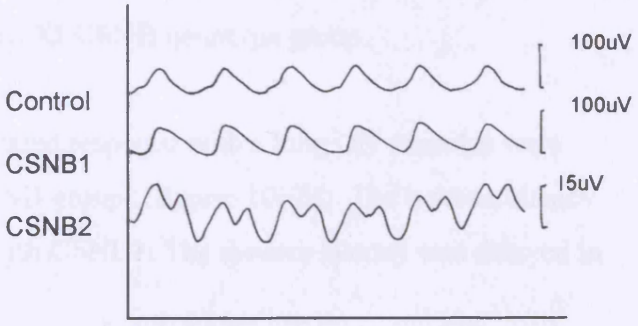

ii) 30 Hz flicker latency scatterplot and error bar chart. The 30Hz flicker latency was prolonged in the majority of subjects from each group although the mean group latencies were comparable.

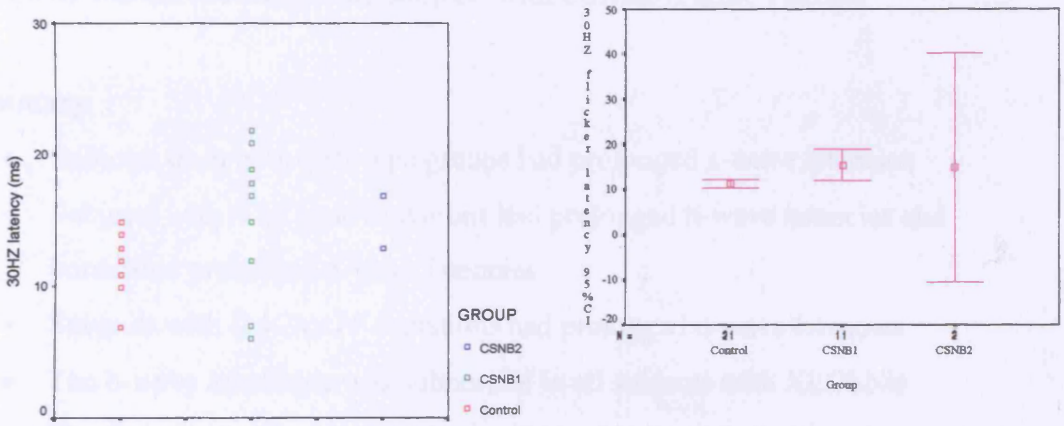

iii) 30 Hz flicker amplitude scatterplot and error bar chart. The response amplitude was subnormal in both CSNB2 patients (*CACNA1F* mutation).

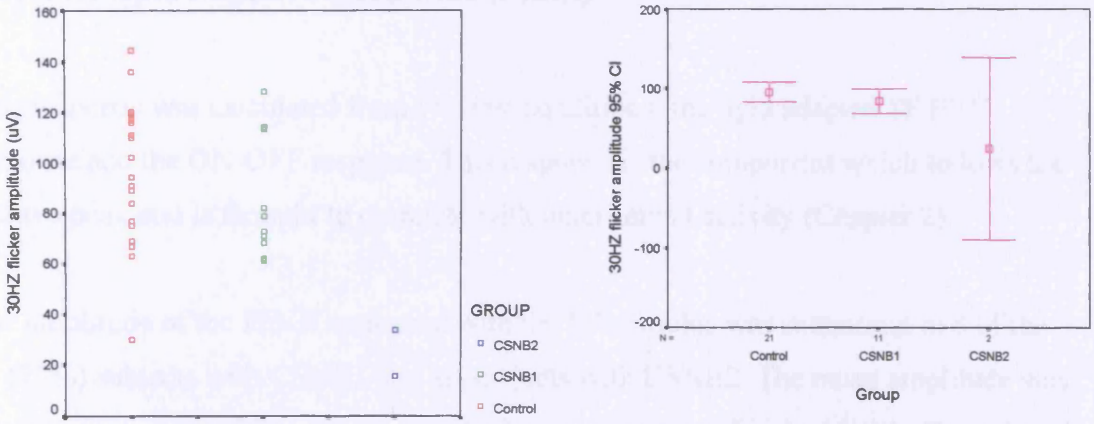

10.5 ON-OFF response

Representative ON-OFF responses are shown in Figure 10i(i). The test was performed on 16 controls and 2 subjects from each XLCSNB genotype group.

The a-wave latencies of the cone mediated response with a long ON stimulus were prolonged in all subjects in the XLCSNB groups (Figure 10i(ii)). The b-wave latency was prolonged in 1 of the 2 subjects with CSNB1. The d-wave latency was delayed in both subjects with CSNB2.

The a-wave amplitude was subnormal in one control and one of the 2 subjects with CSNB2. The b-wave amplitude was subnormal in all XLCSNB subjects. The d-wave amplitude was subnormal in both subjects with CSNB2 (Figure 10i(iii)).

Summary

- Subjects from both genotype groups had prolonged a-wave latencies
- Subjects with *NYX* gene mutations had prolonged b-wave latencies and borderline prolonged d-wave latencies
- Subjects with *CACNA1F* mutations had prolonged d-wave latencies
- The b-wave amplitude was subnormal in all subjects with XLCSNB
- The d-wave amplitude was subnormal in subjects with *CACNA1F* mutations

10.6 Photopic negative Response (PhNR)

This response was calculated from two test conditions: the light adapted SF ERG response and the ON-OFF response. This response is the component which follows the b-wave peak and is thought to correlate with inner retinal activity (Chapter 2).

The amplitude of the PhNR measured with the SF stimulus was subnormal in 8 of the 11 (73%) subjects with CSNB1 and all subjects with CSNB2. The mean amplitude was lower in these two subject groups than in the control group (Figure 10j(i)). The reduced PhNR amplitude was confirmed by the results using the ON-OFF (i.e. long flash stimulus) response conditions (Figure 10j(ii)).

Summary

- The PhNR was subnormal in the majority of XLCSNB subjects
- The PhNR to b-wave amplitude ratio was lower in XLCSNB subjects than in controls

Figure 10i: ON-OFF response

i)Representative ON-OFF responses
Note the reduced d-wave amplitude in the CSNB2 subject
PhNR=photopic negative response
d=dwave (OFFresponse)

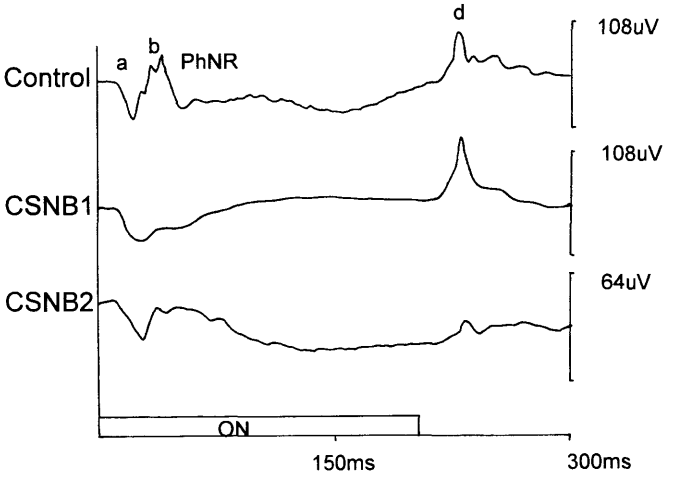

Figure 10i(ii): ON-OFF response Scatterplots of a-, b and d-wave latencies. The latencies were prolonged in the majority of XLCSNB subjects. :

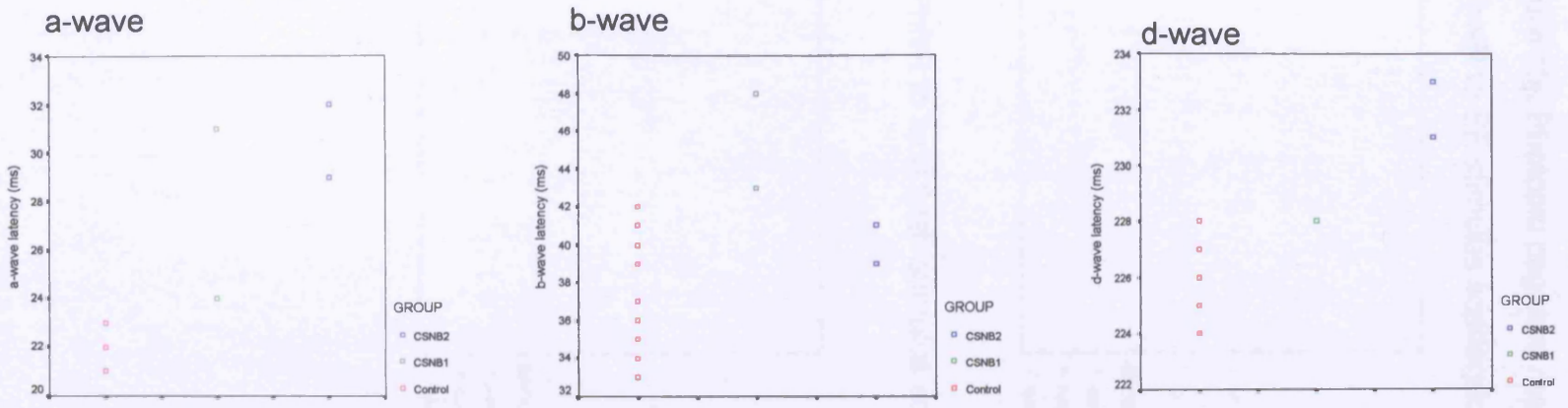

iii) Scatterplots of a-, b- and d-wave amplitudes.b-wave amplitude was subnormal in all XLCSNB subjects. the d-wave was subnormal in both CSNB2 (*CACNA1F* mutation) subjects.

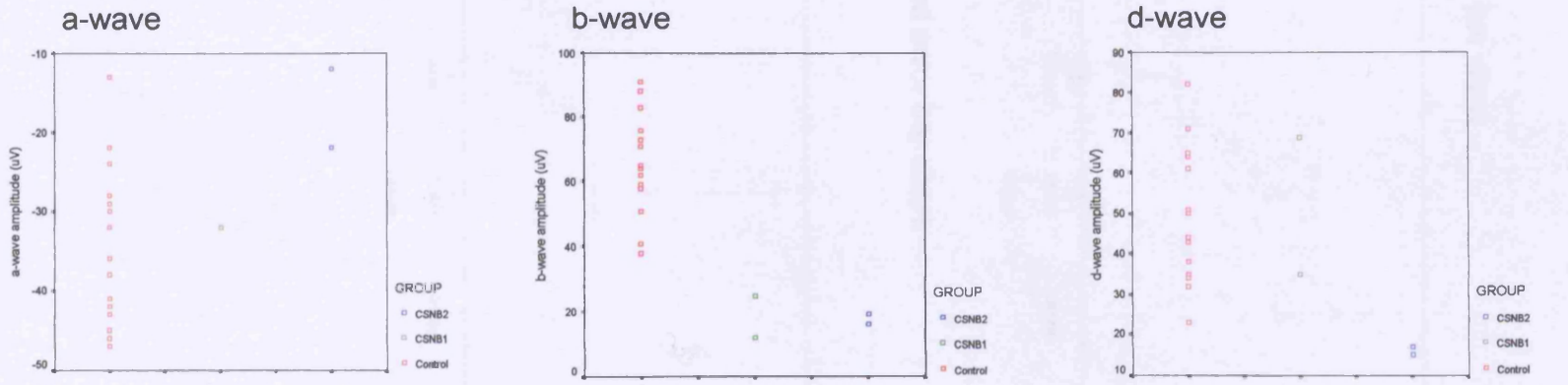

Figure 10j: Photopic negative response

i) PhNR to SF stimulus scatterplot and error bar chart

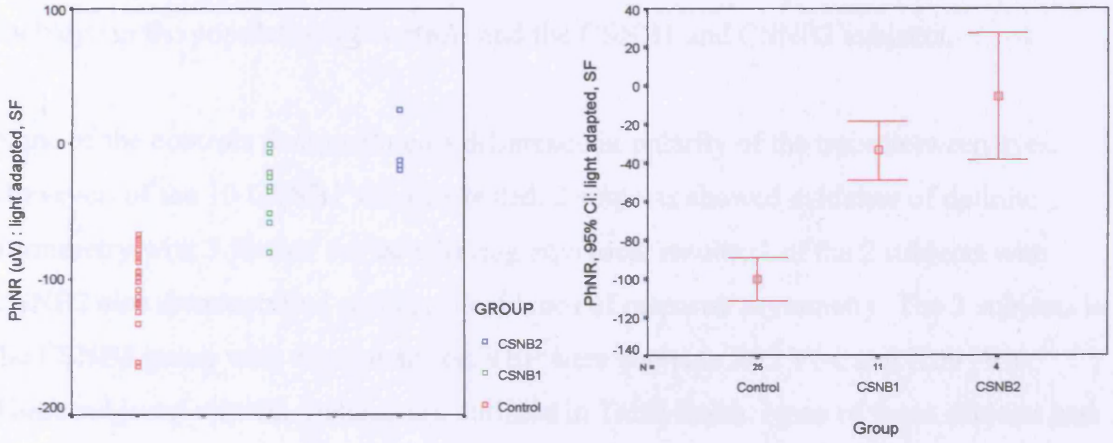

ii) PhNR to long flash stimulus scatterplot and error bar chart

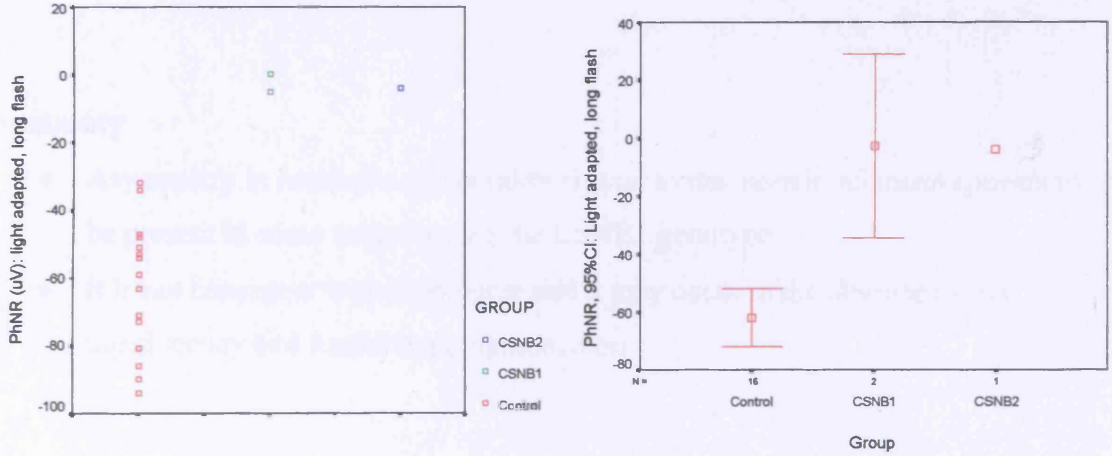

10.7 Visual Evoked Potential

Figure 10k illustrates the differential potentials (difference response) for stimulation of each eye in the population of controls and the CSNB1 and CSNB2 subjects.

None of the controls demonstrated a difference in polarity of the trace between eyes. However, of the 10 CSNB1 subjects tested, 2 subjects showed evidence of definite asymmetry with 3 further subjects having equivocal results; 1 of the 2 subjects with CSNB2 also demonstrated equivocal evidence of response asymmetry. The 2 subjects in the CSNB1 group with asymmetry on VEP were subjects X05 VI-6 and X09 IV-6. These subjects' clinical features are outlined in Table 8a&b. None of these subjects had iris translucency on SLE. Infero-temporal hypopigmentation with foveal hypoplasia was noted in X05 VI-6 only. Two other affected members from pedigree X05 showed no evidence of response asymmetry.

Summary

- Asymmetry in hemispheric laterality similar to that seen in albinism appears to be present in some subjects with the CSNB1 genotype
- It is not consistent within pedigree and it may occur in the absence of iris translucency and fundal hypopigmentation

Figure 10k: Pattern onset VEP: "difference response" left occipital-right occipital

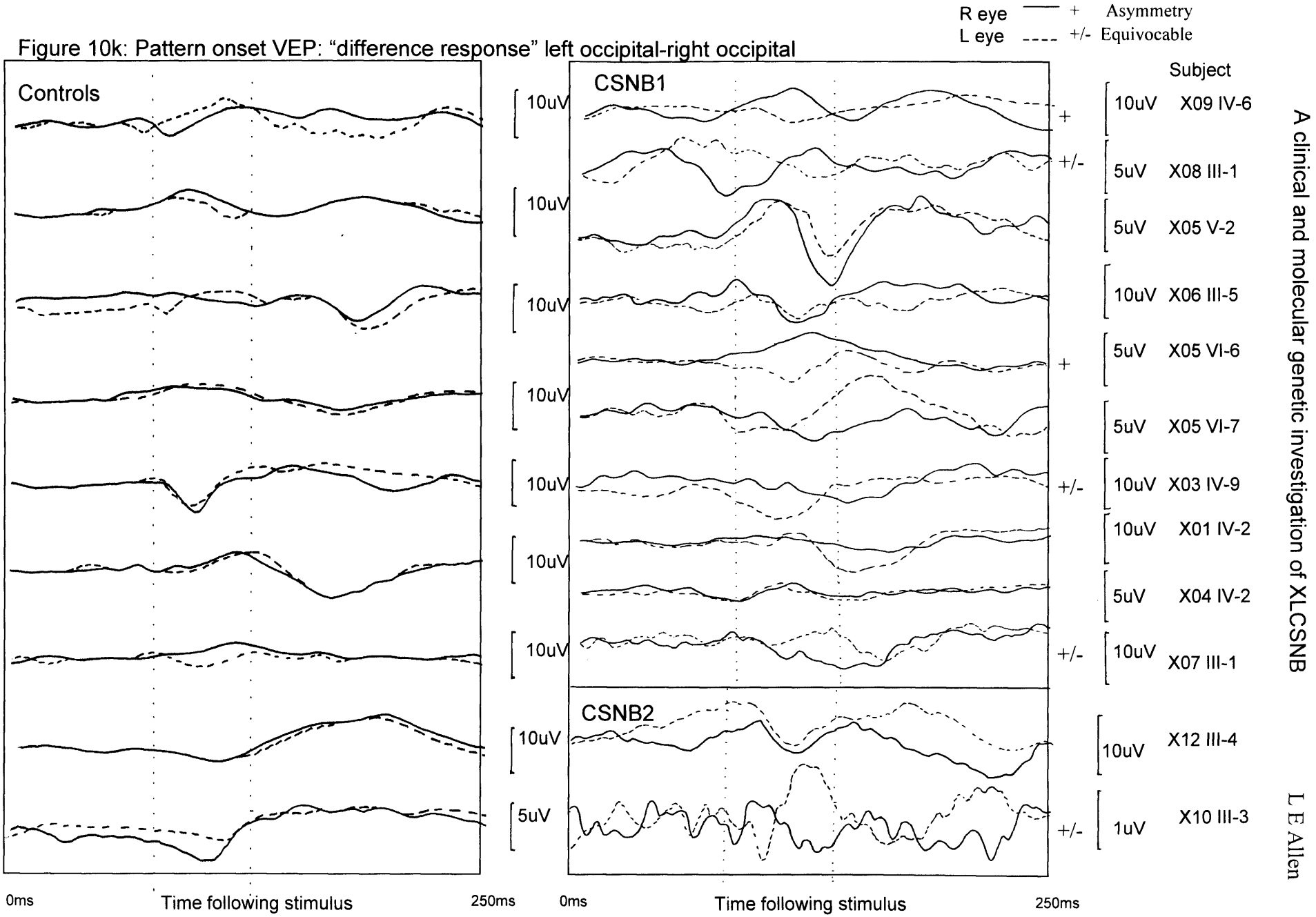

Chapter 11 Discussion

11.1 Molecular Genetic findings

Mutation screening of *CACNA1F* and *NYX* genes identified a causative mutation in 14 of the 15 families tested (Zito, Allen et al. 2003). Although *NYX* gene mutations were much more prevalent than *CACNA1F* gene mutations, this may be a chance finding rather than a true indication of the relative proportion of genotype in the UK due to the small size of the sample. No mutations were found in one X-linked pedigree (X02). Since the phenotype of these subjects was similar to that described for subjects with *NYX* mutations, it is likely that the causative mutation in this pedigree may be present in the undefined promoter region, in alternatively transcribed exons or deep within the introns of the *NYX* gene. Alternatively the causative mutation may be in a different gene: a third locus for XLCSNB in Xp21.1 has been previously described in two families (Bergen, ten Brink et al. 1996). The affected members in these families had very poor rod-mediated responses and were similar in phenotype to affected members of pedigree X02. Support for another XLCSNB locus at Xp21.1 is given by the presence of CSNB1 phenotype electrophysiological changes in Xp21 deletion syndrome (Oregon Eye Disease) (Weleber, Pillers et al. 1989; Pillers, Seltzer et al. 1993).

11.2 Clinical examination in XLCSNB

The small number of subjects and the preponderance of pedigrees with the CSNB1 (*NYX* gene mutations) genotype compared to the CSNB2 (*CACNA1F* gene mutations) limits the meaningful application of quantitative statistics to the results.

There was no evidence in our patient group to suggest a progressive deterioration in visual function. Although several subjects had noted deterioration in visual acuity with age, this could be explained by concurrent pathology. There was a high degree of inter- and intra-familial variability in clinical phenotype but a high concordance between the eyes of each subject, despite the presence of amblyopia. This suggests that other genetic or environmental factors may influence clinical severity. Mild peripheral iris

translucency was identified in only one CSNB1 genotype subject. This feature was not present in any other affected member in his pedigree and was not associated with features of pigment dispersion syndrome. Although not previously reported in subjects with XLCSNB, iris translucency has been identified in subjects with a diagnosis of AIED (Witkop, Quevedo et al. 1983; van Dorp, Eriksson et al. 1985) and supports the speculation that these conditions are one and the same (Hawksworth, Headland et al. 1995). Optic disc tilt accompanied by infero-temporal retinal hypopigmentation was present in most subjects, a minority of whom also had foveal hypoplasia. Although usually ascribed to high myopia, optic disc tilt and sectoral hypopigmentation was seen in the majority of subjects with low degrees of myopia and astigmatism, suggesting that it may be a characteristic of XLCSNB itself. Infero-temporal retinal hypopigmentation was accompanied by a more severe reduction in scotopic threshold sensitivity in the supero-nasal visual field.

The clinical features and effect on visual function of XLCSNB are extremely variable and there appears to be no consistent clinical, psychophysical or electrophysiological feature that enables the distinction of Åland Island Eye Disease from CSNB2. Additionally, mutations in the *CACNA1F* gene have been identified in the majority of patients with a clinical diagnosis of AIED (Andrassi, Alitalo et al. 1999; Wutz, Sauer et al. 2002). The existence of AIED as a distinct entity seems unlikely.

11.3 "Complete" versus "incomplete" clinical forms of XLCSNB

Both genotype groups showed the typical "negative-wave" ERG configuration of XLCSNB due to a grossly sub-normal b-wave response. Miyake based his clinical classification of XLCSNB on the basis of absent rod-mediated responses in the "complete" form on electrophysiological and psychophysical testing (Miyake, Yagasaki et al. 1986). It has been postulated that the "complete" XLCSNB phenotype results from *NYX* gene mutations and the "incomplete" XLCSNB phenotype results from *CACNA1F* gene mutations (Bech-Hansen, Naylor et al. 1998; Bech-Hansen, Naylor et al. 2000; Pusch, Zeitz et al. 2000). The results from this study show that rod-mediated responses can be recorded in both genotypic forms of XLCSNB.
The evidence for residual rod function includes:

- Biphasic dark adapatation curves in subjects from both genotype groups
- Scotopic threshold responses recorded in both genotype groups
- Scotopic spectral sensitivity curves indicating mediation by a desensitized rod system in both genotype groups
- ERGs showing recordable scotopic b-wave responses in subjects from both genotype groups

These findings demonstrate that mutations in both the *NYX* and *CACNA1F* genes result in desensitization of the scotopic system. Although rod-mediated inner retinal responses tend to be more severely affected in CSNB1 as illustrated by a lower scotopic b-/a-wave ratio, rod-mediated responses can be identified in the majority of subjects from each genotype group. Although this is not the first report of detectable rod-mediated b-waves in subjects with *NYX* gene mutations, more commonly they are described as absent in this genotype (Pusch, Zeitz et al. 2000; Scholl, Langrova et al. 2001). Possible explanations for the high detection rate in our study compared to some of the earlier work includes the use of ISCEV standard stimuli with a Ganzfeld system and modern, sophisticated amplifying and averaging techniques in addition to differences in dark adaptation between laboratories. The data from this study suggests that the current clinical classification into "complete" and "incomplete" phenotypic forms on the basis of an absent scotopic response is not justified.

11.4 CSNB1 versus CSNB2

Having shown that a functioning but desensitized scotopic system is present in both genotypic forms of XLCSNB, other psychophysical and electrophysiological characteristics can help to elucidate other differences in retinal pathophysiology between CSNB1 and CSNB2.

Although rod and cone photoreceptor function has previously been accepted as normal, recent studies, including this one, have demonstrated possible rod photoreceptor dysfunction in CSNB1 (*NYX* gene mutations) and possible cone photoreceptor dysfunction in CSNB2 (*CACNA1F* gene mutations) (Hansen, Asefzadeh et al. 2001; Scholl, Langrova et al. 2001; Langrova, Gamer et al. 2002; Allen, Zito et al. 2003). These deductions are based on a sub-normal a-wave response, which may represent a

true abnormality in the hyperpolarization of the photoreceptor due to the molecular defect in each genotypic form of XLCSNB or which, since the ERG is a composite waveform, may be a phenomenon secondary to abnormalities of other cells in the retinal circuitry: OFF bipolar cell activity is known to shape the a-wave in photopic conditions (Sieving, Murayama et al. 1994).

The profoundly sub-normal scotopic b-wave (leading to b-/a-wave ratio less than 1) which is the characteristic feature of both forms of XLCSNB has lead to the assumption that synaptic transmission between rod photoreceptors and ON rod bipolar cells is blocked. In addition, abnormalities of photopic, cone-mediated b-waves in subjects with CSNB2 have been identified in this study and others, suggesting an additional abnormality in synaptic transmission between cone photoreceptors and cone ON bipolar cells (Krill and Martin 1971; Miyake, Yagasaki et al. 1986). Previous studies have shown a reduction in peripheral s-cone sensitivity using blue on yellow perimetry and s-cone ERG in CSNB1; since s-cone responses are channelled only via the cone ON bipolar system, it follows that CSNB1 also affects the cone ON bipolar cell pathway (Kamiyama, Yamamoto et al. 1996; Terasaki, Miyake et al. 1999). Photopic ON-OFF responses, as demonstrated in this study and others, show that the cone OFF bipolar cell response is sub-normal in CSNB2 but normal in CSNB1; indicating an additional site of dysfunction in the CSNB2 group (Miyake, Yagasaki et al. 1987; Houchin, Purple et al. 1991; Langrova, Gamer et al. 2002).

Other electrophysiological differences are apparent between the two groups. Oscillatory potential (OP) wavelets 1-3 are thought to represent rod and cone-mediated ON-circuitry responses whilst OP wavelet 4 is derived from (cone-mediated) OFF responses (Lachapelle, Rousseau et al. 1998; Langrova, Gamer et al. 2002). In mesopic conditions, this study demonstrated that the early OP wavelets derived from Standard Flash stimulation under mesopic conditions were absent in all subjects with CSNB1 but present (although abnormal in waveform) in all subjects with CSNB2. In photopic conditions OP are absent in subjects with CSNB2 but normal in CSNB1 subjects (Lachapelle, Little et al. 1983; Tremblay, Laroche et al. 1995; Langrova, Gamer et al. 2002). The response to 30Hz frequency flicker stimulation is grossly subnormal with a characteristic biphasic waveform in CSNB2 but normal in amplitude in CSNB1 (Miyake, Horiguchi et al. 1987; Ruether, Apfelstedt-Sylla et al. 1993; Tremblay, Laroche et al.

1995). Studies of the fast and slow rod ERG pathways show that although the slow pathway is blocked in CSNB1, the rod-cone-coupling (fast rod pathway) and cone OFF bipolar pathway still function (Scholl, Langrova et al. 2001).
In summary, these electrophysiologic characteristics suggest that CSNB1 causes a near total defect in transmission in the rod and cone ON retinal pathway in the presence of a functioning fast rod pathway and cone OFF bipolar cell pathway. CSNB2 causes a less severe disruption in the rod and cone ON pathway but additionally disrupts the cone OFF pathway, preventing efficient utilization of the fast rod pathway (see Figure 11a and b) (Scholl, Langrova et al. 2001; Langrova, Gamer et al. 2002).

11.5 Other electrophysiological abnormalities in XLCSNB

The photopic negative response is a relatively recently described characteristic in the ERG waveform thought to be derived from the activity of retinal ganglion cells, and has been shown to be selectively reduced in amplitude in glaucoma and optic atrophy (Viswanathan, Frishman et al. 2001; Gotoh, Machida et al. 2004). This response has not previously been studied in XLCSNB but was found to be sub-normal in the majority of CSNB1 subjects and all CSNB2 subjects in our group. This suggests that there is an additional defect in retinal ganglion cell function in both genotypic forms.

Crossed asymmetry was demonstrated on the pattern onset VEP in two CSNB1 subjects. This feature has previously been regarded as diagnostic of ocular and oculo-cutaneous albinism (Apkarian, Reits et al. 1983). The subjects with crossed asymmetry in this study did not have iris translucency but one did have tilted discs with infero-temporal hypopigmentation and foveal hypoplasia. A previous study has identified crossed asymmetry in the majority of CSNB2 subjects tested when using a flash stimulus (Tremblay, De Becker et al. 1996). A postulated cause for crossed asymmetry in XLCSNB is a disruption in the time relationship between melanogenesis and ganglion cell development leading to optic tract disorganization (Tremblay, De Becker et al. 1996). Since nyctalopin is thought to be involved in the establishment of neuronal contacts during fetal development, it is possible that its absence may play some part in ganglion cell misrouting in CSNB1. This issue requires further investigation and a study comparing the VEP in XLCSNB and ocular albinism is currently underway.

Figure 11a: Abnormal retinal circuitry in CSNB1

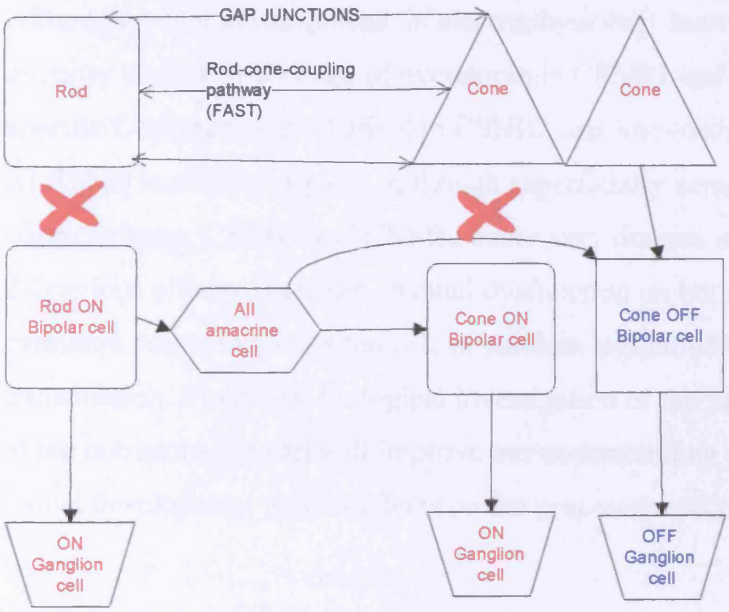

Near complete absence of signal transmission

Figure 11b; Abnormal retinal circuitry in CSNB2

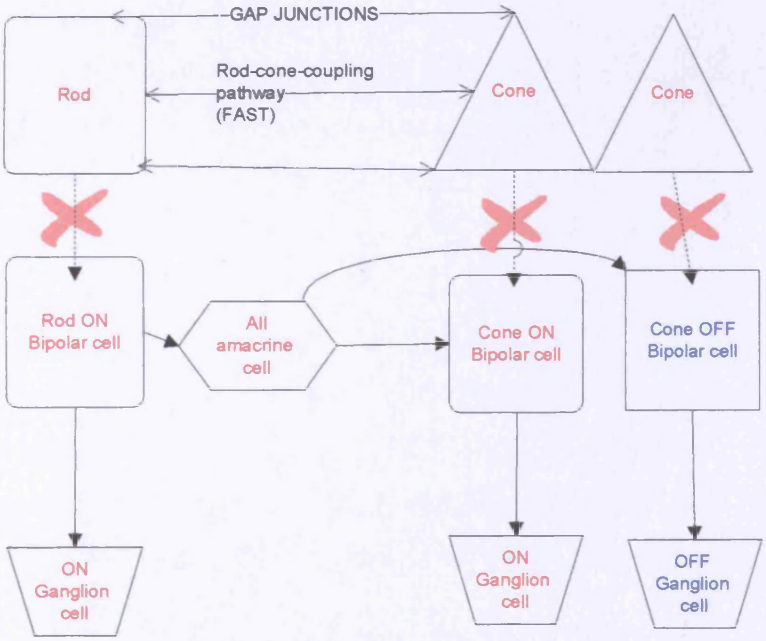

Subnormal signal transmission

11.6 Future developments

Although recent developments in electrophysiology have elucidated the defects in retinal circuitry caused by absence of nyctalopin in CSNB1 and the dysfunction of the retina specific L-type calcium channel in CSNB2, our knowledge of the pathophysiology of XLCSNB is still incomplete. Although superficially similar in their basic ERG characteristics, CSNB1 and CSNB2 cause very distinct inner retinal abnormalities. The deleterious effect of calcium channel dysfunction on both the ON and OFF inner retinal pathways points to the central role of calcium regulation in the mediation of signal transmission. Molecular biological investigation of the function of nyctalopin and study of the nob mouse model will improve our understanding of the role of this protein during retinal development and its effects on the processes and pathways within the inner retina.

Chapter 12 Summary

The clinical classification of XLCSNB into "complete" and "incomplete" forms on the basis of the absence of rod-mediated responses does not correlate with genotype. This study has shown that although phenotypic differences are present in subjects with CSNB1 (*NYX* gene mutations) and CSNB2 (*CACNA1F* gene mutations), these differences are in the function of the inner retinal circuitry.

All subjects in this study, regardless of genotype, had evidence of a functioning but desensitized rod mediated response, although responses tended to be more severely depressed in CSNB1. Absence of nyctalopin severely interferes with functioning of the rod and cone-mediated ON inner retinal pathway. Absence of a functioning retina specific L-type calcium channel results in sub-normal transmission through the rod and cone–mediated ON inner retinal pathway and, in addition, impaired transmission through the cone-mediated OFF inner retinal pathway. These functional differences can be assessed by comparing the electrophysiological responses of the inner retina: the absence of scotopic oscillatory potentials in CSNB1 and the grossly sub-normal and characteristically biphasic appearance of the 30Hz flicker response in CSNB2 serve as practical phenotypic markers which can be assessed during the basic ISCEV standard ERG procedure.

The finding of residual rod-mediated responses in subjects with proven *NYX* gene mutations suggests that the current clinical classification of XLCSNB into "complete" and "incomplete" forms is unsatisfactory. A more suitable classification, utilizing the phenotypic differences in inner retinal function and their correlation with genotype, would be the terms CSNB1 and CSNB2, the clinical features of which are summarized in Table 12.

Table12: Comparison between CSNB1 and CSNB2 (phenotypc differences in bold)

	CSNB1	**CSNB2**
Causative gene mutation	*NYX*	*CACNA1F*
Protein function affected	Nyctalopin	A1 subunit of retina specific L-type calcium channel
Clinical Examination		
Visual acuity	Variably reduced (6/9-6/60)	Variably reduced (6/9-6/60)
Nystagmus	Frequent	Frequent
Strabismus and amblyopia	Frequent	Frequent
High Myopia	Frequent	Frequent
Optic disc tilt and sectoral hypopigmentation	Frequent	Frequent
Psychophysics		
Colour vision	Normal	Normal
Dark adaptation	Biphasic (monphasic in some studies)	Biphasic
Scotopic perimetry	Rod and cone threshold elevation	Rod and cone threshold elevation
Electrophysiology		
Scotopic b-wave amplitude	Sub-normal (absent in some studies)	Sub-normal
Scotopic oscillatory potentials	**Absent**	**Present**
Photopic b-wave amplitude	**Normal**	**Sub-normal**
Photopic oscillatory potentials	**Present**	**Absent**
30Hz flicker response	**Normal amplitude, saw tooth waveform**	**Grossly sub-normal, biphasic waveform**
OFF response	**Normal**	**Sub-normal**

References

al- Jandal, N., Farrar, G., Kiang, A., Humphries, M., Bannon, N., Findlay, J., Humphries, P., and Kenna, P. (1999). "A novel mutation within the rhodopsin gene causing autosomal dominant congenital stationary night blindness." *Human Mutation*, 13(1), 75-81.

Aldred, M. A., Dry, K. L., Sharp, D. M., Van Dorp, D. B., Brown, J., Hardwick, L. J., Lester, D. H., Pryde, F. E., Teague, P. W., Jay, M., and et al. (1992). "Linkage analysis in X-linked congenital stationary night blindness [published erratum appears in Genomics 1994 Jul 1;22(1):255]." *Genomics*, 14(1), 99-104.

Alitalo, T., Kruse, T. A., Forsius, H., Eriksson, A. W., and de la Chapelle, A. (1991). "Localization of the Aland Island eye disease locus to the pericentromeric region of the X chromosome by linkage analysis." *Am J Hum Genet*, 48(1), 31-8.

Allen, L. E., Zito, I., Bradshaw, K., Patel, R. J., Bird, A. C., Fitzke, F. W., Yates, J. R., Trump, D., Hardcastle, A. J., and Moore, A. T. (2003). "Genotype-phenotype correlation in British Families with X-Linked congenital stationary night blindness." *British Journal of Ophthalmology*, 87(11), 1413-1420.

Andrassi, M., Alitalo, T., and Meindl, A. (1999). "High prevalence of CACNA1F mutations in families with X-linked incomplete CSNB (CSNB2) but no evidence for mutations in Aland eye disease (AIED) and X-linked nystagmus." *Investigative ophthalmology and visual science*, 40(4), S469.

Apkarian, P., Reits, D., Spekreijse, H., and Van Dorp, D. (1983). "A decisive electrophysiological test for human albinism." *Electroencephalography and clinical neurophysiology*, 55, 513-531.

Arden, G. B., and Hogg, C. R. (1985). "Rod-cone interactions and analysis of retinal disease." *Br J Ophthalmol*, 69(6), 404-15.

Auerbach, E., Godel, V., and Rowe, H. (1969). "An electrophysiological and psychophysical study of two forms of congenital night blindness." *Invest Ophthalmol*, 8(3), 332-45.

Ayoub, G. S., and D.R.Copenhagen. (1991). "Application of a fluorometric method to measure glutamate release from single photoreceptors." *J Neurosci Methods*, 37, 7-11.

Ball, S. L., Pardue, M. T., McCall, M. A., R.G., G., and Peachey, N. S. (2003). "Immunohistochemical analysis of the outer plexiform layer in the nob mouse shows no abnormalities." *Visual Neuroscience*, 20(3), 267-272.

Barricks, M. E., Flynn, J. T., and Kushner, B. J. (1977). "Paradoxical pupillary responses in congenital stationary night blindness." *Arch Ophthalmol*, 95(10), 1800-4.

Bech-Hansen, N. T., Boycott, K. M., Gratton, K. J., Ross, D. A., Field, L. L., and Pearce, W. G. (1998a). "Localization of a gene for incomplete X-linked congenital stationary night blindness to the interval between DXS6849 and DXS8023 in Xp11.23." *Hum Genet*, 103(2), 124-30.

Bech-Hansen, N. T., Field, L. L., Schramm, A. M., Reedyk, M., Craig, I. W., Fraser, N. J., and Pearce, W. G. (1990). "A locus for X-linked congenital stationary night blindness is located on the proximal portion of the short arm of the X chromosome." *Hum Genet*, 84(5), 406-8.

Bech-Hansen, N. T., Moore, B. J., and Pearce, W. G. (1992). "Mapping of locus for X-linked congenital stationary night blindness (CSNB1) proximal to DXS7." *Genomics*, 12(2), 409-11.

Bech-Hansen, N. T., Naylor, M. J., Matbaum, T. A., Sparkes, R. L., Koop, B., Birch, D. G., Bergen, A. A. B., Prinsen, C. F. M., Polomeno, R. C., Gal, A., Drack, A. V., Musarella, M. A., Jacobson, S. G., Young, R. S. L., and Weleber, R. G. (2000). "Mutations in NYX, encoding the leucine-rich proteogycan nyctalopin, cause X-linked complete congenital stationary night blindness." *Nature Genet*, 26, 319-323.

Bech-Hansen, N. T., Naylor, M. J., Maybaum, T. A., Pearce, W. G., Koop, B., Fishman, G. A., Mets, M., Musarella, M. A., and Boycott, K. M. (1998b). "Loss-of-function mutations in a calcium-channel alpha1-subunit gene in Xp11.23 cause incomplete X-linked congenital stationary night blindness." *Nat Genet*, 19(3), 264-7.

Bergen, A. A., ten Brink, J. B., Riemslag, F., Schuurman, E. J., Meire, F., Tijmes, N., and de Jong, P. T. (1996). "Conclusive evidence for a distinct congenital stationary night blindness locus in Xp21.1." *J Med Genet*, 33(10), 869-72.

Bergen, A. A., ten Brink, J. B., Riemslag, F., Schuurman, E. J., and Tijmes, N. (1995). "Localization of a novel X-linked congenital stationary night blindness locus: close linkage to the RP3 type retinitis pigmentosa gene region." *Hum Mol Genet*, 4(5), 931-5.

Bessant, A. R., Ali, R. R., and Bhattacharya, S. S. (2001). "Molecular genetics and prospects for therapy of the inherited retinal dystrophies." *Current opinion in genetics and development*, 11, 307-316.

Bok, D. (1985). "Retinal photoreceptor-pigment epothelium interactions." *Invest Ophthalmol Vis Sci*, 26, 1659-1565.

Boycott, K. M., Pearce, W. G., Musarella, M. A., Weleber, R. G., Maybaum, T. A., Birch, D. G., Miyake, Y., Young, R. S., and Bech-Hansen, N. T. (1998). "Evidence for Genetic Heterogeneity in X-Linked Congenital Stationary Night Blindness." *Am J Hum Genet*, 62(4), 865-75.

Brown, P., and Wald, G. (1964). "Visual pigments in single rods and cones of the human retina." *Science*, 144, 45-49.

Carr, R., and Siegel, I. M. (1964). "Electrophysiological aspects of several retinal diseases." *Am J Ophthalmol*, 58, 95-107.

Carr, R. E. (1974). "Congenital stationary nightblindness." *Trans Am Ophthalmol Soc*, 72, 448-87.

Carr, R. E., and Ripps, H. (1967). "Rhodopsin kinetics and rod adaptation in Oguchi's disease." *Investigative Ophthalmology*, 6, 426-436.

Carr, R. E., Ripps, H., Siegel, I. M., and Weale, R. A. (1966). "Visual functions in congenital night blindness." *Invest Ophthalmol*, 5(5), 508-14.

Carroll, F. D., and Haig, C. (1952). "Congenital stationary night blindness without ophthalmoscopic or other abnormalities." *Trans Am Ophthalmol Soc*, 50, 193-209.

Catterall, W. A. (1995). "Structure and function of voltage-gated ion channels." *Annu Rev Biochem*, 64, 493-531.

Cibis, G. W., Fitzgerald, K. M., Harris, D. J., Rothberg, P. G., and Rupan, M. (1993). "The effects of dystrophin gene mutations on the ERG in mice and humans." *Invest Ophthalmol Vis Sci*, 34, 3646-3652.

Colotto, A., Falsini, B., Salgarello, T., Iarossi, G., Galan, M. E., and Scullica, L. (2000). "Photopic negative response of the human ERG: losses associated with glaucomatous damage." *Investigative Ophthalmology and Visual Science*, 41, 2205-2211.

Cunier, F. (1838). "Historie d'une hemerolpie, hereditaire depuis deux siecles dans une famille de la commune de Vendemian, pres Monpellier." *Ann Soc Med de Gand*, 4, 385-395.

Curcio, C. A., Sloan, K. R., Laina, R. E., and Hendrickson, A. E. (1990). "Human photoreceptor topography." *J Comp neurol*, 292, 497-523.

Daw, N. W., Jensen, R. J., and Brunken, W. J. (1990). "Rod pathways in mammilian retinae." *Trends in Neurosciences*, 13, 110-115.

De Becker, I., Riddell, D. C., Dooley, J. M., and Tremblay, F. C. (1994). "Correlation between electroretinogram findings and molecular analysis in the Duchenne muscular dystrophy phenotype." *Br J Ophthalmol*, 78, 719-722.

de Jong, P. T., Zrenner, E., van Meel, G. J., Keunen, J. E., and van Norren, D. (1991). "Mizuo phenomenon in X-linked retinoschisis. Pathogenesis of the Mizuo phenomenon." *Arch Ophthalmol*, 109(8), 1104-8.

Dizhoor, A., Ray, S., and Kumar, S. (1991). "Recoverin: A calcium sensitive activator of retinal rod guanylate cyclase." *Science*, 251, 915-920.

Donders, F. (1855). "Torpeur de la retine congenitale hereditaire." *Ann Ocul (Paris)*, 34, 270-273.

Downes, S. M., Fitzke, F. W., Holder, G. E., Payne, A. M., Bessant, D. A. R., Bhattacharya, S. S., and Bird, A. C. (1999). "Clinical features of codon 172 RDS macular dystrophy." *Arch Ophthal*, 117, 1373-1383.

Doyle, J. L., and Stubbs, L. (1998). "Ataxia, arrythmia and ion-channel gene defects." *Trends Genet*, 14, 92-98.

Dryja, T. P., Berson, E. L., Rao, V. R., and Oprian, D. D. (1993). "Heterozygous missense mutation in the rhodopsin gene as a cause of congenital stationary night blindness." *Nat Genet*, 4(3), 280-3.

Dryja, T. P., Hahn, L. B., Reboul, T., and Arnaud, B. (1996). "Missense mutation in the gene encoding the alpha subunit of rod transducin in the Nougaret form of congenital stationary night blindness." *Nat Genet*, 13(3), 358-60.

Ferris, F. L., Kassoff, A., Bresnick, G. H., and Bailey, I. (1982). "New visual acuity charts for clinical research." *Am J Ophthalmol*, 94, 91-96.

Fitzke, F. W. (1995). "Recent developments in psychophysics." Recent advances in Ophthalmology.

Forsius, H., and Eriksson, A. W. (1964). "Ein neues Augensyndrom mit x-chromosomal Transmission. Eine Sippe mit Fundusalbinismus, Fovealhypoplasie, Nystagmus, Myopie, Astigmatismus und Dyschromatopsie." *Klinische Monatsblaetter fur Augenheilkunde*, 144, 447-457.

Franceschetti, A., and Chrome-Brecioux, N. (1951). "Fudus albipunctatus cum hemeralopie." *Ophthalmologica*, 121, 111-116.

Francois, J., Verriest, G., DeRouck, A., and DeJean, C. (1956). "Les fonctions visuelles dans l'hemeralopie essentielle nougarine." *Ophthalmologica*, 132, 244-257.

Fuchs, S., Nakazawa, M., Maw, M., Tamai, M., Oguchi, Y., and Gal, A. (1995). "A homozygous 1-base pair deletion in the arrestin gene is a frequent cause of Oguchi disease in Japanese." *Nat Genet*, 10(3), 360-2.

Gal, A., Orth, U., Baehr, W., Schwinger, E., and Rosenberg, T. (1994). "Heterozygous missense mutation in the rod cGMP phosphodiesterase beta- subunit gene in autosomal dominant stationary night blindness [published erratum appears in Nat Genet 1994 Aug;7(4):551]." *Nat Genet*, 7(1), 64-8.

Gal, A., Schinzel, A., Orth, U., Fraser, N. A., Mollica, F., Craig, I. W., Kruse, T., Machler, M., Neugebauer, M., and Bleeker-Wagemakers, L. M. (1989). "Gene of X-chromosomal congenital stationary night blindness is closely linked to DXS7 on Xp." *Hum Genet*, 81(4), 315-8.

Glass, I. A., Good, P., Coleman, M. P., Fullwood, P., Giles, M. G., Lindsay, S., Nemeth, A. H., Davies, K. E., Willshaw, H. A., Fielder, A., and et al. (1993). "Genetic mapping of a cone and rod dysfunction (Aland Island eye disease) to the proximal short arm of the human X chromosome." *J Med Genet*, 30(12), 1044-50.

Gotoh, Y., Machida, S., and Tazawa, Y. (2004). "Selective loss of the photopic negative response in patients with optic nerve atrophy." *Archives of Ophthalmology*, 122(3), 341-346.

Gregg, R. G., Mukhopadhyay, S., S.I., C., Ball, S. L., Pardue, M. T., McCall, M. A., and Peachey, N. S. (2003). "identification of the gene and the mutation responsible for the mouse nob phenotype." *Investigative Ophthalmology and Visual science*, 44(1), 378-384.

Haim, M. (1986). "Congenital stationary night blindness." *Acta Ophthalmol (Copenh)*, 64(2), 192-8.

Hansen, R. M., Asefzadeh, B., and Fulton, A. B. (2001). "Rod photoreceptor function in congenital stationary night blindness (CSNB)." *Invest Ophthalmol Vis Sci*, 42(4), S77.

Hardcastle, A. J., David-Gray, Z. K., Jay, M., Bird, A. C., and Bhattacharya, S. S. (1997). "Localization of CSNBX (CSNB4) between the retinitis pigmentosa loci RP2 and RP3 on proximal Xp." *Invest Ophthalmol Vis Sci*, 38(13), 2750-5.

Hardcastle, A. J., Thiselton, D. L., Van Maldergem, L., Sake, B. K., Jay, M., Plant, C., Taylor, R., Bird, A. C., and Bhattacharya, S. (1999). "Mutations in the RP2 gene cause disease in 10% of familial XLRP assessed in the study." *Am J Hum Genet*, 64, 1210-1215.

Hawksworth, N. R., Headland, S., Good, P., Thomas, N. S., and Clarke, A. (1995). "Aland island eye disease: clinical and electrophysiological studies of a Welsh family." *Br J Ophthalmol*, 79(5), 424-30.

Heckenlively, J. R., Martin, D. A., and Rosenbaum, A. L. (1983). "Loss of electroretinographic oscillatory potentials, optic atrophy, and dysplasia in congenital stationary night blindness." *Am J Ophthalmol*, 96(4), 526-34.

Heynen, H., Wachtmeister, L., and Norren, D. v. (1985). "Origin of the oscillatory potentials in the primate retina." *Vision Res*, 25, 1365-1370.

Hill, D. A., Arbel, K. F., and Berson, E. L. (1974). "Cone electroretinograms in congenital nyctalopia with myopia." *Am J Ophthalmol*, 78(1), 127-36.

Hittner, H. M., Borda, R. P., and Justice, J., Jr. (1981). "X-linked recessive congenital stationary night blindness, myopia, and tilted discs." *J Pediatr Ophthalmol Strabismus*, 18(1), 15-20.

Hocking, A. M., Shinomura, T., and McQuillan, D. J. (1998). "Leucine-rich repeat glycoproteins of the extracellular matrix." *Matrix Biol.*, 17(1), 1-19.

Hogan, K., Powers, P. A., and Gregg, R. G. (1994). "Cloning of the human skeletal muscle a-subunit of the dihydropyrimidine-sensitive L-type calcium channel (CACNL1A3)." *Genomics*, 24, 608-609.

Hood, D., and Finkelstein, M. (1986). "Sensitivity to light." The handbook of perception and human performance., K. Boff, L. Kaufman, and J. Thomas, eds., John Wiley, New York.
Hood, D. C., and Greenstein, V. (1990). "Models of the normal and abnormal rod system." *Vision Res*, 30(1), 51-68.

Horowitz, D. S., and Krainer, A. R. (1994). "Mechanisms for selecting 5' splice sites in mammalian pre-mRNA splicing." *Trends Genet*, 10(3), 100-106.

Houchin, K. W., Purple, R. L., and Wirtschafter, J. D. (1991). "X-linked congenital stationary night blindness and depolarising bipolar cell function." *Invest Ophthalmol Vis Sci*, 32, 1229.
Iozzo, R. V. (1997). "The family of the small leucine-rich proteoglycans: key regulators of matrix assembly and cellular growth." *Crit. Rev. Biochem. Mol. Biol.*, 32, 141-174.

Jensen, H., Warburg, M., Sjo, O., and Schwartz, M. (1995). "Duchenne muscular dystrophy: negative electroretinograms and normal dark adaptation. Reappraisal of assignment of X linked incomplete congenital stationary night blindness." *J Med Genet*, 32(5), 348-51.

Kamiyama, M., Yamamoto, S., Nitta, K., and Hayasaka, S. (1996). "Undetectable S cone electroretinogram b-wave in complete congenital stationary night blindness." *Br J Ophthalmol*, 80(7), 637-9.

Kandori, F. (1959). "Very rare cases of congenital nonprogressive night blindness with flecked retina." *Jap J Ophthalmol*, 13, 383-386.

Kandori, F., Tamai, A., Kurimoto, S., and Fukunaga, K. (1972). "Fleck retina." *Am J Ophthalmol*, 73(5), 673-85.

Khouri, G., Mets, M. B., Smith, V. C., Wendell, M., and Pass, A. S. (1988). "X-linked congenital stationary night blindness. Review and report of a family with hyperopia [see comments]." *Arch Ophthalmol*, 106(10), 1417-22.

Kobe, B., and Deisenhofer, J. (1994). "The leucine-rich repeat: a versatile binding motif." *Trends Biol. Sci.*, 19, 415-421.

Koch, K.-W. (1991). "Purification and identification of photoreceptor guanylate cyclase." *J Biol Chem*, 266, 8634-36.

Kohl, S., Marx, T., Giddings, I., Jagle, H., Jacobson, S. G., Apfelstedt-Sylla, E., Zrenner, E., Sharpe, L. T., and Wissinger, B. (1998). "Total colourblindness is caused by mutations in the gene encoding the alpha subunit of the cone photoreceptor cGMP-gated cation channel." *Nature Genetics*, 19, 257-259.

Kolb, H., and Famligetti, E. V. (1974). "Rod and cone pathways in the inner plexiform layer of the cat retina." *Science*, 186, 47-49.

Krantz, D. E., and Zipursky, S. L. (1990). "Drosophila chaoptin; a member of the leucine-rich repeat family is a photoreceptor cell specific adhesion molecule." *EMBO J*, 9(6), 1969-1977.
Krill, A. E., and Martin, D. (1971). "Photopic abnormalities in congenital stationary nightblindness." *Invest Ophthalmol*, 10(8), 625-36.

Kriss, A., and Russell-Eggitt, I. (1992). "Electrophysiological assessment of visual pathway function in infants." *Eye*, 6, 145-153.

Lachapelle, P., Little, J. M., and Polomeno, R. C. (1983). "The photopic electroretinogram in congenital stationary night blindness with myopia." *Invest Ophthalmol Vis Sci*, 24(4), 442-50.

Lachapelle, P., Rousseau, S., McKerral, M., Benoit, J., Polomeno, R. C., Koenekoop, R. K., and Little, J. M. (1998). "Evidence supportive of a functional discrimination between photopic oscillatory potentials as revealed with cone and rod mediated retinopathies." *Doc Ophthalmol*, 95(1), 35-54.

Langrova, H., Freidburg, C., Besch, D., Zrenner, E., and Apfelstedt-Sylla, E. (1999). "Abnormalities of the long flash (ON-OFF) ERG in congenital stationary night blindness of the Schubert-Bornshein type.[ARVO abstract]." *Invest Ophthalmol Vis Sci*, 40, S719.

Langrova, H., Gamer, D., Friedberg, C., Besch, D., Zrenner, E., and Apfelstedt-Sylla, E. (2002). "Abnormalities of the long flash ERG in congenital stationary night blindness of the Schubert-Bornshein type." *Vision Research*, 42, 1475-1483.

Lauber, H. (1910). "Die sogenannte Retinitis puncata albescens." *Klin Monatsbl Augenheilkd*, 48, 133-148.

Lee, R., Fowler, A., and McGuinness, J. (1990). "Amino acid and cDNA sequence of bovine phosducin, a soluble phosphoprotein from photoreceptor cells." *J Biol Chem*, 265, 15867-70.

Leibrock, C. S., Reuter, T., and Lamb, T. D. (1998). "Molecular basis of dark adaptation in rod photoreceptors." *Eye*, 12, 511-520.

Margolis, S., Siegel, I. M., and Ripps, H. (1987). "Variable expressivity in fundus albipunctatus." *Ophthalmology*, 94(11), 1416-22.

Marmor, M. F. (1977). "Fundus albipunctatus: a clinical study of the fundus lesions, the physiologic deficit, and the vitamin A metabolism." *Doc Ophthalmol*, 43(2), 277-302.

Marmor, M. F. (1990). "Long-term follow-up of the physiologic abnormalities and fundus changes in fundus albipunctatus." *Ophthalmology*, 97(3), 380-4.

Marmor, M. F., and Zrenner, E. (1998). "Standard for clinical electroretinograohy (1999 update)." *Doc Ophthalmol*, 97, 143-156.

Masland, R. H. (2001). "The fundamental plan of the retina." *Nature neuroscience*, 4, 877-884.

Maturana, H. R., Lettvin, J. Y., and McCullock, W. S. (1960). "Anatomy and physiology of vision in the frog." *J Gen Physiol*, 43, 129-135.

Mears, A. J., Hiriyanna, S., Vervoort, R., Yashar, B., Gieser, L., Fahrner, S., Daiger, S. P., Heckenlively, J. R., Sieving, P. A., Wright, A. F., and Swaroop, A. (2000). "Remapping of the RP15 locus for X-linked cone-rod degeneration to Xp11.4-p21.1, and identification of a de novo insertion in the RPGR exon ORF15." *Am J Hum Genet*, 67(4), 1000-3.

Meindl, A., Dry, K., and Herrmann, K. (1996). "A gene (RPGR) with homology to the RCCI guanine nucleotide exchange factor is mutated in X-linked retinitis pigmentosa." *Nat Genet*, 13, 35-42.

Merin, S., Rowe, H., Auerbach, E., and Landau, J. (1970). "Syndrome of congenital high myopia with nyctalopia. Report of findings in 25 families." *Am J Ophthalmol*, 70(4), 541-7.

Miyake, Y. (1989). "X-linked congenital stationary night blindness [letter; comment]." *Arch Ophthalmol*, 107(5), 635-6.

Miyake, Y., Gto, S., Ando, F., and Ichikawa, H. (1983). "Vitreous fluorophotometry in congenital stationary nightblindness." *Arch Ophthalmol*, 101(4), 574-6.

Miyake, Y., Horiguchi, M., Ota, I., and Shiroyama, N. (1987a). "Characteristic ERG-flicker anomaly in incomplete congenital stationary night blindness." *Invest Ophthalmol Vis Sci*, 28(11), 1816-23.

Miyake, Y., Horiguchi, M., Terasaki, H., and Kondo, M. (1994). "Scotopic threshold response in complete and incomplete types of congenital stationary night blindness." *Invest Ophthalmol Vis Sci*, 35(10), 3770-5.

Miyake, Y., and Kanai, A. (1992). "A Japanese pedigree of autosomal dominant congenital stationary night blindness with variable expressivity." *Ophthalmic Paediatrics and Genetics*, 13(4), 211-217.

Miyake, Y., and Kawase, Y. (1984). "Reduced amplitude of oscillatory potentials in female carriers of X- linked recessive congenital stationary night blindness." *Am J Ophthalmol*, 98(2), 208-15.

Miyake, Y., Yagasaki, K., and Horiguchi, M. (1987b). "A rod-cone dysfunction syndrome with separate clinical entity: incomplete-type congenital stationary night blindness (Miyake)." *Prog Clin Biol Res*, 247, 137-45.

Miyake, Y., Yagasaki, K., Horiguchi, M., and Kawase, Y. (1987c). "On- and off-responses in photopic electroretinogram in complete and incomplete types of congenital stationary night blindness." *Jpn J Ophthalmol*, 31(1), 81-7.

Miyake, Y., Yagasaki, K., Horiguchi, M., Kawase, Y., and Kanda, T. (1986). "Congenital stationary night blindness with negative electroretinogram. A new classification." *Arch Ophthalmol*, 104(7), 1013-20.

Mizuo, G. (1913a). "On a new discovery in the dark adaptation of Oguchi's disease." *Acta Soc Ophthalmol Jap*, 17, 1148-1150.

Mizuo, G. (1913b). "On a new discovery in the dark adaptation of Oguchi's disease." *Acta Societatis Ophthalmologicae Japonicae*, 17, 1148-1150.

Mollon, J. D., Astell, S., and Reffin, J. P. (1991). "A minimalist test of colour vision." Colour vision deficiencies, B. Drum, Moreland, J.D., Serra, A., ed., Kluwer, Dordrecht.

Musarella, M. A., Weleber, R. G., Murphey, W. H., Young, R. S., Anson-Cartwright, L., Mets, M., Kraft, S. P., Polemeno, R., Litt, M., and Worton, R. G. (1989). "Assignment of the gene for complete X-linked congenital stationary night blindness (CSNB1) to Xp11.3 [see comments]." *Genomics*, 5(4), 727-37.

Nakazawa, M., Wada, Y., Fuchs, S., Gal, A., and Tamai, M. (1997). "Oguchi disease: phenotypic characteristics of patients with the frequent 1147delA mutation in the arrestin gene." *Retina*, 17(1), 17-22.

Nettleship, E. (1907). "A history of congenital stationary night blindness in nine consecutive generations." *Trans Ophthalmol Soc UK*, 27, 269-293.

Newman, E. A., and Odette, L. L. (1984). "Model of electroretinogram b-wave generation: a test of the K+ hypothesis." *J Neurophysiol*, 51, 164-183.

Noble, K. G., Carr, R. E., and Siegel, I. M. (1990). "Autosomal dominant congenital stationary night blindness and normal fundus with an electronegative electroretinogram." *Am J Ophthalmol*, 109(1), 44-8.

Noble, K. G., Margolis, S., and Carr, R. E. (1989). "The golden tapetal sheen reflex in retinal disease." *Am J Ophthalmol*, 107(3), 211-7.

Nose, A., Takeiki, M., and Goodman, C. S. (1994). "Ectopic expression of connectin reveals a repulsive function during growth guidance and synapse formation." *Neuron*, 13, 525539.
Oguchi, C. (1907). "Ueber einen fall von eigenartiger hemeralopie." *Nippon Gankakai Zasshi*, 11, 123-134.

Ott, J., Bhattacharya, S., and J.D., C. (1990). "Localising multiple X chromosome-linked retinitis pigmentosa loci using multiple homogeneity tests." *Proc Natl Acad USA*, 87, 701-704.

Pardue, M. T., McCall, M. A., LaVail, M. M., Gregg, R. G., and Peachey, N. S. (1998). "A naturally occurring mouse model of X-linked congenital stationary night blindness." *Invest Ophthalmol Vis Sci*, 39(12), 2443-9.

Pearce, W. G., Reedyk, M., and Coupland, S. G. (1990). "Variable expressivity in X-linked congenital stationary night blindness." *Can J Ophthalmol*, 25(1), 3-10.

Pellegata, N. S., Dieguez-Lucena, J. L., Joensuo, T., Lau, S., Montgomery, K. T., Krahe, R., Kivela, T., Kucherlapati, R., Forsius, H., and de la Chapelle, A. (2000). "Mutations in KERA encoding keratocan cause cornea plana." *Nature Genetics*, 25(1), 91-95.

Pillers, D. A., Seltzer, W. K., Powell, B. R., Ray, P. N., Tremblay, F., La Roche, G. R., Lewis, R. A., McCabe, E. R., Eriksson, A. W., and Weleber, R. G. (1993a). "Negative-configuration electroretinogram in Oregon eye disease. Consistent phenotype in Xp21 deletion syndrome." *Arch Ophthalmol*, 111(11), 1558-63.

Pillers, D. M., Bulman, D. E., and Weleber, R. G. (1993b). "Dystrophin expression in the human retina is required for normal function as defined by electroretinography." *Nature Genet*, 4.

Pokorny, J., and Smith, V. (1994). "Colour vision and night vision." Retina, R. SJ.., ed., Mosby, St Louis.

Pragnell, M. (1994). "Calcium channel b-subunit binds to a conserved motif in the I-II cytoplasmic linker of the a1-subunit." *Nature*, 368, 67-71.

Price, M. J., Judisch, G. F., and Thompson, H. S. (1988). "X-linked congenital stationary night blindness with myopia and nystagmus without clinical complaints of nyctalopia." *J Pediatr Ophthalmol Strabismus*, 25(1), 33-6.

Pusch, C. M., Zeitz, C., Brandau, O., Pesch, K., Achatz, H., Feil, S., Scharfe, C., Maurer, J., Jacobi, F. K., Pinckers, A., Andreasson, S., Hardcastle, A., Wissinger, B., Berger, W., and Meindl, A. (2000). "The complete form of X-linked congenital stationary night blindness is caused by mutations in a gene encoding a leucine-rich repeat protein." *Nature Genet*, 26(3), 324-7.

Quigley, M., Roy, M. S., Barsoum-Homsy, M., Chevrette, L., Jacob, J. L., and Milot, J. (1996). "On- and off-responses in the photopic electroretinogram in complete- type congenital stationary night blindness." *Doc Ophthalmol*, 92(3), 159-65.

Rao, V. R., Cohen, G. B., and Oprian, D. D. (1994). "Rhodopsin mutation G90D and a molecular mechanism for congenital night blindness." *Nature*, 367(6464), 639-42.

Regan, B. C., Reffin, J. P., and Mollon, J. D. (1994). "Luminance noise and the rapid determination of discrimmination ellipses in colour deficiency." *Vision Research*, 34, 1279-1299.

Riggs, L. (1954). "Electroretinography in cases of night blindness." *Am J Ophthalmol*, 38(II), 70-78.

Ripps, H. (1982). "Night blindness revisited: From man to molecules." *Invest Ophthalmol Vis Sci*, 23, 588-602.

Rosenberg, T., Schwartz, M., and Simonsen, S. E. (1990). "Aland eye disease (Forsius-Eriksson-Miyake syndrome) with probability established in a Danish family." *Acta Ophthalmol (Copenh)*, 68(3), 281-91.

Ruether, K., Apfelstedt-Sylla, E., and Zrenner, E. (1993). "Clinical findings in patients with congenital stationary night blindness of the Schubert-Bornschein type." *Ger J Ophthalmol*, 2(6), 429-35.

Schmitz, F., Holbach, M., and Drenckhahn, D. (1993). "Colocalisation of retinal dystrophin and actin in postsynaptic dendrites of rod and cone photoreceptor synapses." *Histochemistry*, 100, 473-479.

Schmitz, Y., and Witkovsky, P. (1997). "Dependence of photoreceptor glutamate release on a dihydropyridine-sensitive calcium channel." *Neuroscience*, 78, 1209-1216.

Scholl, H. E., Langrova, H., Pusch, C. M., Wissinger, B., Zrenner, E., and Apfelstedt-Sylla, E. (2001a). "Slow and fast rod ERG pathways in patients with X-linked complete stationary

night blindness carrying mutations in the NYX gene." *Invest ophthalmol Vis Sci*, 42, 2728-2736.

Scholl, H. P., Langrova, H., Pusch, C. M., Wissinger, B., Zrenner, E., and Apfelstedt-Sylla, E. (2001b). "Slow and fast rod ERG pathways in patients with X-linked congenital stationary night blindness carrying mutations in the NYX gene." *Invest Ophthalmol Vis Sci*, 42, 2728-2736.

Schubert, G., and Bornscein, H. (1952). "Beitrag zur Analyse des menschlichen Elektroretinogramms." *Ophthalmologica*, 123, 396-412.

Schultz, D. (1990). "Cloning, chromosomal localization and functional expression of the a1 subunit of the L-type voltage dependent calcium channel from normal heart." *Proc. Natl. Acad. Sci. USA*, 90, 6228-6232.

Schuster, A. (1996). "The IVS6 segment of the L-type calcium channel is critical for the action of dihydropyridines and phenylalamines." *EMBO J*, 15, 2365-2370.

Schwahn, U., Lenzner, S., Dong, J., Feil, S., Hinzmann, B., van Duijnhoven, G., Kirschner, R., Hemberger, M., Bergen, A. A., Rosenberg, T., Pinckers, A. J., Fundele, R., Rosenthal, A., Cremers, F. P., Ropers, H. H., and Berger, W. (1998). "Positional cloning of the gene for X-linked retinitis pigmentosa 2." *Nat Genet*, 19(4), 327-32.

Schwartz, E. A. (1986). "Synaptic transmission in amphibian retinae during conditions unfavourable for calcium entry into presynaptic terminals." *J Physiol*, 376, 411-428.
Schwartz, M., and Rosenberg, T. (1991). "Aland eye disease: linkage data." *Genomics*, 10(2), 327-32.

Seymour, A. B., Dash-Modi, A., O'Connell, J. R., Shaffer-Gordon, M., Mah, T. S., Stefko, S. T., Nagaraja, R., Brown, J., Kimura, A. E., Ferrell, R. E., and Gorin, M. B. (1998). "Linkage analysis of X-linked cone-rod dystrophy: localization to Xp11.4 and definition of a locus distinct from RP2 and RP3." *Am J Hum Genet*, 62(1), 122-9.

Sharp, D., Arden, G., Kemp, C., CR., H., and Bird, A. (1990). "Mechanisms and sites of loss of scotopic sensitivity: a clinical analysis of congenital stationary night blindness." *Clin Vision Sci*, 5(3), 217-230.

Shinohara, T., Donoso, L., and Tdusa, M. (1988). *Progress in retinal research.*, Pergammon Press, Oxford.

Siegel, I., and Carr , R. (1979). "Electrodiagnostic and psychophysical testing in retinal disease." *Invest ophthalmol.*

Siegel, I. M., Greenstein, V. C., Seiple, W. H., and Carr, R. E. (1987). "Cone function in congenital nyctalopia." *Doc Ophthalmol*, 65(3), 307-18.

Sieving, P. A., Frishman, L. J., and Steinberg, R. H. (1986). "Scotopic threshold response of the proximal retina in cat." *J neurophysiol*, 56, 1049-1053.

Sieving, P. A., Murayama, K., and Naarendorp, F. (1994). "Push-pull model of the primate photopic electroretinogram: a role for the hyperpolarising neurons in shaping the b-wave." *Visual Neuroscience*, 11, 519-532.

Sieving, P. A., and Nino, C. (1988). "Scotopic threshold response (STR) of the human electroretinogram." *IOVS*, 29, 1608-1614.

Sieving, P. A., Richards, J. E., Naarendorp, F., Bingham, E. L., Scott, K., and Alpern, M. (1995). "Dark-light: model for nightblindness from the human rhodopsin Gly-90-- >Asp mutation." *Proc Natl Acad Sci U S A*, 92(3), 880-4.

Smith, L. A. (1996). "A Drosophila calcium channel a1 subunit gene maps to a genetic locus associated with behavioral and visual defects." *J Neurosci*, 16, 7868-7879.

Snell, R. S., and Lemp, M. A. (1989). *Clinical anatomy of the eye.*, Blackwell Scientific Publications, Inc.

Steinmetz, R. L., Haimovici, R., Jubb, C., Fitzke, F. W., and Bird, A. C. (1993). "Symptomatic abnormalities of dark adaptation in patients with agerelated Bruch's membrane change." *Br J Ophthalmol*, 77, 549-554.

Stockton, R. A., and Slaughter, M. M. (1989). "B-wave of the electroretinogram: a reflection of bipolar cell activity." *J Gen Physiol*, 93, 101-122.

Strom, T. M., Nyakatura, G., Apfelstedt-Sylla, E., Hellebrand, H., Lorenz, B., Weber, B. H., Wutz, K., Gutwillinger, N., Ruther, K., Drescher, B., Sauer, C., Zrenner, E., Meitinger, T., Rosenthal, A., and Meindl, A. (1998). "An L-type calcium-channel gene mutated in incomplete X-linked congenital stationary night blindness." *Nat Genet*, 19(3), 260-3.
Stuhmer, W. (1989). "Structural parts involved in activation and inactivation of the sodium channel." *Nature*, 339, 597-603.

Terasaki, H., Miyake, Y., Nomura, R., Horiguchi, M., Suzuki, S., and Kondo, M. (1999). "Blue-on-yellow perimetry in the complete type of congenital stationary night blindness." *Invest Ophthalmol Vis Sci*, 40(11), 2761-4.

Tremblay, F., De Becker, I., Cheung, C., and LaRoche, G. R. (1996). "Visual evoked potentials with crossed asymmetry in incomplete congenital stationary night blindness." *Invest Ophthalmol Vis Sci*, 37(9), 1783-92.

Tremblay, F., Laroche, R. G., and De Becker, I. (1995). "The electroretinographic diagnosis of the incomplete form of congenital stationary night blindness." *Vision Res*, 35(16), 2383-93.

van Dorp, D. B., Eriksson, A. W., Delleman, J. W., van Vliet, A. G., Collewijn, H., van Balen, A. T., and Forsius, H. R. (1985). "Aland eye disease: no albino misrouting." *Clin Genet*, 28(6), 526-31.

Varelmann, H. (1925). "Die Vererbung der hemeralopie mit myopia." *Arch Augenheilkd*, 96, 385-405.

Viswanathan, S., Frishman, L. J., Robson, J. G., and Walters, J. W. (2001). "The photopic negative response of the flash electroretinogram in primary open angle glaucoma." *IOVS*, 42, 514-521.

Volker-Dieben, H. J., and Went, L. N. (1975). "Ophthalmologic and genetic study of a family with nyctalopia and myopia." *Ophthalmologica*, 171, 358-359.

Waardenberg, P. J., Eriksson, A., and Forsius, H. (1969). "Aland eye disease (syndroma Forsius-Eriksson)." *Progress in Neuro-Ophthalmology*, 2, 336-339.

Wassle, H., and Boycott, B. B. (1991). "Functional architecture of the mammilian retina." *Physiol Rev*, 71(447-480).

Wassle, H., Grunert, U., Chun, M. H., and Boycott, B. B. (1995). "The rod pathway of the macaque monkey retina: identification of AII amacrine cells with antibodies against calretinin." *J Comp Neurol*, 361, 537-551.

Weleber, R. G., Pillers, D. A., Powell, B. R., Hanna, C. E., Magenis, R. E., and Buist, N. R. (1989). "Aland Island eye disease (Forsius-Eriksson syndrome) associated with contiguous deletion syndrome at Xp21. Similarity to incomplete congenital stationary night blindness." *Arch Ophthalmol*, 107(8), 1170-9.

White, T. (1940). "Linkage and crossing over in the human sex chromosomes." *Journal of Genetics*, 40, 403-437.

Williams, M. E. (1992). "Structure and functional expression of the alpha 1, alpha 2 and beta subunits of a novel neuronal calcium channel subtype." *Neuron*, 8, 71-84.

Witkop, C. J., Quevedo, W. C., and Fitzpatrick, T. B. (1983). "Albinism and other disorders of pigment metabolism." The Metabolic Basis of Inherited Disease, J. B. Stanbury, ed., McGraw-Hill Book Co., New York.

Wolf, E., and Weber, U. (1984). *Night blindness with a tritan colour vision defect.*, Dr W Junk Publishers The Hague, Boston, Lancashire.

Wutz, K., Sauer, C., Zrenner, E., Lorenz, B., Alitalo, T., Broghammer, M., Hergersberg, M., de la Chapelle, A., Weber, B., Wiisinger, B., Meindl, A., and Pusch, C. (2002). "Thirty distinct CACNA1F mutations in 33 families with incomplete type of XLCSNB." *Eurpoean Journal of Human Genetics*, 10(8), 449-456.

Yamamoto, H., and Simon, A. (1999). "Mutations in the gene encoding 11-cis retinol dehydrogenase cause delayed dark adaptation and fundus albipunctatus." *Nat genetics*, 22, 188-191.

Yamamoto, S., Sippel, K. C., Berson, E. L., and Dryja, T. P. (1997). "Defects in the rhodopsin kinase gene in the Oguchi form of stationary night blindness [see comments]." *Nat Genet*, 15(2), 175-8.

Yamazaki, A., Hayashi, F., and Tatsumi, M. (1990). "interactions between the subunits of transducin and cyclic GMP phosphodiesterase in Rana caresbeiana rod receptors." *J Biol Chem*, 265, 11539-42.

Yau, K.-W., and Nakatani, K. (1985). "Light suppressible, cGMP-sensitive conductance in the plasma membrane of a truncated rod outer segment." *Nature*, 313, 310-315.

Young, R. S., Chaparro, A., Price, J., and Walters, J. (1989). "Oscillatory potentials of X-linked carriers of congenital stationary night blindness." *Invest Ophthalmol Vis Sci*, 30(5), 806-12.

Zito, I., Allen, L. E., Patel, R. J., Meindl, A., Bradshaw, K., Yates, J. R., Bird, A. C., Erskine, L., Cheetham, M. E., Webster, A. R., Poopalasundram, S., Moore, A. T., Trump, D., and Hardcastle, A. J. (2003). "Mutations in the CACNA1F and NYX genes in British CSNB families." *Human Mutation*, 21(2), 169-171.

Appendix A: Patient information sheet

CONGENITAL STATIONARY NIGHT BLINDNESS RESEARCH INFORMATION SHEET

Congenital Stationary Night Blindness (CSNB) is a rare, inherited visual disorder and little is known about its cause. By examining families affected by CSNB, we hope to improve our knowledge of the condition so that we may improve our understanding of the condition, counsel families with CSNB more effectively and possibly, in the future, develop new forms of therapy. We would be very grateful if you and/or other members of your family could help us in this research.

CSNB

The term *CSNB* describes a group of inherited retinal disorders that cause poor night vision and a degree of visual loss which remains stable throughout life. The commonest type is the X-linked form which only affects the males in the family, the gene fault may be 'carried' by female members of the family who may have no visual problems themselves but are at risk of passing the disorder on to their sons. A less common form may affect males or females without a family history of the condition. CSNB typically causes visual problems in the dark but can also reduce daytime, colour and distance vision and cause nystagmus (wobbly eyes). Little is known about the defect in the retina which causes CSNB, but we hope to improve our understanding of the condition by using specialised visual tests and gene studies in our examination of affected families.

What participating in our research would mean for you or your child:

A standard eye examination will be required which will take about 60 minutes (there will be a shortened examination for young children). If a blood sample has not already been taken at your local surgery, a small sample of blood will be taken from you and/or older children. This blood sample will be used for the genetic research of CSNB and will not provide a personal result for you, although we will inform you of the advances that have been made as a result of the study.

Some adults and older children will be asked to attend Addenbrooke's Hospital, Cambridge or Moorfields Eye Hospital, London for more sophisticated tests, including examination of visual fields and measurement of vision at low light levels,

which may take several hours to complete. Although you have probably had similar tests performed in your own hospital, it is only by performing these tests in standardised manner that we can be sure to identify and compare the different forms of CSNB. We will provide your ophthalmologist with a detailed report of our findings but otherwise the results will be kept strictly confidential. Your travelling expenses to either centre will be reimbursed.

During the initial examination we will need to dilate your (or your child's) pupils with drops. This procedure is conducted routinely in eye clinics and often causes temporary sensitivity to bright light and blurring of near vision. It is advisable for you to bring sunglasses for you or your child to wear after the examination to prevent dazzle and you should not drive for 5-6 hours.

We should greatly appreciate your help in our research, if you would like further information before deciding whether to participate, we would be very happy to discuss any concerns you might have. We do not expect an explanation if you decide against participating or if you decide to withdraw from the study at any stage, nor will withdrawal from the project affect your future treatment in any way.

Appendix B: Patient Database Sheet

Congenital Stationary Night Blindness - History

Patient code AD 1001a

First Name xxxx

Last Name xxxx

Age 11

Nyctalopa ☑

Colour deficiency ☐

Comments Mother says he has always had bad vision at night

Medications Nil

POH Myopic since 2-3 years of age

Previous Eye surgery Nil

PMH Nil

Congenital Stationary Night Blindness - Examination

Patient code	AD 1001a

First Name		**Last Name**	
XXXX		XXXX	
Snellen VAR	6/9	**Snellen VAL**	6/9
		Snellen BEO	6/9
LogMAR R		**LogMAR L**	
Near type BEO	N5	**LogMAR BEO**	
Ishihara		**Mollon-Reffin**	
Full		T2,D1,P1	
Paradoxical pupils	☐	**City university test:**	Full
Transllumination	☐	**Nystagmus**	☑
		Nystagmus type:	Latent
IOP R	0	**IOP L**	0
Refraction		**Refraction L**	
		Strabismus type:	
Strabismus	☐		
Fundus Normal	☐		
Lens opacity	No		
Disc abnormality	tilted discs		
Other fundal abnormality	foveal hypoplasia		

Appendix C: Recipes and sequencing protocols

C.1 Buffer recipes

NEB Buffer

Tris 670mM
(Sigma Chemicals, USA)
Ammonium sulphate 166mM
(BDH laboratory supplies, UK)
Magnesium Chloride 1M
(Fisons Scientific UK Ltd)
T 0.1 E (10mM Tris, 0.1mM EDTA)
pH adjusted to pH 8.8 with hydrochloric acid

P1 Buffer

Potassium chloride 2M
(Fisons Scientific UK Ltd)
Tris 1M
(Sigma Chemicals, USA)
Magnesium chloride 1M
(Fisons Scientific UK Ltd)
Gelatin 1%
(BDH laboratory supplies, UK)
Distilled water

Sequencing Loading Buffer

Formamide 95%
(Reidel-de Haen, Germany)
EDTA 20mM
(Sigma Chemicals, USA)
Bromophenol blue 0.05%
(BDH laboratory supplies, UK)
Xylene cyanol 0.05%
(ICN pharmaceuticals Inc. USA)

C.2 PCR product purification

Qiaquick PCR purification kits (Qiagen Ltd. UK) were used to prepare each PCR exon product prior to sequencing according to the manufacturers instructions. This system utilises the selective binding properties of a silica-gel membrane. The binding buffer provided with the kit is optimised for the efficient recovery of single and double stranded DNA fragments from 100bp to 10kb and for the quantitiative (99.5%) removal of primers under 40 bases and unincorporated nucleotides. The sample is drawn through the silica-gel membrane using a vacuum and DNA adsorbs to the silica-membrane in the presence of high salt while contaminants pass through. Impurities are washed away and the purified DNA fragment is eluted with Tris buffer (provided in kit).

C.3 Automated sequencing protocol for the ABI 373 sequencer

The DNA to be sequenced was used as a single-stranded template for the synthesis of new DNA strands by a DNA polymerase (provided in the ABI Prism Big Dye Terminator Cycle Sequencing Ready Reaction Kit, PE Applied Biosystems, USA).

In addition to the normal nucleotide precursors, this DNA synthesis reaction is carried out in the presence of base-specific dideoxynucleotides (ddNTPs). These are analogs of the normal dNTPs but lack a hydroxyl group at the 3' and 2' carbon position. The ddNTP can be incorporated into the growing DNA chain but cannot participate in phosphodiester bonding at its 3' carbon, resulting in abrupt termination of chain synthesis. The Big Dye terminators provided in the Sequencing Kit contain fluorophores specific for each ddNTP. During the electrophoresis run, a laser beam is focused at a specific constant position on the gel. As the individual DNA fragments migrate past this position the laser causes the dyes to fluoresce. Maximum fluorescence occurs at different wavelengths for the four dyes. The intensity profiles of each of the coloured dyes is recorded electronically and the interpreted sequence is stored in a computer database.

C.3.1Sequencing Reaction

The following reagents were mixed in a labelled 0.5µl eppendorph tube:

Purified PCR product	5µl
Specified buffer (kit)	2µl
Primer (10ng/µl)	1µl

Big Dye Terminator (last)	2µl

The thermal cycle for the sequencing reaction was:

96E for 30 seconds

50E for 15 seconds

60E for 4 minutes

This was repeated 25 times. Following completion of the sequencing reaction, samples were stored at 4EC prior to purification.

The sequencing product was purified by the addition of:

3M sodium acetate (pH4.8)	2µl
(Fisons Scientific Equipment UK)	
95% ethanol (ice cold)	50µl
(Fisher Scientific UK)	

Each sample was then mixed by vortex and placed at -20EC for 25 minutes to precipitate the DNA. The samples were then centrifuged at 13,000rpm for 20 minutes to allow a DNA pellet to form. The supernatant was carefully removed and discarded. The pellet was washed with 200µl of ice-cold 75% ethanol and further centrifuged for 2 minutes. The supernatent was removed and discarded with care not to dislodge the DNA pellet. The samples were flash dried to remove any remaining ethanol.

C.3.2 Preparation of the sequencing gel

The sequencing plates were cleaned using water only and left to air dry. The following reagents were combined in a beaker and stirred:

Distilled water	18.4ml
Acrylamide bis(30%)	7.2ml
(Anachem Ltd. UK)	
Urea	24g
(BDH Laboratory supplies UK)	
Amberlite resin	1g
(BDH Laboratory supplies UK)	

10X TBE (1L)

Tris	108g
Boric acid	55g
(Fisher Scientific UK)	
EDTA	7.44g

4.8mls of 10X TBEwas applied to the filter of a *Nalgene* (Nalg Nunc International USA) disposable filter flask and drawn through using a vacuum. The acrylamide/urea mixture was then added to the filter. The contents of the flask (the gel mix) were then left to degas for 20 minutes.

C.3.3 Pouring the gel

The clean glass sequencing plates were laid horizontally using supports, the plates separated by spacers. To catalyse the polmerisation of the gel, the following were added:

10% Ammonium persulphate	240µl
(BDH Laboratory supplies UK)	
TEMED (NNN'N' tetramethylethylenediamine)	
(Sigma Chemicals Co USA)	26.4µl

The polymerising gel mixture was then swiftly poured between the glass plates using a 50ml syringe. Any bubbles which had occurred during pouring were hooked out and the comb was introduced. The gel was allowed to polymerise for 2 hours.

C.3.4 Starting the sequencer

An initial plate check to determine the presence of optical contamination of the gel and plates was performed. If satisfactory, the upper and lower reservoirs were filled with 1X TBE. The comb was then removed from the gel, the excess acrylamide rinsed from the upper gel border and the gel was then pre-run for 30 minutes at 500mv.

C.3.5 Preparing the specimens for loading

A formamide loading buffer was used to ensure the DNA specimens were in a single-stranded state. (see buffer recipe C1). The pellet of DNA formed after the purification procedure was resuspended in 3.5µl of formamide loading buffer and heated on the PCR block at 95E for 2 minutes. The samples were then put on ice prior to loading on the sequencing gel.

Appendix D: Publications derived from this research

Presentations

Allen LE, Moore, AT.

Congenital Stationary Night Blindness: evidence for a genotype/phenotype correlation. *European Paediatric Ophthalmology Group*, Cambridge, September 2000.

Allen, L.E., Bradshaw, K., Fitzke, F.W., Bird, A.C., Yates, J.R.W., Moore, A.T., Trump, D. Retinal function testing in X-linked CSNB can identify patients with mutations in the CSNB2 gene. *Association for Research in Vision and Ophthalmology.* IOVS 2000 41(4):S884

Publications

To date four publications have been accepted by peer reviewed journals from the research detailed in this thesis:

Zito, I., Allen, L.E., Patel, R.J., Meindl, A. Bradshaw, K., Yates, J.R. Bird, A.C. Erskine, L., Cheetham, M.E., Webster, A.R., Poopalasundaram, S., Moore, A.T., Trump, D., Hardcastle, A.J. (2003) Mutations in the CACNA1F and NYX genes in British CSNB families. *Human Mutation.* 21(2):169-171.

Allen, L.E., Zito, I., Bradshaw, K. Patel, R.J., Bird,A.C., Fitzke, F.W., Yates, J.R., Trump, D., Hardcastle, A.J., Moore, A.T. (2003) Genotype-phenotype correlation in British Familes with X-linked congenital stationary night blindness. *British Journal of Ophthalmology* 87:1413-1420.

Bradshaw, K., Newman, D.K., Allen, L.E., Moore. A.T. Abnormalities of the scotopic threshold response correlated with gene mutation in X-linked retinoschisis and congenital stationary night blindness (2003). *Documenta Ophthalmologica.* 107:155-164

Bradshaw, K., Allen, L.E., Trump, D., Hardcastle,A.J., George, N., Moore, A.T. A comparison of ERG abnormalities in X-linked retinoschisis and X-linked congenital stationary night blindness(2004) *Documenta Ophthalmologica 108:135-145.*

Appendix E: Pedigrees

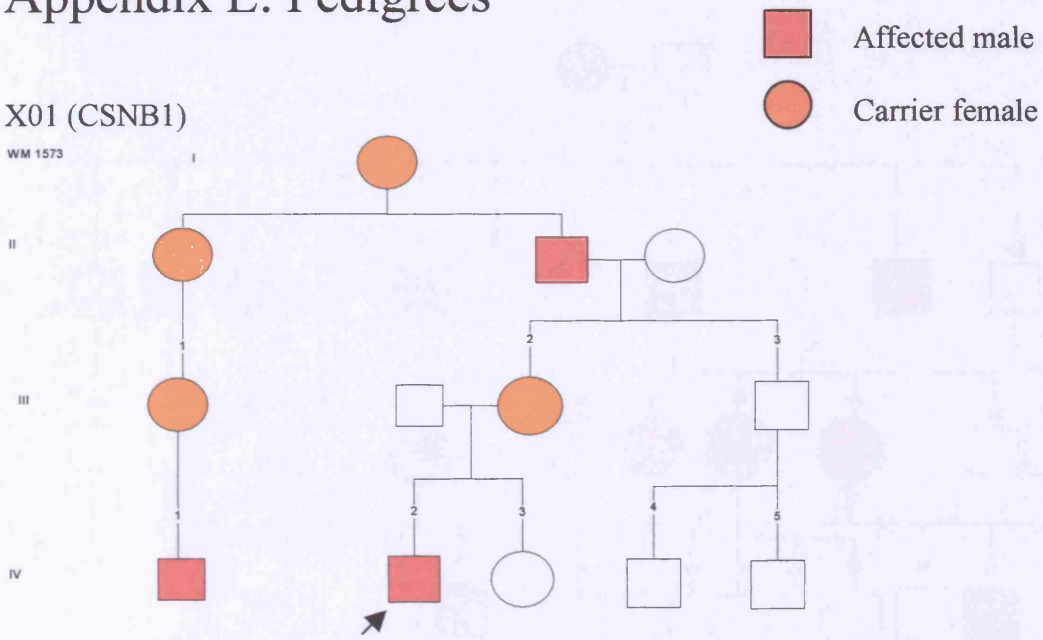

X02 (No mutation identified)

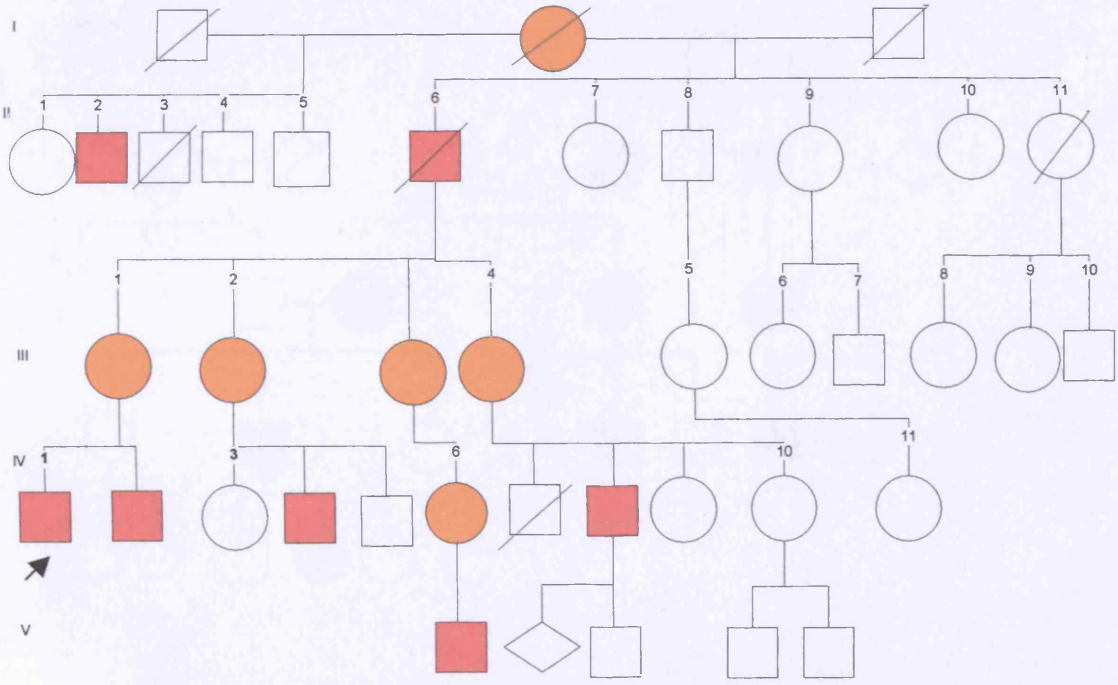

X03 (CSNB1)

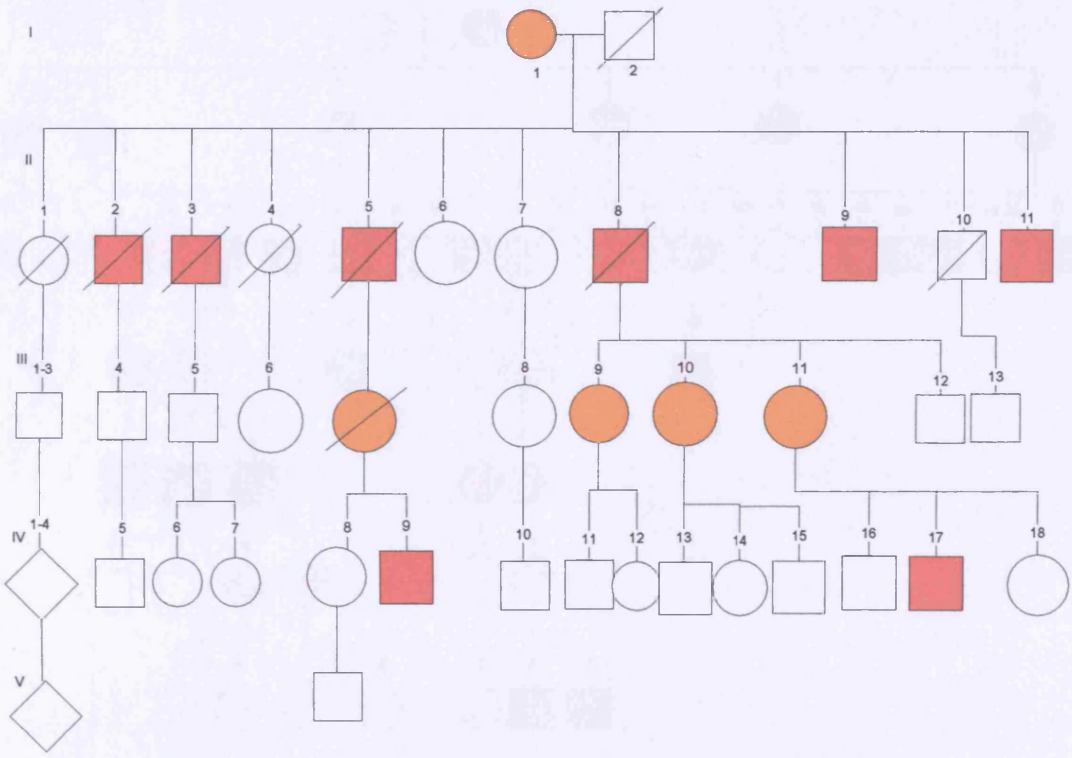

X04 (CSNB1)

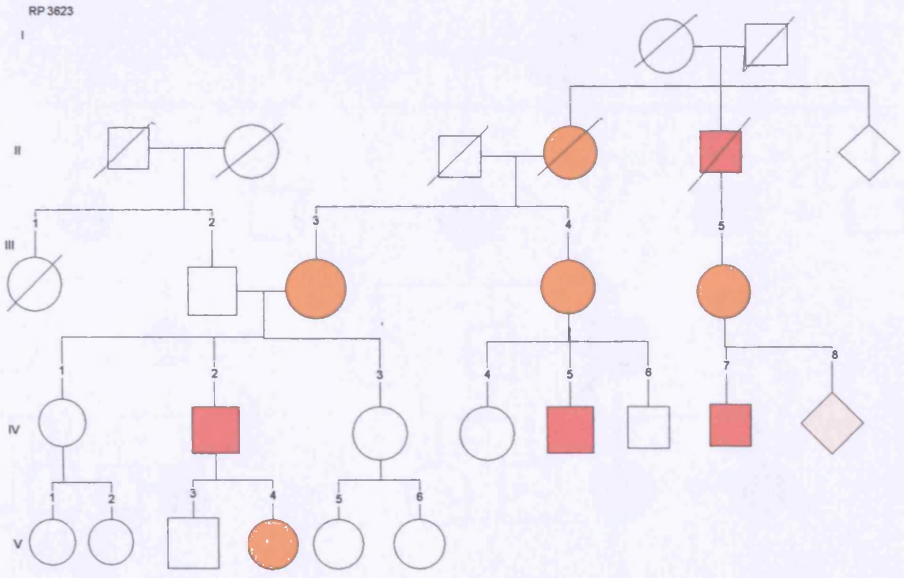

X05 (CSNB1)

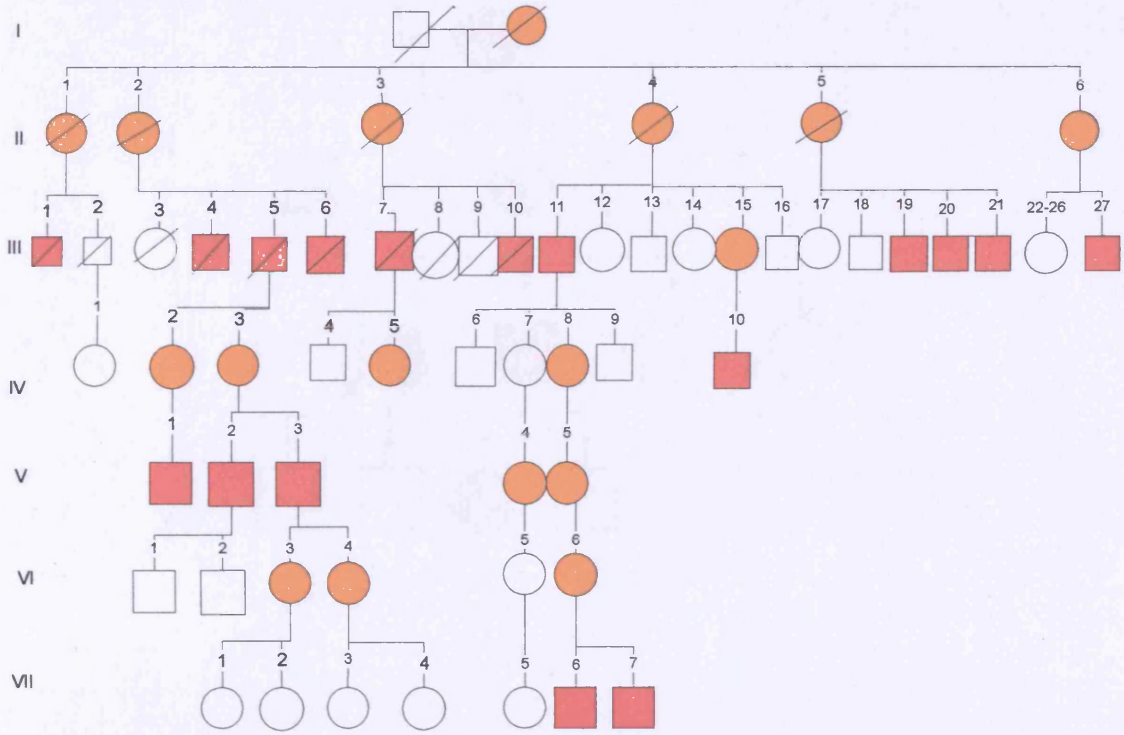

X06 (CSNB1)

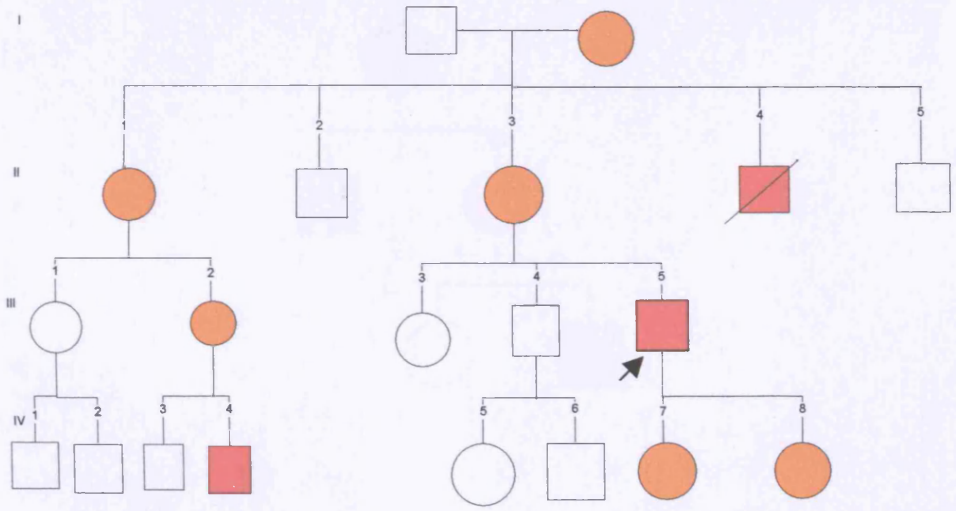

X07 (CSNB1)

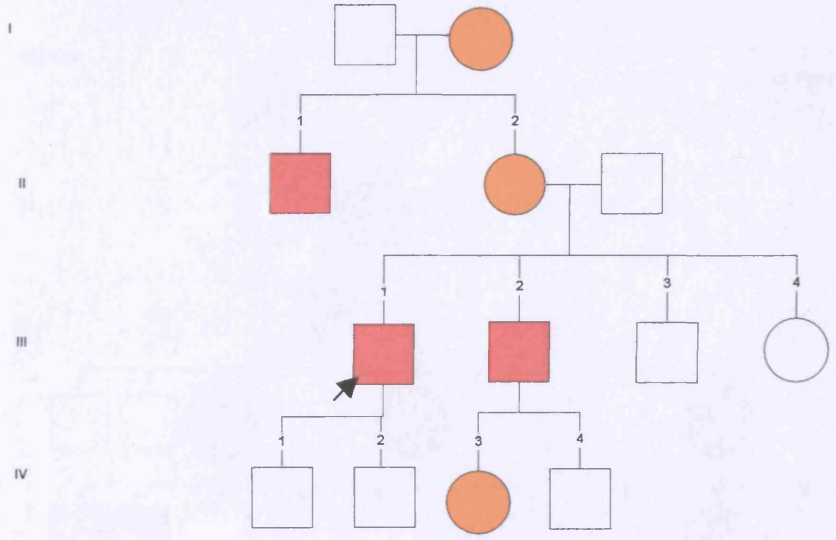

X08 (CSNB1)

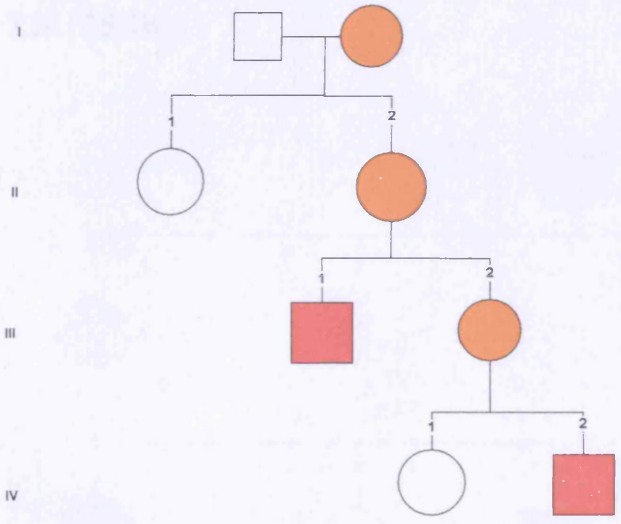

X09 (CSNB1)

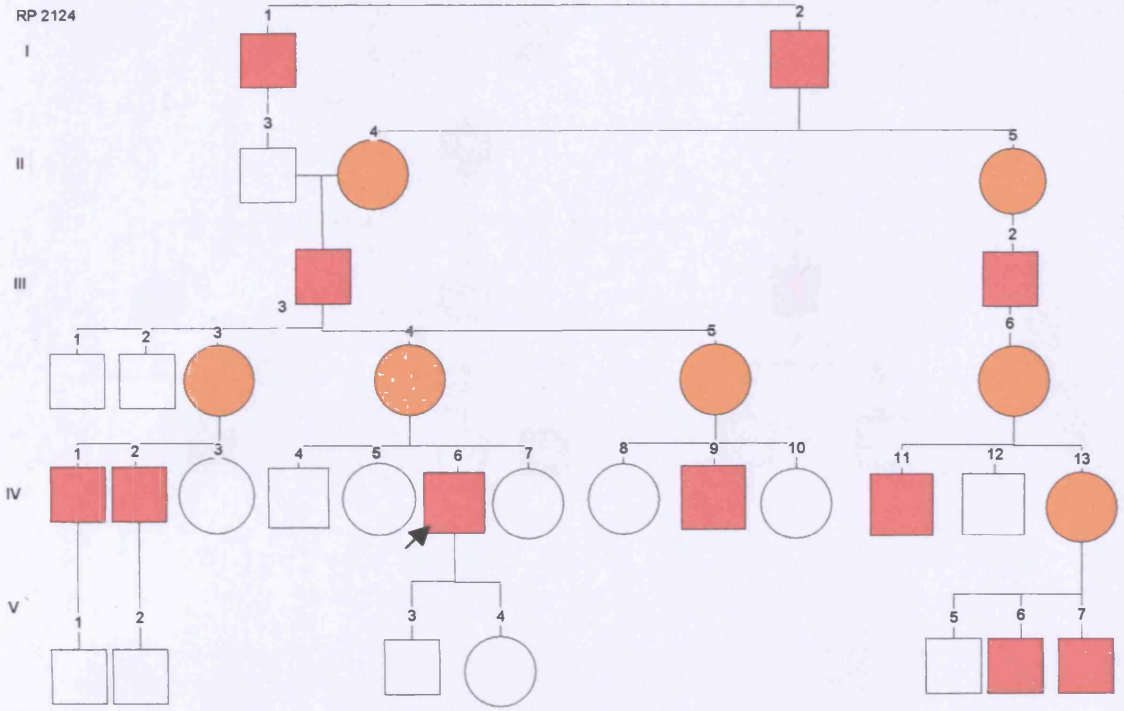

X10 (CSNB2)

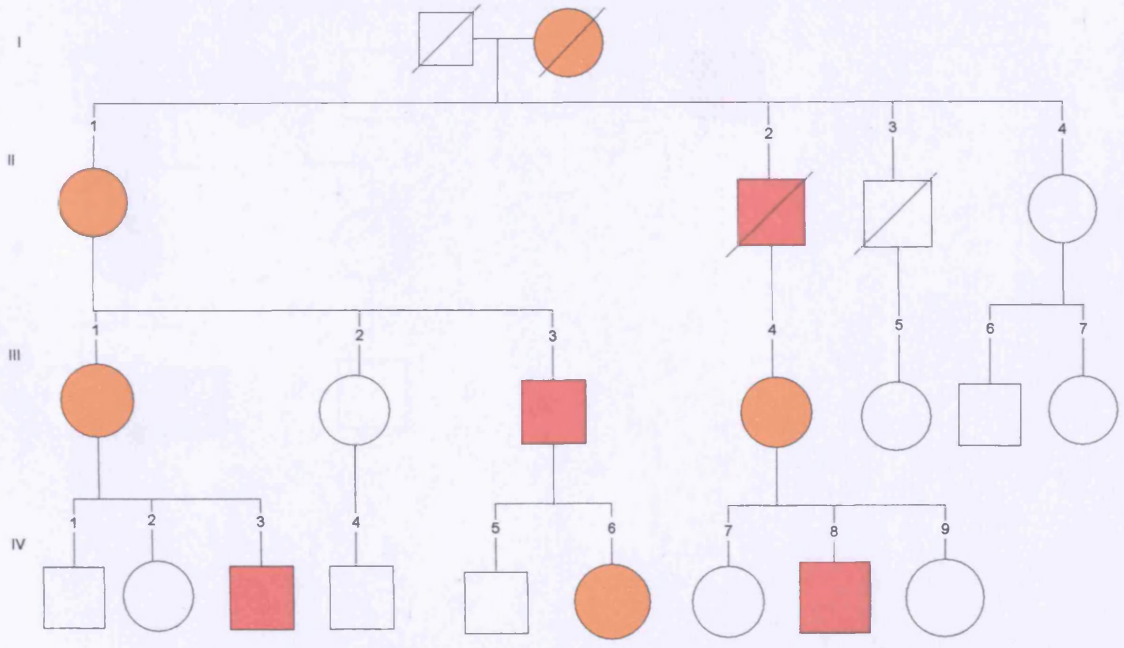

X11 (CSNB2)

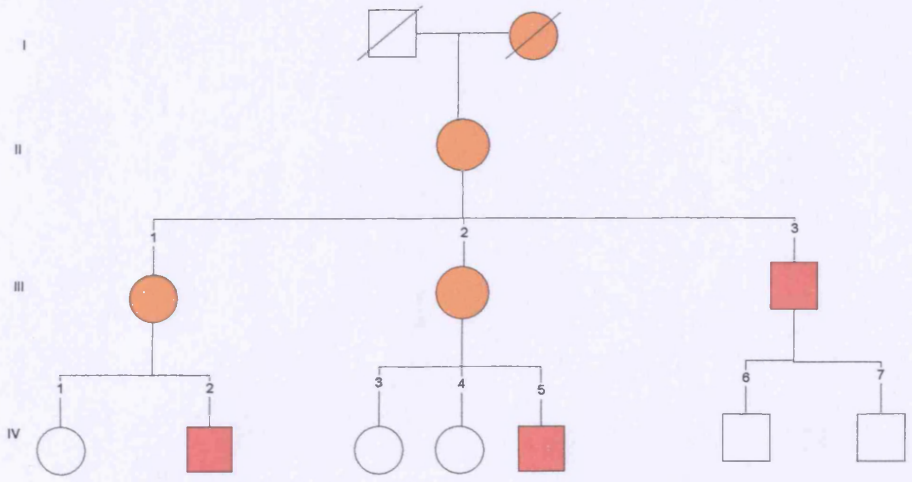

X12 (CSNB2)